Effect of kisspeptin on testes and accessory sex glands in prepubertal rats

By

FAIQAH RAMZAN

~~(M.Sc)~~

Department of Animal Sciences
Faculty of Biological Sciences
Quaid-i-Azam University
Islamabad, Pakistan
2010

Effect of kisspeptin on testes and accessory sex glands in prepubertal rats

A thesis submitted in the partial fulfillment of the requirements for the degree of

Doctor of Philosophy

In

Animal Physiology

By

FAIQAH RAMZAN
(M.Sc)

Department of Animal Sciences
Faculty of Biological Sciences
Quaid-i-Azam University
Islamabad, Pakistan
2010

IN THE NAME OF ALLAH THE MOST MERCIFUL AND MIGHTY

O my Lord! Open for me my chest
(Grant me Self-confidence,
Contentment and boldness)
And ease my task for me,
And loose the knot from my tongue that they
understand my speech (words)

Surah 20, Ta Ha (Al-Quran)

Dedicated to…

My Parents…

For their support throughout my education and inculcating the sense of responsibility and independence

My Brothers and sister…

For their love and support

My Teachers and mentors…

For the arduous task of imparting knowledge in an often disillusioned student

My Friends…

For putting up with me

My Family…

For their support

DECLARATION

The material contained in this thesis is my original work and I have not presented any part of this thesis/work elsewhere for any other degree. I have tried my best to avoid plagiarism. I understand that I may be held responsible in case faulty, non authentic or plagiarized results found in the dissertation.

FAIQAH RAMZAN

CERTIFICATE

This is to certify that the dissertation, submitted by **Mrs. Faiqah Ramzan** is accepted in its present form by the Department of Animal Sciences, Faculty of Biological Sciences, Quaid-i-Azam University, Islamabad, as satisfying the thesis requirement for the degree of Doctor of Philosophy in Animal Sciences (Animal Physiology).

SUPERVISOR:

Dr. Irfan Zia Qureshi

EXTERNAL EXAMINER:

Prof. Dr. A. R. Shakoori

EXTERNAL EXAMINER:

Prof. Dr. Arif Siddiqui

CHAIRMAN:

Prof. Dr. M. Shahab

Dated: **June 09, 2011**

CONTENTS

ACKNOWLEDGEMENTS

*All praises are to **Allah Almighty**, the most gracious, the most merciful, who has created all that exists and guides us in darkness and helps us in difficulties. Peace and blessings be upon **Prophet Mohammad (Peace be upon him)**, who is a seal of the Prophets and the true universal Messenger of Allah who enabled us to recognize our creator.*

I would like to extend my heartfelt appreciation to my PhD supervisor, Dr Irfan Zia Qureshi for his diligent guidance, instruction, patience, moral and social support during the course of my research and training for which I will always feel indebted.

I am grateful to Prof. Dr. Muhammad Shahab, Chairman, Department of Animal sciences, Quaid-i-Azam University, Islamabad for the gift of acyline, valuable suggestions and providing all research facilities at the department to accomplish this work.

Sincere thanks are due to Mrs. Shehnaz Murtaza, Deputy Chief Scientist,Nuclear Institute of Oncology and Radiotherapy (NORI) hospital, Islamabad and her staff for guidance on radioimmunoassay. I am grateful to Dr. Yousaf Zafar, DG, NIBGE, Dr. Sohail Hameed, Principal Scientific Officer and M. Javed Iqbal, Incharge Electron Microscopy Division, NIBGE, Faisalabad, for sincere guidance and help in electron microscopy. I am also grateful to Prof. Dr. Wasim Ahmad for his gracious help.

Without the valuable support and constant encouragement from my parents, mother in law, husband and daughter, who adjusted with the inconveniences and disturbances during the course of this study, this work would not have been a reality. I offer them my heartfelt thanks.

I would like to extend my sincere thanks to my lab fellows Dr. Tariq Mehmood, Fariha, Riaz, Nosheen and Qamer for their skillfull assistances, helpful attitude and cheerful companionship. My thanks are also due to Johar, Dr. Rizwan, Sadia, Sumaira for their cooperation, encouragement and help. I appreciate the moral support and encouragements of all my juniors including Saba, Naila, Shabana, Nosheen, Mehwish, Humera, Naheed and Dilnaz.

I am grateful to my brothers, sister and other members of family, for the keen interest shown and encouragement given to me in completing this work.

Above all, from the innermost core of my heart I thank the Almighty in helping me to complete this work.

The study was supported by an indigenous PhD research fellowship awarded by the Higher Education Commission (HEC), Islamabad, Pakistan.

Faiqah Ramzan

ABBREVIATIONS

Abbreviations	Full Name
%	Percentage
µg	Microgram
µl	Microlitre
ANOVA	Analysis of variance
DPA	Diphenyleamine
EDTA	Ethylene Diamine Tetra Acetate
FSH	Follicle stimulating hormone
GnRH	Gonadotropin releasing hormone
i.p.	Intraperitoneal
Icv	Intracerebroventricular
LH	Luteinizing hormone
Min	Minute
°C	Degree Centigrade
P	Picomol
PBS	Phosphate Buffered Saline
PFA	Paraformaldehyde
s.c.	Subcutaneous

TABLES

FIGURES

PHOTOMICROGRAPHS

ELECTRON MICROGRAPHS

ABSTRACT

Hypothalamus-derived kisspeptins are critical regulators of reproduction in nearly all mammalian species including the humans. These small peptides mediate their actions through the GnRH loop system. How kisspeptins regulate gonadal maturation in sexually immature male mammals remains elusive. To address this, two sets of experiments were done: firstly, kisspeptin was administered as subchronic (12 days) twice daily i. p. doses at three different dosage regimens: 15 pmol (10 pg), 1.5 nmol (1 ng) and 1.5 μmol (1 μg), to prepubertal male Sprague Dawley rats (PND 35), secondly, kisspeptin effects were further evaluated indirectly by blocking GnRH action using acyline as an antagonist. Rats were assigned to four experimental groups namely: control saline treated, kisspeptin alone, saline with acyline pretreatment and kisspeptin with acyline pretreatment. Effects on spermatogenesis, secretion of testosterone and pituitary gonadotropins, the LH and FSH, DNA parameters and histomorphology of testicular tissue and accessory sex glands, seminal vesicle and prostate, were studied. Major scientific approaches applied were; radioimmunoassay, light and electron microscopy, DNA extraction, electrophoresis and morphometrical measurements. Spermatogenesis was studied histologically at stage VII of the spermatogenic cycle. Data were analyzed statistically.

Results showed that at end of the treatments plasma FSH levels were not altered in any of the treatment groups. LH and testosterone concentrations were reduced in the 1 ng ($p < 0.05$) and 1 μg kisspeptin groups ($p < 0.01$), while no significant change was observed at 10 pg dose. At 1 ng and 1 μg kisspeptin doses, testicular parameters that decreased significantly were mainly: the number of type A spermatogonia ($p < 0.05$; $p < 0.01$), preleptotene spermatocytes ($p < 0.05$), pachytene spermatocytes ($p < 0.01$; $p < 0.001$), step 7 spermatids ($p < 0.05$; $p < 0.001$), elongated spermatids and daily sperm production ($p < 0.05$; $p < 0.001$), while at 10 pg dose the decrease was non significant. Sertoli cell efficiency and total support capacity of each Sertoli cell decreased significantly at all doses. Meiotic index decreased ($p < 0.05$) only at 1 μg dose; while coefficient of mitosis increased at 1 ng and 1 μg ($p < 0.01$) doses both. Histomorphology showed scant round and elongated spermatids, intratubular vacuolizations, multinucleated giant cells and atrophied germinal epithelium. Ultrastructure evidenced vacuolated mitochondria in Sertoli cells,

involuted acrosome, degenerated and vacuolated Leydig cells and thin basal laminae. DNA ladder assay showed fragmentation of DNA into smaller fragments of variable sizes. On quantification, DNA damage that occurred to the testicular tissue was 20 ± 2.04, 36 ± 1.85 and 60.18 ± 3.37, at 10 pg, 1 ng and 1 μg doses respectively. In the second set of experiments plasma FSH ($p < 0.001$) and LH ($p < 0.001$) decreased in the saline (acyline pretreated) treated group, and as well as in the kisspeptin (acyline pretreated) treated group at the end of the experiment. Testosterone levels decreased ($p < 0.01$) in saline (acyline pretreated) and kisspeptin (acyline pretreated) treated groups ($p < 0.001$). Seminiferous tubular diameter decreased non-significantly while seminiferous tubular epithelial height decreased highly significantly ($p < 0.001$) in treated groups as compared to control. In saline (acyline pretreated) treated group, type A spermatogonia ($p < 0.001$), preleptotene spermatocytes ($p < 0.05$), pachytene spermatocytes ($p < 0.01$), step 7 spermatids ($p < 0.001$), elongated spermatid head count and daily sperm production ($p < 0.01$) decreased as compared to control testes. In the kisspeptin (acyline pretreated) treatment group, only type A spermatogonia ($p < 0.001$), decreased significantly, while other parameters remained unaffected. Histomorphological observations demonstrated loss of germ cells, abnormal germ cell associations and germ cell maturation arrest in saline (acyline pretreated) treated group, while seminiferous tubules of rats treated with kisspeptin (acyline pretreated) revealed partial restoration of spermatogenesis. DNA damage to the testicular tissue was 36 ± 0.07 and 14 ± 1.17 with saline (acyline pretreated) and kisspeptin (acyline pretreated) treatment respectively.

Seminal vesicle weights decreased significantly ($p < 0.01$) at 1 μg kisspeptin dose. The epithelial height of secretory acini of seminal vesicle decreased at 10 pg ($p<0.05$), 1 ng and 1μg doses ($p < 0.001$). Histological observations demonstrated dilated lumen and decrease in epithelial folds and height of epithelial cells. Ultrastructure showed disorganization of the organelles involved in the secretory process such as dilatation of the endoplasmic reticulum, disorganization of the Golgi complex and decrease in the number of secretory granules in principal cells of the seminal vesicle. DNA damage to the seminal vesicle was 19.54 ± 1.98, 38.06 ± 2.09 and 58.18 ± 2.59 at 10 pg, 1 ng and 1 μg doses respectively. In the second set of experiments seminal vesicle weights remained unaffected. Epithelial height of secretory acini of seminal vesicle decreased ($p < 0.05$) in both the saline (acyline

pretreated) and kisspeptin (acyline pretreated) treated groups as compared to the control. Histological and ultrastructural examination showed degeneration of the tissue in saline (acyline pretreated) treated group, while it nearly restored to normal in the kisspeptin (acyline pretreated) treated group. DNA damage was 20.87 ± 0.98 and 19.03 ± 1.71 with saline (acyline pretreated) and kisspeptin (acyline pretreated) treatment respectively.

Prostate weights decreased significantly ($p < 0.05$) at 1 μg treatment dose of kisspeptin. The epithelial height of secretory acini of prostate decreased at 10 pg ($p < 0.05$), 1 ng and 1μg doses ($p < 0.001$). Histology and ultrastructure demonstrated, decrease in epithelial cell height, epithelial folding and dilatation of the organelles with kisspeptin treatment. DNA damage to the prostatic tissue was 20.74 ± 2.18, 43.60 ± 2.39 and 58.18 ± 2.59 at 10 pg, 1 ng and 1 μg doses respectively. In the second set of experiments, prostate weights were unaltered. Epithelial height of secretory acini of prostate gland decreased ($p < 0.001$) in saline (acyline pretreated) and ($p < 0.05$) in kisspeptin (acyline pretreated) treated groups. Histologically, the prostate tissue was degenerated and regressed with saline (acyline pretreated) treatment but showed a restoration of structure to normal with kisspeptin (acyline pretreated) treatment. DNA damage to the gland was 26.60 ± 1.71 and 14.02 ± 1.27 with saline (acyline pretreated) and kisspeptin (acyline pretreated) treatments respectively.

The present findings indicate that subchronic kisspeptin administration may act as a suppressor of pubertal maturation during non-pubertal states and a partial recovery of the testicular tissue and accessory sex glands occur with acyline pretreatment.

INTRODUCTION

INTRODUCTION

1.1 Puberty

Puberty is characterized by rapid interactive endocrine, anatomical and morphological changes. It is the transitional period between the juvenile and adult state in which sexual maturation begins in the hypothalamic–pituitary–gonadal (HPG) system, leading to the development of secondary sex characteristics and fertility. The three primary controllers in the HPG axis are: (i) neurosecretory neurons within the hypothalamic arcuate nucleus (ARC) that release gonadotropin-releasing hormone (GnRH), (ii) the pituitary gonadotropes, which secrete luteinizing hormone (LH) and follicle stimulating hormone (FSH) and lactotropes that secrete prolactin (PRL), and (iii) the gonadotropin-responsive elements within the testes, the Leydig and Sertoli cells.

1.1.1 Pubertal maturation in male rat

Although the release of GnRH, gonadotropins, gonadal steroids and, the steroid positive and negative feedback are relatively consistent across mammalian species, however several differences do appear between the human and rat pubertal progression. For example, male rodents do not display a postnatal period of testicular quiescence analogous to that in the human juvenile period, but instead show initiation and progression of testicular development at a very early age (Ojeda and Urbanski, 1994).

Postnatal sexual development in the male rat has been classified into four distinctive periods including the (i) neonatal, postnatal day (PND 1-7), (ii) infantile (PND 8-21), (iii) juvenile, (PND 22-35), and (iv) peripubertal, (PND 36- 55 or 60), at which time the first mature spermatozoa appear in the vas deferens (Clegg, 1960; Ojeda *et al.,* 1980). Testicular development and function are dependent on many factors. It is known that gonadotropins secreted by the pituitary gland act on the Sertoli cells, either directly through FSH or via LH action on the Leydig cells. Sertoli cells in turn regulate germ cell differentiation (Hansson *et al.,* 1983; Sanborn *et al.,* 1983).

Compared to humans where spermatogenesis starts at puberty (12-14 years of age), germ cell proliferation in rat starts very early; the first meiotic cells appearing within 2 weeks after birth (Tanner, 1962). The development of the testis in Sprague-Dawley rat is morphologically well described. In newborn rat the seminiferous cords contain only undifferentiated Sertoli cells and gonocytes but most gonocytes are differentiated into spermatogonia at about 10 days post natal (Roosen-Runge and Leik, 1968). The first primary spermatocytes appear at PND 12 or 13, and formation of the occluding inter-Sertoli cell junctions takes place between PND day 15 and 19 Vitale *et al.*, 1973; Hagenas *et al.*, 1981). First meiotic divisions are observed at PND 4, and spermatids in the Golgi phase appear at PND day 25 (Knorr *et al.*, 1970). First ature spermatids, "testicular spermatozoa" are evident at PND 44, but not until ut PND 56 days of age is the frequency of such late spermatids the same as in the lt testis (Ekwall *et al.*, 1984). By 48 days postnatal a considerable number of liated, more or less degenerated, testicular cells are found in the epididymis. occurs a 17-fold increase in testicular weight but only a 7-fold increase in body t between day PND 20 and 60. Tubular diameter increases about 2.5 times this period while the total tubular length increases about three times (Ekwall *et* t).

atogenesis

natogenesis involves four basic processes: spermatogonial development l subsequent cell mitotic divisions), meiosis (DNA synthesis and two ons to yield haploid spermatids), spermiogenesis (spermatid olving differentiation of head and tail structures), and spermiation ease of mature sperm into the tubule lumen). These processes occur in all mammals and are well described at the morphological level nt, 1952; Clermont, 1972; de Kretser and Kerr, 1988; Russell et nd some primate species (e.g., *Macaca fascicularis*), germ cell rderly and recognizable cell associations (or stages) along the that a single stage can be seen within a tubule cross section umans and some other primates (e.g., marmosets) however, intertwining helical pattern such that cross section from a

Compared to humans where spermatogenesis starts at puberty (12-14 years of age), germ cell proliferation in rat starts very early; the first meiotic cells appearing within 2 weeks after birth (Tanner, 1962). The development of the testis in Sprague-Dawley rat is morphologically well described. In newborn rat the seminiferous cords contain only undifferentiated Sertoli cells and gonocytes but most gonocytes are differentiated into spermatogonia at about 10 days post natal (Roosen-Runge and Leik, 1968). The first primary spermatocytes appear at PND 12 or 13, and formation of the occluding inter-Sertoli cell junctions takes place between PND day 15 and 19 (Vitale *et al.*, 1973; Hagenas *et al.*, 1981). First meiotic divisions are observed at PND 24, and spermatids in the Golgi phase appear at PND day 25 (Knorr *et al.*, 1970). First mature spermatids, "testicular spermatozoa" are evident at PND 44, but not until about PND 56 days of age is the frequency of such late spermatids the same as in the adult testis (Ekwall *et al.*, 1984). By 48 days postnatal a considerable number of exfoliated, more or less degenerated, testicular cells are found in the epididymis. There occurs a 17-fold increase in testicular weight but only a 7-fold increase in body weight between day PND 20 and 60. Tubular diameter increases about 2.5 times during this period while the total tubular length increases about three times (Ekwall *et al.*, 1984).

1.2 Spermatogenesis

Spermatogenesis involves four basic processes: spermatogonial development (stem cell and subsequent cell mitotic divisions), meiosis (DNA synthesis and two meiotic divisions to yield haploid spermatids), spermiogenesis (spermatid development involving differentiation of head and tail structures), and spermiation (the process of release of mature sperm into the tubule lumen). These processes occur along similar lines in all mammals and are well described at the morphological level (Leblond and Clermont, 1952; Clermont, 1972; de Kretser and Kerr, 1988; Russell *et al.*, 1990). In rodents and some primate species (e.g., *Macaca fascicularis*), germ cell development occurs in orderly and recognizable cell associations (or stages) along the seminiferous tubule, such that a single stage can be seen within a tubule cross section (Russell *et al.*, 1990). In humans and some other primates (e.g., marmosets) however, the stages are arranged in an intertwining helical pattern such that cross section from a

single seminiferous tubule may contain up to six identified stages (Schulze and Rehder, 1984).

The stem cells for the spermatogenic process are termed spermatogonial stem cells, and these undergo infrequent mitotic divisions. They can undergo several rounds of mitosis without completing cytokinesis, beginning the pathway by which groups of spermatogonia then proceed to enter meiosis and are termed first as primary spermatocytes and then secondary spermatocytes. The latter divides to form spermatids, haploid cells that are transformed during spermatogenesis into spermatozoa (Kerr *et al.*, 2006).

The process of spermatogenesis requires the creation of a special environment within the seminiferous tubule which is provided by the Sertoli cells that also form the blood-testis barrier (Setchell and Waites, 1975). Furthermore the unusual cellular nature of the product of spermatogenesis, namely the spermatozoa, creates a specific requirement within the epithelium that supports the migration of a population of cells that proliferate at the base of the tubule and move progressively toward the lumen of the tubule as the cells differentiate (Kerr *et al.*, 2006).

1.2.1 Spermatogonia

The cells that divide by mitosis and represent the pool of cells from which meiosis and spermatogenesis proceed are termed "spermatogonia". Spermatogonia were first identified as separate entities from the Sertoli cells by von Ebner in 1871, but the term spermatogonia was first applied to this class of cells by von La Valette and St. George in 1876 (cited by Donnel *et al.*, 2006).

According to Regaud (1901, cited by Donnel *et al.*, 2006) on the basis of differences in the chromatin patterns of nuclei, two types of spermatogonia in the rat are recognizable, the "dusty" cell and the "crusty" cells. The dusty cells nucleus contain fine pale stained chromatin granulation, whereas the crusty cells nuclei contain coarse granules of heavily stained chromatin lying in close proximity to the nuclear membrane. Later, Allen (1918, cited by Donnel *et al.*, 2006) devised another terminology that persists until today; the cells equivalent of the dusty were named

"sprmatogonia type A" while the crusty cell were termed "spermatogonia type B". In case of rat, spermatogonia with nuclear characteristics intermediate between type A and type B can be identified principally on the basis of fine plaques of chromatin present closer to the nuclear membrane; named therefore intermediate spermatogonia (Clermont and Leblond, 1953). Later studies in rat showed that based on nuclear morphology, three types of spermatogonial cell types are usually present which include: (i) four classes of type A spermatogonia, (ii) the intermediate spermatogonia and lastly, (iii) type B spermatogonia (Clermont, 1962). Similar subtypes can also be identified in other species such as the mouse (Oakberg, 1956), ram (Ortavant, 1959), bull (Hochereau, 1968), and guinea pig (Clermont, 1960) with the number of generations of spermatogonia varying significantly (Clermont, 1972; de Rooij *et al.*, 2000).

Light microscopic examination of spermatogonia demonstrate that they have a poorly staining cytoplasm, while whole mounts of seminiferous tubules show that they remain connected by intercellular bridges such that large numbers are effectively linked together (Fawcett *et al.*, 1959; Huckins, 1971; Dym and Fawcett, 1971). Since spermatogonia act as stem cells for spermatogenesis, they are usually found at sites closer to the basal lamina to allow formation of the germ cell clones. In the adult testis these clones are histologically recognized as different stages of the spermatogenic cycle during testicular maturation. Initially, during the process of maturation the spermatogenesis is asymmetrical but becomes uniformly distributed around the circumference of the entire tubule at later stages of development. Similar asymmetry first, and then symmetrical arrangement of spermatogonial cells has also been demonstrated after spermatogonial transplantation (Parreira *et al.*, 1998).

Being mobile structures, moving at the rate of 60 μm per day along the length of the recipient tubule, spermatogonia support early spermatogenesis (Nagano *et al.*, 1999). As Sertoli cells accommodate a finite number of spermatogonia along the basal lamina, spermatogonia find preferential sites within the tubules, suggesting that spermatogina establish separate niches in association with Sertoli cells (Meachem *et al.*, 2001; Shinohara *et al.*, 2001; Shinohara *et al.*, 2002; Ryu *et al.*, 2003). The spermatogonia are located at a basal position within the epithelium developing

extensive contact with the tubular basement membrane (Vilar *et al.*, 1962; Nicander *et al.*, 1961). The degree of contact with the basement membrane decreases and finally all contact is lost upon transformation of type B spermatogonia into prelepotene primary spermatocytes (Rowley *et al.*, 1971). Spermatogonia are remained connected by intercellular bridges due to the incomplete cytokinesis occurring during mitosis. These bridges which are 2 to 3 μm in width and usually do not contain organelles or microtubules were originally identified by Watson, (1952). They are limited by the cell membrane, which is more electron-dense in this region, and separated from the adjacent Sertoli cell membrane by an intercellular space of approximately 200 A^{o} (Dym and Fawcett, 1971; Moens *et al.*, 1972).

1.2.2 Spermatocytes

The germ cells that undergo meiotic divisions are the primary and secondary spermatocytes (Clermont, 1960). These pass through two meiotic divisions; in the first, primary spermatocyte chromosomes appear as pairs of chromatids. Heterologous chromosomes then pair by synapsis to form bivalents. Each member of the bivalent pair subsequently moves to the daughter cells, termed secondary spermatocytes that contain haploid number of chromosomes. The total DNA content is however equivalent to that of somatic cells because each chromosome is composed of a pair of daughter chromatids, After a relatively short duration, the second meiotic division results into separation of the chromatids of each chromosome to move into daughter cells in a pattern similar to that of mitotic division. The daughter cells now called spermatids, contain the haploid number of chromosomes and half the DNA content of somatic cells (Kerr *et al.*, 2006).

1.2.2.1 Primary spermatocytes

The primary spermatocytes arising from type B spermatogonia are characterized by spherical nuclei with features similar to the type B spermatogonia lacking any details of chromosomal structure. At this stage they are termed preleptotene spermatocytes and are actively engaged in DNA synthesis (Swift, 1950), the mechanism by which each chromosome, when it condenses is composed of a pair

of chromatids, the total DNA content representing twice the diploid content (Kerr *et al.*, 2006).

Montogomery (1901, cited by Kerr *et al.*, 2006) showed that during the first meiotic division, distinct pairs of chromosomes were visible in primary spermatocytes and suggested that each pair was composed of a chromosome of maternal or paternal origin. Their pairing was originally suggested to be end to end (Montogomery, 1901; Sutton, 1903) but was subsequently shown to be side to side (Winiwater, 1901) (references cited by Kerr *et al.*, 2006).

The prophase of the first meiotic division (prophase I) is characteristically of longer duration. During this stage, the primary spermatocytes show condensation of chromosomes which in the leptotene stage, appear as single filamentous strands attached at each end to the nuclear membrane (Wettstein and Sotelo, 1967). Although at this stage the chromosomes are already composed of two chromatids, these do not become evident until later in prophase. The zygotene stage is characterized by a further thickening of the chromosomal elements to commence the process of synapsis. The mechanism whereby homologous chromosomes recognize each other to pair as bivalents depends on the chromatin organization that facilitates recognition of homologous sequences on each chromosome (Kerr *et al.*, 2006).

The pachytene stage is marked by the completion of synapsis. Here further thickening and shortening of the chromosomes occur. At this stage the chromosomes appear as paired structures (Painter, 1923). It is during his stage the exchange of chromosomal material between maternal and paternal homologous chromosomes occurs by crossing over, with the chromosomes linked at such sites by chiasmata. Nuclear and cytoplasmic growth occurring at this stage causes these cells to become the largest of the germ cell line. The paired chromosomes partially separate but remain joined at chiasmata as desynapsis occurs during the next phase, the diplotene. In the last phase termed diakinesis, further shortening of chromosomes occurs and they detach from the nuclear membrane. Each chromosome composing of two chromatids can now be seen (Kerr *et al.*, 2006).

Diakinesis is the immediately followed by dissolution of the nuclear membrane, appearance of the spindle, and the attachment of the bivalents to the equator of the spindle during. This stage is characterized as metaphase I. Next, anaphase I results in the movement of the members of each bivalent to opposite poles of the spindle resulting ultimately into daughter cells, termed secondary spermatocytes. These contain haploid number of chromosomes, each constituting of two chromatids. As with other cell divisions within the seminiferous epithelium, cytokinesis is incomplete, and the secondary spermatocytes remain joined by intercellular bridges. Primary spermatocytes are joined to each other by intercellular bridges similar to those found between spermatogonia. They are separated from adjacent Sertoli cells by a distinct intercellular space that is modified in some regions by desmosome-like structures (Kaya and Harrison, 1976; Russell, 1977).

1.2.2.2 Secondary spermatocytes

Secondary spermatocytes were first described by von Ebner (1888, cited by Kerr *et al.*, 2006). They undergo second meiotic division. These cells have a short life span before they complete meiosis to form spermatids and are therefore relatively infrequently found in histological sections of the testis (Heller and Clermont, 1964). The secondary spermatocytes have haploid number of chromosomes, an observation first made by Montgomery (1912, by Kerr *et al.*, 2006). Although their DNA content is still diploid and but when they complete meiosis the resultant spermatids have both the haploid DNA and chromosomal content. Secondary spermatocytes are spherical, intermediate in size between primary spermatocytes and spermatids and are situated closer to the lumen of the seminiferous tubules. Their spherical nuclei contain a homogeneous chromatin network throughout which are dispersed large globular chromatin masses. Nucleoli are often centrally placed. Light and electron microscopic studies have shown that these cells are joined by intercellular bridges identical to those found between other germ cells (Nicander, 1967; Dym and Fawcett, 1971; Holstein and Roosen-Runge, 1981).

1.2.3 Spermatids

Spermatids are formed from the secondary spermatocytes. von La Valette and St. George (1885, cited by Kerr *et al.*, 2006) were the first who described these cells. The process of spermiogenesis transforms the spermatids into spermatozoa. This transformation involves a complex sequence of events and because no cell division is involved, it is essentially a metamorphosis in which a conventional cell is converted into a highly organized motile structure. Although the major features of spermiogenesis are common to all species, the details differ in each species due to the distinguishing morphological features between spermatozoa as determined by genetic features. Ultrastructural studies have shown that the changes can be grouped into; (i) formation of the acrosome, (ii), nuclear changes (iii), development of the flagellum (iv), reorganization of the cytoplasm and cell organelles, and (v) spermiation relationships of the Sertoli cells and spermatids (Kerr *et al.*, 2006).

Newly formed spermatids are spherical and are smaller in size than the secondary spermatocytes and are normally found at the luminal aspect of the seminiferous epithelium. They have centrally positioned spherical nuclei, a well-developed Golgi complex adjacent to which are present the centrioles. The mitochondria are dispersed and lie at the periphery near the plasma membrane. In addition, the chromatoid body, a chromophilic electron-dense mass, can be observed lying adjacent to the Golgi complex at a more perinuclear location (Leblond and Clermont, 1952; Daoust and Clermont, 1955).

1.3 The Sertoli cell

Enrico Sertoli (1865, cited by Kerr *et al.*, 2006) was the first who identified these cells as individual elements extending from the basement membrane to lumen of the seminiferous tubules, enveloping clusters of associated germ cells. The Sertoli cells are situated along the basal lamina of the seminiferous tubules. Their basic function is to create an appropriate microenvironment for the development of germ cells (Li and Heindel, 1998). The Sertoli cell is responsible for orchestrating germ cells through sequential phases of mitosis, meiosis and differentiation. Clones of germ cells then pass through several stage specific cell associations until the elongated

spermatids are released into the lumen of the seminiferous tubule, a process called spermiation. The Sertoli cell is a fundamental component of the architectural structure of the seminiferous epithelium providing physical support to the germ cells, which are enveloped in the Sertoli cell cytoplasm. The tight junctions between the Sertoli cells make up the blood-testis barrier that forms, (i) a basal compartment containing spermatogonia and early spermatocytes and, (ii) an adluminal compartment isolating the spermatocytes and the spermatids from surrounding tissue and the blood stream. Synchronized 'lifting' of early meiotic spermatocytes through the tight junctions from the basal compartment to the adlumininal compartment is another important function of the Sertoli cell. Furthermore, Sertoli cell is also responsible for providing nutrition to the germ cells by transporting sugars, amino acids, lipids and metallic elements. Sertoli cells also secrete inhibin, androgen binding protein, sulphated glucoprotein 1 and 2, and metal carrier proteins, paracrine factors of prime importance for spermatogenesis (Clermont, 1993). Lastly, the Sertoli cell also bears phagocytotic properties and eliminates dead germ cells as well as residual bodies and the remains of the cytoplasm of the released spermatids (Russell and Sinha Hikim, 1995).

1.4 The Leydig cell

Interstitial Leydig cells are the chief source of testicular androgens (Christenson and Mason, 1965; Hall *et al.*, 1969) and are the predominant site for steroidogenic enzymes (Wattenberg, 1958; Levy *et al.*, 1959). They are located in clear spaces separating individual seminiferous tubules. Leydig cells together with other constituents are found closer to the blood vessels thereby facilitating the passage of steroids into circulation (Fawcett *et al.*, 1970). Leydig cells usually display round or irregular cell shapes but adopt elliptical profiles when present close to blood vessels or to the tubule (Schulze, 1984). Leydig cell nuclei are often eccentrically placed with heterochromatin associated with the inner nuclear envelop. Smooth endoplasmic reticulum, which provides binding sites on its surface for numerous enzymes necessary for steroidogenesis is the dominant cytoplasmic organelle of the Leydig cells, most often showing great diversity of structure (Kerr *et al.*, 2006).

Leydig cell mitochondria are of variable in size in a given cell and also between different species (Christensen, 1975). Within mitochondria, side chain of

cholesterol is known to occur possibly on the surface cristae (Prince, 1999). The correlation that exists between testosterone secretion and the amount of smooth endoplasmic reticulum and Golgi membranes indicates the central role played by these organelles in determining the secretory capacity of a single Leydig cell (Ewing *et al.*, 1979).

1.5 The cycle of the seminiferous epithelium

Spermatogenesis in any given area within the seminiferous tubules proceeds in a characteristic cyclic pattern whereby, a well-defined series of events occur that follow a precise and orderly sequence. The events are extremely well-timed and occur at intervals with respect to one another giving rise to a precise number of distinct cellular associations, each consisting of one or two generations of spermatogonia, spermatocytes and spermatids. According to Clermont (1972), "the sequence of events occurring from the disappearance of given cellular association to its reappearance constitutes one cycle of the seminiferous epithelium".

The spermatogenic process comprising the organization of cell types within the seminiferous epithelium is highly organized (Regaud, 1901, cited by Kerr et al., 2006). The germ cells at different developmental phases form easily identifiable collections are termed "cell association". Leblond and Clermont (1952) divided the process of spermatogenesis in the rat into 14 stages or cell associations using the periodic acid–Schiff reaction to stain the acrosome of spermatids together with nuclear morphology. The complete sequence of 14 stages or cell associations constitute one cycle of the seminiferous epithelium (Fig. 1.1).

1.6 Wave of the seminiferous epithelium

Different stages of the seminiferous cycle are distributed in an orderly sequence along the length of the seminiferous tubule. The distribution of cellular associations at any given time is responsible for generation of the wave of the seminiferous epithelium (Curtis, 1918, cited by Kerr *et al.*, 2006; Perey *et al.*, 1961; Courot *et al.*, 1970). The typical arrangement of cellular associations along the length of rat seminiferous tubule is shown in Fig. 1.2.

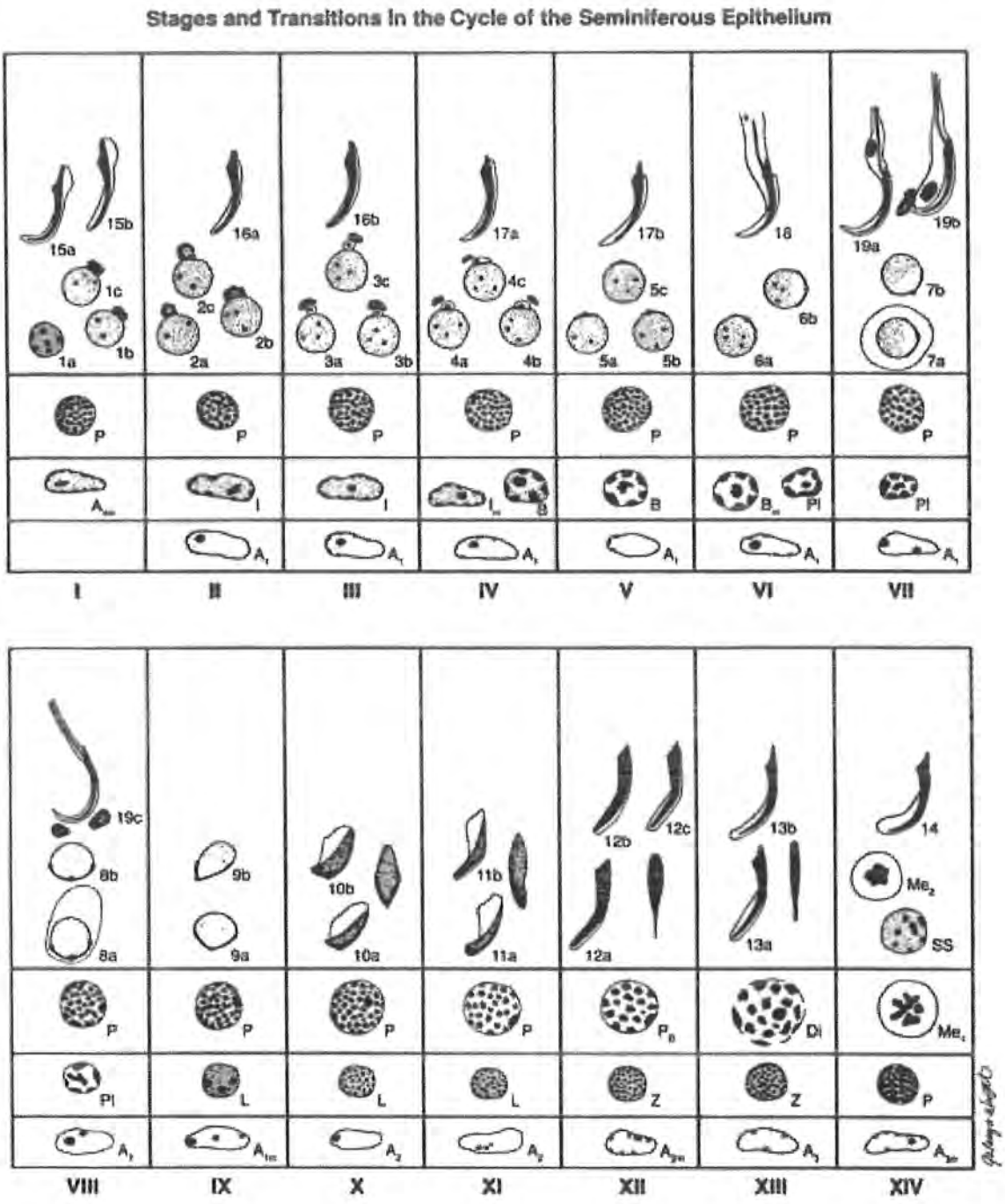

Figure 1.1 The 14 stage cycle of rat seminiferous epithelium (Taken from Leblond and Clermont, 1952).

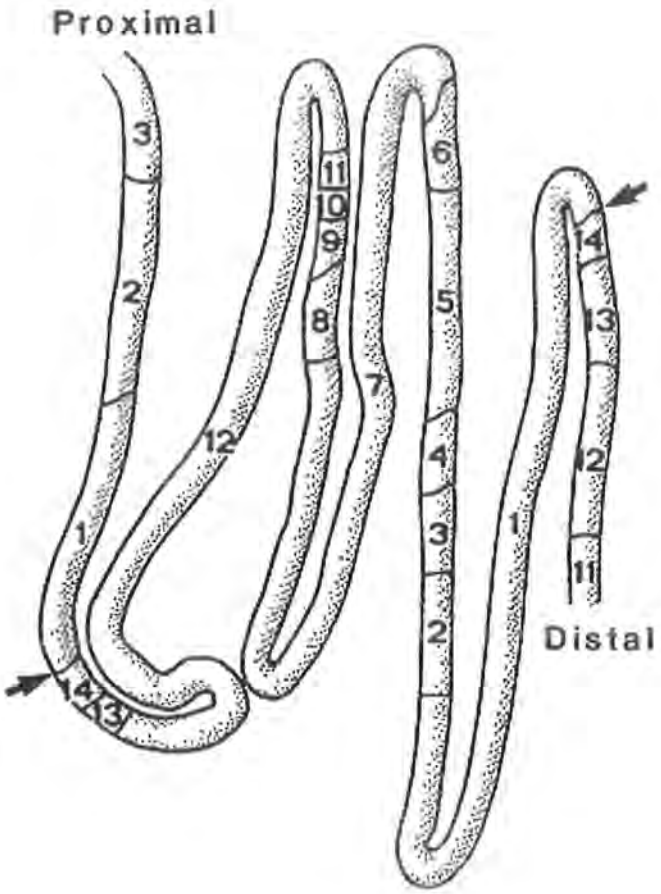

Figure 1.2 Stages of spermatogenesis (spermatogonial wave) as they occur along the tubule (Taken from de Kretser and Kerr, 1994, in "The Physiology of Reproduction" Ed E Knobil and Neill, 2006).

1.7 Seminal vesicles

The seminal vesicle is an accessory sex gland and is composed of tubular alveoli. Its mucosa is thrown into a complex system of folds whereby the epithelium is present over the lamina propria (Gonzales, 1989). Conversion of testosterone to dihydrotestosterone (DHT) as a result of alpha-reductase activity occurs in seminal vesicles. Localization of the LH/hCG receptor makes seminal vesicle a potential target for direct regulation by LH (Tao *et al.*, 1998). The sex differentiation of the seminal vesicle and its growth are both androgen dependent (Higgins and Burchell, 1978; Lieber *et al.*, 1980). In men the secretory activity of the seminal vesicle has

been found to be directly proportional to serum testosterone (Gonzales, 1994). Similarly in rat, an increase in serum testosterone or treatment with androgens also increases the secretory activity of seminal vesicle (Higgins and Burchell, 1978; Fawell and Higgins, 1984; Zanato *et al.*, 1994), resulting into increased seminal vesicle weight (Almenara *et al.*, 2000).

The secretory proteins and the constituents of the seminal vesicle are well characterized and are considered to be important for sperm motility and metabolism. These include fructose and prostaglandins (Luke and Coffey, 1994); the former is considered to be a marker for seminal vesicular function. The measurement of fructose is therefore included by WHO as a measure of function of these glands (WHO, 1999). Notably, there exists an inverse relationship between the sperm count and the concentration of fructose (Gonzales and Villena, 2001). The inverse correlation between seminal fructose and motile sperm suggests that only motile sperms consume fructose after ejaculation) by a process known as fructolysis (Lewis-Jones *et al.*, 1996). Accordingly, at higher sperm counts, the concentration of fructose is lower explaining why azoospermic and oligozoospermic men have a higher concentration of fructose as compared to normozoospermic or polyzoospermic men. However, other studies in contrast do not regard fructose concentration to be a very reliable source of function of seminal vesicle since these have been unable to find a direct correlation between fructose concentration and sperm motility (Pahdke *et al.*, 1973; Biswas *et al.*, 1978; Gonzales *et al.*, 1988). Nonetheless there exists evidence which suggests that the seminal vesicles are important for sperm motility (Gonzales, 1989). Moreover in humans, seminal vesicle is the source of nitric oxide synthase and the secretion of fructose by the gland may be improved by an increase in nitric oxide production (Zini *et al.*, 2001).

1.7.1 Histology of seminal vesicle

The seminal vesicles are elongated saccular organ with numerous lateral outpocketings from an irregularly branched lumen. They arise as evaginations of the ductus deferens. The wall consists of an external connective tissue layer rich in elastic fibers, a middle layer of smooth muscle and an epithelium resting upon a layer of loose connective tissue. The mucosa forms an intricate system of thin, primary folds,

which branch into secondary and tertiary folds. These project far into the lumen and anastomose frequently. In this way numerous cavities in different sizes are formed, separated by thin branching partitions. All of these cavities open into central cavity, but in sections many of them may seem to be isolated (Bloom and Fawcett, 1976).

The epithelium is pseudostratified and consists of rounded basal cells lodged between larger cuboidal or low columnar cells. The epithelial cells contain numerous secretion granules. The secretion of seminal vesicle is a slightly yellowish, viscid liquid. In sections it appears as coagulated, deeply staining masses in the lumen. The muscular wall of the seminal vesicles is provided with a plexus of nerve fibres and contains small sympathetic ganglia (Bloom and Fawcett, 1976).

1.8 Prostate gland

The prostate gland, a chestnut shaped organ surrounding the base of urethra is a hormone-dependent accessory sex gland (Sugimura *et al.*, 1986; Cunha *et al.*, 2002). It varies among different animal species in its anatomy, biochemistry and pathophysiology. It is known that smooth muscle of the prostate gland helps in semen expulsion (Anderson *et al.*, 2006). Mammalian prostate is a glandular organ comprising of epithelial and stromal cells, the activities of which are regulated by a number of hormones such as steroids, prolactin, growth factors, neuropeptides and biogenic amines (Lee *et al.*, 1997; Hedlund *et al.*, 1997; Reiter *et al.*, 1999). It secretes a clear or milky alkaline fluid of pH 7.29, which is discharged by the excretory duct in the prostatic urethra at the time of emission of semen. About 10-30% of the volume of seminal fluid is contributed by the prostate. Together with spermatozoa it constitutes the semen. The acidity of the vaginal tract is neutralized by alkalinity of the seminal fluid thus prolonging the lifespan of the sperm. Seminal plasma contains a very high concentration of zinc, citric acid, fructose, phosphorylcholine, spermine, free amino acids, prostaglandins and various enzymes; most of these are contributed by prostate (Luke and Coffey, 1994).

Human and rodent prostate are although very different anatomically, at cellular level they are quite similar. A pseudostratified epithelium lines the ductal gland that consists of distinct cell types, the secretory and basal cells (McNeal, 1968;

Hayward *et al.*, 1996; El-Alfy *et al.*, 1999). Neuroendocrine cells are also present but are rare and scattered throughout the acini and ducts (di Saint' Agnese and Cockett, 1996). The exocrine portion of the prostatic epithelium is made by the columnar shape secretory cells that synthesize and secrete proteins such as prostate-specific antigen (PSA) and prostatic acid phosphatase (PAP) into the ductal network and lumen. The apical portion of secretory cells faces lumen while the basal aspect is towards the basla cells and the basement membrane (McNeal, 1968; 1981; 1988).

Flattened, non-secretory epithelial cells, called basal cells, are present below the secretory cells. They are androgen independent yet they do respond to androgens (De Marzo *et al.*, 1998). Although the exact function of these cells is not known, they are believed to play a role in modulation and mediation of endocrine, paracrine and other regulatory functions (El-Alfy *et al.*, 2000). In humans, they form a bordering around the basement membrane (Fawcett and Keynes, 1986), while in other animal species they are scattered in appearance (Fawcett and Keynes, 1986; Gartner and Hiatt, 1997) as indicated by their ratio to that of the luminal cell, which is 1:1 in human, 1:7 in mouse, dog, monkey and rat (El-Alfy *et al.*, 2000).

1.8.1 Macroscopic description of the rat prostate

The prostate gland of rat is present around its urethera, and unlike the human prostate, it presents a lobar organization (Jesik *et al.*, 1982). It constitutes of three lobes that, according to their position around the proximal region of the urethra, can be designated as ventral, dorsal, and lateral lobes. The three pairs of lobes are connected to the urethra by connective tissue and the ductal excretory system. Each lobe is composed of a complex system of ducts proximally joining to the urethra and distally finishing in many secretory acini that divide into branches and are present in close proximity close to the prostate capsule (Fig. 1.3).

The individual lobes do not encircle the urethra completely (Cunha *et al.*, 1987), explaining why rodents, unlike humans, do not suffer symptoms of the lower urinary tract due to enlargement of the prostate (Maini *et al.*, 1997). All the components of the prostate are surrounded by a thin connective tissue capsule. Since anatomic distinction between the dorsal and lateral lobes is not discernible, these

lobes are considered as a single element, the dorso-lateral lobe. Histologically, the glandular component of rat prostate has tubo-alveolar type appearance. All the tubo-alveoli from a lobe drain through a number of excretory ducts (Hayashi *et al.*, 1991; Timms *et al.*, 1994; Kinbara and Cunha, 1996).

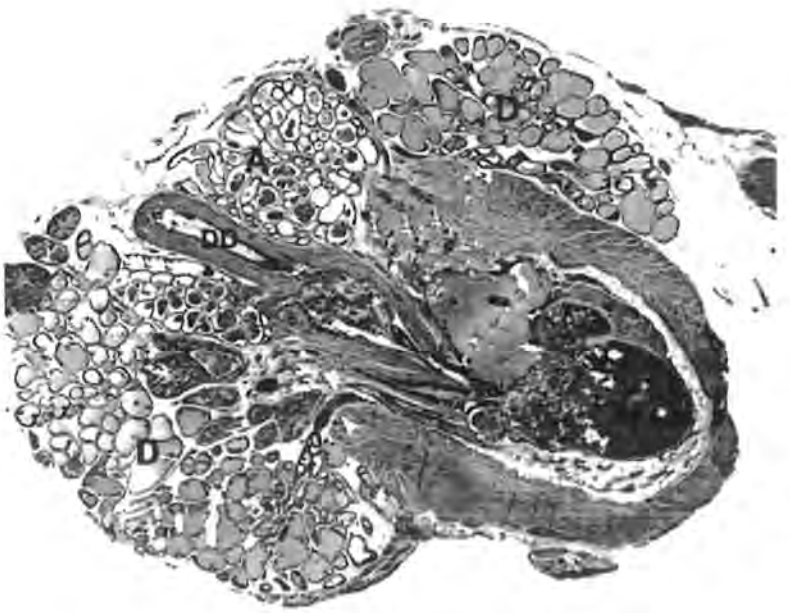

Figure 1.3 Transverse section of rat prostate showing: ampular region (A); dorsolateral region (D) and deferent duct (DD) (Taken from Ingelmo and Santamaría, 2007).

The ventral and lateral lobes drain into the urethra by means of two or three principal ducts, which show a so-called "oak tree" branching pattern (Sugimura *et al.*, 1986). The ducts from lateral lobes have two regions, namely: type I, formed by 5-7 long ducts that spread cranially toward the seminal vesicles and, type II formed by 5-6 short ducts that branch out caudally to the neck of the urinary bladder. The ventral lobe shows 2-3 pairs of thin ducts originating in the central portion of every lobe and following a parallel course to the layers of smooth muscle in the wall of the urethra

(Hayashi *et al.*, 1991; Timms *et al.*, 1994; Kinbara and Cunha, 1996). The dorsal lobes drain to the urethra with 10–14 narrow ducts (5–6 for each side) having a mixed morphology between acinus and duct. The more posterior acini of the dorsal lobes lead into the medial zone of the urethra by four or five ducts. The remaining acini drain by means of ducts that penetrate into the roof of the dorsal urethra (Hayashi *et al.*, 1991; Timms *et al.*, 1994; Kinbara and Cunha, 1996). These ducts have a "palm tree" branching pattern (Sugimura *et al.*, 1986).

1.8.2 Anatomic relationships of the prostate

Rat prostate is present in intimate anatomic relationships with several other structures that include; the ampular glands, the seminal vesicles, the coagulating glands, the deferent ducts, the ureters, the urinary bladder, and the urethra. The ampular glands surrounding the distal portion of the deferent ducts (Fig. 1.3) are considered integrating part of the prostate because their secretion contributes to the composition of the prostatic fluid (Ingelmo and Santamaría, 2007).

1.8.3 Histology of rat prostate

The rat prostate is composed of two components, epithelial and stromal, which vary in proportion across species. In the adult rat, the ratio of stroma to epithelium is 1:5, while in the human prostate the stroma and the epithelial cells are present in equal proportion (DeKlerk and Coffey, 1978; Bartsch and Rohr, 1980).

1.8.3.1 Histology of the acini

Acini are the sceretory units of the prostate (Nemeth and Lee, 1996). The ventral acini are highly contorted structures, especially the peripheral units located near the prostate capsule. These show abundant circumvolutions and are smaller than the central acini situated near the urethra. Stroma made up of loose connective tissue surrounds the acini. The luminal secretion of the acini is pale and eosinophilic. The epithelial cells lining the ventral acini showing basophilic cytoplasm are predominantly columnar in shape, and are intermingled occasionally with the cuboidal cells. Basal cells, located between the basal membrane and the columnar cells show an irregular stratum. The basal cells are cubic or flattened; with ovoid

nuclei and scant cytoplasm that does not reach the acinar lumen (Nemeth and Lee, 1996; Arriazu *et al.*, 2005).

The acini of the lateral lobe are comparatively bigger than those of the ventral lobe, variable in size, and highly convoluted in shape. The acinar secretions are intensely eosinophilic. The epithelial cells are cuboidal or columnar, containing centrally positioned nuclei. The acini from dorsal lobes are less contorted than the ventral and lateral ones and are loosely distributed within the stroma. The luminal secretions present an intermediate staining between those seen with the ventral and lateral lobes. The secretion is characterized by intense eosinophily and the presence of nonstained holes (bubbles) (Ingelmo and Santamaría, 2007) (Fig. 1.3).

1.9 Rat hypothalamic-pituitary-testicular axis

The primary initiator of puberty onset is undoubtedly the central nervous system (CNS). This is evidenced by the observations that include prepubertal changes in the shape of GnRH secreting neurons, GnRH release, the concentration of neurotransmitters and other trophic molecules within the hypothalamus that regulate GnRH release and, that prior to puberty the male rat is fully capable of responding to GnRH with robust increases in LH and subsequently testosterone and finally, the fact that human chorionic gonadotropin (hCG) fully stimulates steroidogenesis at prepubertal age (Cicero *et al.*, 1986).

1.9.1 Gonadotropin-releasing hormone

GnRH is secreted in a pulsatile manner from the median eminence of the hypothalamus into the hypophyseal portal vessels and in turn, stimulates the release of LH and FSH from the pituitary gland. These processes are controlled by the size and frequency of GnRH pulses, as well as by feedback from androgens and estrogens. Low-frequency GnRH pulses lead to FSH release, whereas high-frequency GnRH pulses stimulate LH release (Dalkin *et al.*, 1989).

1.9.2 Luteinizing hormone (LH) and its receptor

Luteinizing Hormone (LH) is a member of a large family of glycoprotein hormones. This family includes follicle stimulating hormone (FSH), thyroid stimulating hormone (TSH) and human chorionic gonadotropin (hCG) (Pierce and Parsons, 1981). These glycoprotein hormones are each composed of two noncovalently linked subunits, termed the α- and β-subunits. The α-subunit is common to all glycoprotein hormones in the same species. However, the β-subunit varies between glycoprotein hormones and confers hormone specific bioactivity (Catt and Dufau, 1991).

LH is synthesized by the pituitary gonadotropes and released in a pulsatile manner in response to pulses of GnRH. GnRH is delivered to the anterior pituitary via the hypothalamo-hypophyseal portal system (Yen and Jaffe, 1978). The synthesis and release of pituitary gonadotropins are regulated by feedback mechanisms involving the gonadal steroids and peptide hormones (Ying, 1988). LH mainly regulates testosterone production by testicular Leydig cells. Hypophysectomy or reduction of endogenous LH levels by treatment with GnRH antagonists or antibodies results in reduced amounts and activities of steroidogenic enzymes in adult Leydig cells (Lejeune *et al.*, 1998).

LH binds to a specific receptor on Leydig cell memebrane to regulate steroidogenesis. The LH receptor is a member of the G protein-coupled pituitary glycoprotein subfamily of transmembrane receptors (Segaloff and Ascoli, 1993). LH receptors are known to be expressed on Leydig cell surfaces during fetal development, in early postnatal life and from puberty through adult life (Dufau, 1988; Catt and Dufau, 1991; Saez, 1994).

1.9.3 Follicle stimulating hormone (FSH) and its receptor

FSH secretion increases prior to the puberty in the male rat and is known to play vital role in puberty. FSH secretion rises during early postnatal life, reaches a maximum between PND 30 and 40, and falls gradually as testosterone secretion increases, to remain low throughout adulthood (Ketelslegers *et al.*, 1978; Matsumoto

et al., 1986). A maximum release of FSH in response to GnRH is observed between PND 25 and 35 (Dullaart, 1977). FSH induces an increased synthesis and secretion of several Sertoli cell proteins including the inhibin, transferrin and androgen binding protein (Santen, 1995). The hormone inhibin, which is secreted by the seminiferous tubules and inhibits FSH release, plays a role in the increase in serum FSH during puberty. There is an inverse relationship between inhibin levels and serum FSH, with an increase in inhibin from PND 3 to 20 and a decrease at PND 25 (Saito, 1995; Sharpe *et al.,* 1999). FSH binds to receptors located on Sertoli cells to facilitate spermatogenesis at puberty (Steinberger, 1976). It has also been shown to enhance the production of steroid biosynthetic enzymes (Murono and Payne, 1979). Like LH, this gonadotropin is produced and secreted by the pituitary gland as a highly heterogeneous glycoprotein (Moyle and Campbell, 1995). FSH receptors are localized exclusively in the gonads. The FSH receptor belongs to the family of G protein-coupled receptors (Gudermann *et al.,* 1995).

1.9.4 Androgens and androgen receptor

Crucial to the development of the male reproductive tract, the feedback inhibition of the HPG-axis, maintenance of the sex accessory organs, the stimulation and maintenance of spermatogenesis during puberty are a group of steroidogenic hormones called "androgens". Testosterone is one of the major androgens and its presence testosterone is necessary for development of the testes, epididymes, vasa deferentia, seminal vesicles, levator ani/bulbocavernosus (LABC), and other muscles. It is also responsible for stimulating the inguinoscrotal descent of the testes that occurs in rat on PND 15. In comparison, DHT, another androgen, initiates postnatal regression of nipples/areolas and is a key hormone in the development and maintenance of the prostate, urethra, external genitalia and preputial separation (Luke and Coffey, 1994). Testosterone is synthesized and released from fetal Leydig cells during the sex-differentiation of the male fetus. It stimulates the development of the Wollfian ducts to mature into the epididymes, vas deferens, and seminiferous tubules (MacLaughlin and Donahoe, 1998). Testosterone is important for the release of step 19 spermatids from the spermatogenic epithelium into the lumen of the seminiferous tubule. Testosterone is although involved in spermatogenesis, however it appears not

crucial for the spermatogenesis as spermatogenesis continues in adult males after withdrawal of testosterone but at a lower level (Billig *et al.*, 1995).

Testosterone actions are mediated through the androgen receptor that to regulate male sexual development. Testosterone and DHT are the two androgens that bind with highest affinity to the androgen receptor and are the most biologically active forms. Although their affinity to the receptor is similar, the kinetics of dissociation of testosterone and DHT are very different, with the dissociation of testosterone about three times faster than DHT. These differences appear to be due to the fact that most of the testosterone-sensitive tissues in the reproductive tract are derived from the Wolffian duct and are present in close proximity to the testes where there is a higher concentration of testosterone and very low 5 α-reductase activity in the Wolffian duct before puberty (George and Wilson, 1994).

At puberty onset, the GnRH neurons in the male rat undergo morphological changes whereby there occur an increase in the proportion of cells with spiny processes relative to the smooth processes seen prior to puberty (Wray and Hoffman, 1986). As it has been shown that spiny GnRH neurons have a greater number of endings (Jennes *et al.*, 1985), which leads to an enhancement of the pubertal rise of gonadotropin secretion increase in the number of synapses on the cells, appear to be puberty-related. This rise in gonadotropin secretion subsequently stimulates testes growth and maturation. The pulsatile release of GnRH also shows a doubled pulse frequency between the infantile (15 days) and the peripubertal periods (50 days) in the male rat (Bourguignon *et al.*, 1994). The initiator of this increased pulsatility has sometimes been termed the "GnRH-pulse generator", which signifies a network of neurons that are involved in the coordinated synchronous pattern in which GnRH cells discharge their products into the hypophyseal portal blood (Evans and Karsch, 1995). Several observations suggest that this increase in frequency prior to puberty may be due to a combination of changes that take place in neuronal inputs, with "activation of excitatory" or "deactivation of inhibitory" inputs to GnRH neurons (Ojeda and Urbanski, 1994). Among the numerous cell types in the central nervous system that control GnRH neurons, three stimulatory and two inhibitory neurotransmitter systems have been shown to play predominant roles (Crowley *et al.*, 1995).

1.10 LHRH neurons and their transsynaptic control

The soma of most LHRH neurons has a smooth surface during the neonatal infantile periods but LHRH cells with an irregular surface become predominant between weeks 4 and 5 of postnatal life (Wray and Gainer, 1987). Since in the prepubertal rat the total number of LHRH cells do not change despite an increase in the number of spiny cells, evidently smooth LHRH cells are transformed into spiny ones. These morphological changes may reflect an increase in the number of synaptic contact between controlling neuronal networks and LHRH neurons (Jennes *et al.*, 1985).

The qualitative or quantitative changes in synaptic input to LHRH neurons might contribute to at least two events taking place during juvenile development; (i) the prepubertal increase in responsiveness of the hypothalamic pituitary unit and, (ii) the increased capacity of LHRH neurons to release LHRH in response to excitatory amino acids. The cell-cell communication mechanisms that operate in the mature hypothalamus become firmly established during juvenile development and the LHRH neuronal network begins to operate under a dual inhibitory and facilitatory transsynaptic control (Ojeda and Skinner, 2006).

1.10.1 Inhibitory neurotransmission

1.10.1.1 Gamma aminobutyric Acid

γ -Aminobutyric Acid (GABA) is the dominant inhibitory neurotransmitor in the hypothalamus (Decavel *et al.*, 1990). It is synthesized from glutamate via a decarboxylation reaction catalyzed by two forms of the enzyme glutamic acid decarboxylase (GAD). Both the abundance of the mRNAs encoding these two forms (GAD-65 and GAD-67) and GABA concentrations themselves increase in the rat preoptic area (POA), first between neonatal and infantile development (Flügge *et al.*, 1986; Davis *et al.*, 1996; Davis *et al.*, 1999) and then again during the juvenile period (Goroll *et al.*, 1994; Roth *et al.*,1998).

1.10.1.2 Opioid Peptides

A role for endogenous opioides in puberty has been proposed due to the observations that opioid peptides suppress pulsatile LH release (Ferin *et al.*, 1982; Mallory *et al.*, 1989; Kesner *et al.*, 1986) and, that the opioid receptor antagonist naloxone counteracts the negative feedback effects of estrogen on gonadotropins in adult animals (Grosser *et al.*, 1993). In addition, naloxone stimulates LH release in both immature rat and sheep (Cutler *et al.*, 1985; Ebling *et al.*, 1989), and administration of naloxone during early post natal life elicits precocious puberty in female rats (Sirinathsinghji *et al.*, 1985).

1.10.2 Excitatory neurotransmission

1.10.2.1 Glutamatergic neurons

Glutamatergic neurons are considered to be major players among the neuronal systems involved in the excitatory control of LHRH secretion. The facilitatory control they exert on LHRH neurons increases gradually during the infantile-juvenile periods as indicated by the increasing ability of glutamate receptor stimulation to increase LHRH release during this phase of development (Bourguignon *et al.*, 1990).

1.10.2.1 Neuropeptide Y

The neropeptide Y (NPY) has also been implicated in the facilitatory transsynaptic control of rat puberty. For instance, the hypothalamic content of NPY increases during postnatal development of the rat and reaches maximal levels near the time of puberty (Sutton *et al.*, 1988; Corder *et al.*, 1992).

1.11 Metastin/Kisspeptin

About a decade ago, Lee and colleagues (1999) discovered a novel G protein-coupled receptor in the rat termed GPR54. The GPR54 gene encodes a G protein-coupled receptor that shares modest sequence homology with galanin receptors (Lee *et al.*, 1999). GPR54 has been shown to mediate the actions of a unique family of ligands known as kisspeptins (KP), which are derived from the *KISS1* gene. The *KISS1* gene encodes a 145-amino acid peptide that is cleaved into an amidated C-

terminal 54 amino acid product, known as kisspeptin-54 (KP-54) or metastin, now identified to be an endogenous ligand for GPR54 (Kotani *et al.*, 2001; Ohtaki *et al.*, 2001; Stafford *et al.*, 2002). Shorter fragments (*e.g.* kisspeptin-14, kisspeptin-13, and kisspeptin-10) of kisspeptin-54 are generated by further cleavage of the preprohormone. These also bind to GPR54 (Kotani *et al.*, 2001; Stafford *et al.*, 2002; Ohtaki *et al.*, 2001) (Fig. 1.4).

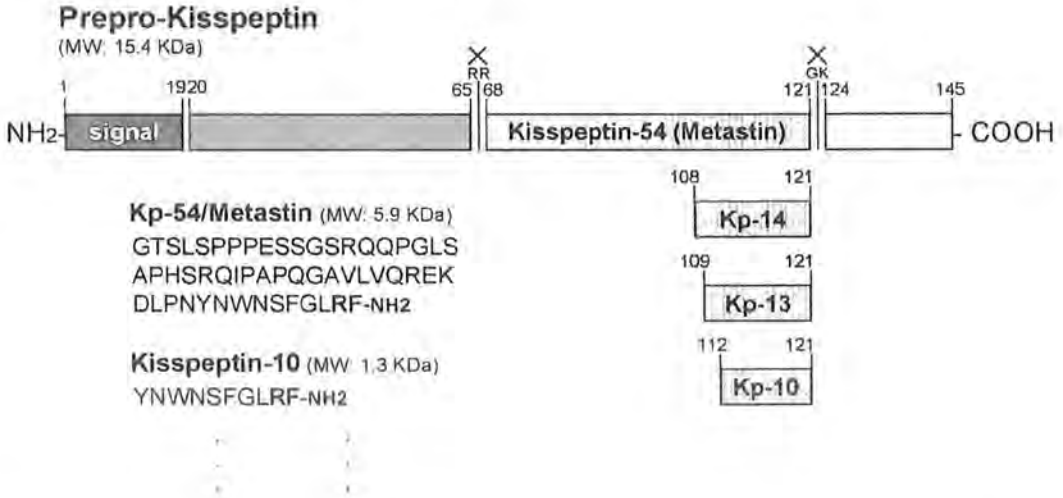

Figure 1.4 Structural features of kisspeptins, generated by cleavage form a common precursor, the prepro-kisspeptin. Prepro-kisspeptin, encoded by the *KiSS-1* gene, is a 145-amino-acid protein that contains a 19-amino-acid signal peptide and a central 54-amino-acid region, flanked by two consensus cleavage sites (denoted by X), which gives rise to metastin or kisspeptin-54. Further cleavage of metastin generates kisspeptins of lower molecular weight: kisspeptin-14 (Kp-14), Kp-13 and Kp-10. All kisspeptins are able to bind and activate GPR54. Besides general structural organization, the complete amino acid sequences of human metastin and kisspeptin-10 are shown. The consensus C-terminal RF-amide motif, hallmark of this peptide super-family, is indicated in bold (Taken from Tena sempere, 2006).

Kisspeptin-54 was originally identified as a metastasis suppresser peptide hence named metastin (Kotani *et al.*, 2001; Ohtaki *et al.*, 2001; Stafford *et al.*, 2002). Later, dysfunctional or deletional mutations in the gene encoding the G protein-coupled receptor, GPR54 were shown to be the cause of hypogonadotropic hypogonadism; a condition characterized by absent or delayed pubertal development

in humans and mice (de Roux *et al.*, 2003; Seminara *et al.*, 2003). Neurons that express kisspeptin are present in the arcuate nucleus (Arc), the periventricular nucleus (PeN), and the anteroventral periventricular nucleus (AVPV) in mice (Gottsch *et al.*, 2004, Smith *et al.*, 2005).

Expression of both the *Kiss-1* and *Gpr 54* mRNA is regulated developmentally as well as hormonally, with a sharp increase at prepubertal age in both male and female rats, changes throughout the estrous cycle in adult females, and increases after gonadectomy that is prevented by sex steroid replacement in both males and females (Navarro *et al.*, 2004a; Irwig *et al.*, 2004). Further evidence came from potent release of LH secretion by kisspeptin has been demonstrated in mice and rats, in both males and females, and in prepubertal, pubertal, and adult rats, as well as in a juvenile agonadal male monkey (Gottsch *et al.*, 2004; Navarro *et al.*, 2004a, b; Shahab *et al.*, 2005). Kisspeptin-54 stimulated secretion of both LH and FSH was shown to be blocked by pretreatment with acyline, a potent GnRH antagonist (Gottsch *et al.*, 2004). Furthermore, chronic central administration of kisspeptin to sexually immature female rats induced early vaginal opening, elevated uterus weight and increased level of serum LH and estrogen (Navarro *et al.*, 2004 b). Similarly, it was found that the transcriptional activity of *Kiss-1* neurons in the Arc is increased significantly after castration and inhibited by testosterone replacement. Thus these neurons act as targets for the negative feedback regulation of GnRH secretion by forebrain, whereas activity of the *Kiss-1* neurons in the AVPV and PeN is reduced with castration and stimulated by testosterone, implicating that they may mediate other testosterone-dependent processes (Smith *et al.*, 2005).

The binding of Kiss1 receptor to Kiss1 peptide leads to the activation of G protein-activated phospholipase C (PLCß), suggesting a Gαq/11-mediated signaling pathway (Kotani *et al.*, 2001; Muir *et al.*, 2001; Stafford *et al.*, 2002; Liu *et al.*, 2008; Constantin *et al.*, 2009) (Fig. 1.5). PLCß activation leads to the generation of the intracellular second messengers, inositol triphosphate (IP3) and diacylglycerol (DAG). These signaling molecules in turn mediate the intracellular Ca^{2+} release and activation of the protein kinase C (PKC), respectively (Stafford, *et al.*, 2002; Constantin *et al.*, 2009). Kisspeptin is thought to stimulate GnRH secretion by

activating transient receptor potential canonical (TRPC)-like channels and inhibiting inwardly rectifying potassium channels (Zhang *et al.*, 2008), likely mediated by DAG and/or Ca^{2+}. Additionally, Kiss1r has been shown to stimulate arachidonic acid release and ERK1/2 and p38 activation, as well as Rho activation, which causes stress fiber formation (Kotani *et al.*, 2001; Castellano *et al.*, 2006).

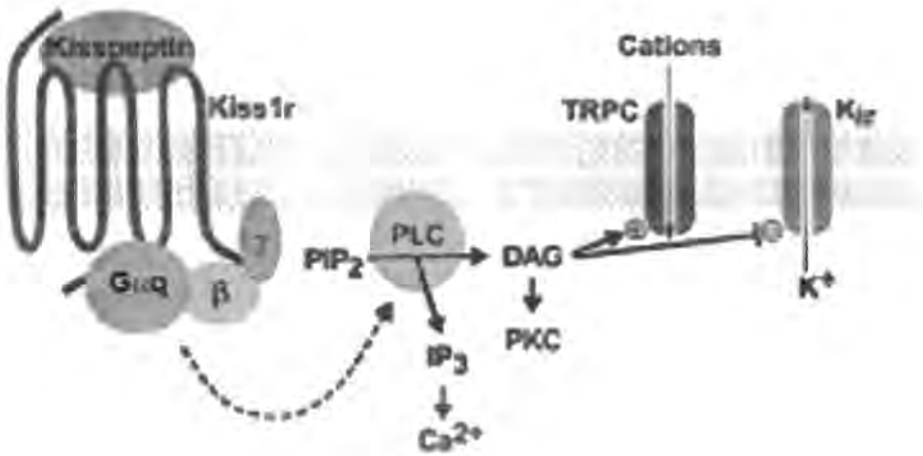

Figure 1.5 Proposed mechanism of neuronal depolarization by kisspeptin binding to its receptor, Kiss1r. Kisspeptin binding to its GPCR, Kiss1r activates the G protein, Gαq, and PLC to cleave phosphatidylinositol 4, 5-bisphosphate (PIP_2) into IP3 and DAG. DAG activates a signal cascade by activating PKC, whereas IP_3 mobilizes calcium ions (Ca^{2+}), which participate in the cascade by activating other proteins. Membrane depolarization is caused by activation (+) of nonselective TRPC cation channels and inhibition (–) of inwardly rectifying potassium channels (Kir), possibly through involvement of DAG (Taken from Oakley *et al.*, 2009).

Kisspeptin can activate a wide variety of signals via GPR54, which involve both typical G-protein (Gaq/11)-coupled cascades, such as PLC–PKC and intracellular Ca^{2+} mobilization, but also MAP kinases ERK1/2- and p38-related pathways, linked to GPCRs as well (Kotani *et al.*, 2001; Becker *et al.*, 2005). From the information gathered to date, it is now beginning to clear that activation of a specific set of interconnected signals is selectively triggered by kisspeptin via GPR54

in a cell type-dependent manner to precisely regulate functions as distinct as stimulation of hormone release and inhibition of cell migration (Castaño *et al.*, 2009). Moreover, rather than being linear straightforward cascades, the pathways activated and required by the kisspeptin/GPR54 system to exert its distinct functions seem to be multiple and intricate, and the mechanisms that enable a given cell to interpret with such a fine precision the kisspeptin signal to convey the correct instructions are still to be determined. In this scenario, it will be important as well to consider other molecular events that, besides intracellular signaling messengers, can significantly influence kisspeptin/GPR54 function. Thus, as pointed out by a recent study in immortalized GT1-7 cells, molecular interaction of GPR54 with other membrane receptors, namely that for GnRH, could play a relevant role in mediating kisspeptin actions (Quaynor *et al.*, 2007). Likewise, there is recent evidence that kisspeptin can suppress metastasis to multiple organs in the apparent absence of GPR54, which would suggest the possible existence of alternate kisspeptin receptors and signaling pathways still to be discovered (Nash *et al.*, 2007). In any event, deciphering of GPR54 signaling mechanisms and pathways in reproductive and nonreproductive tissues still remains a challenging issue that demands the implementation of additional studies using different models, especially on natural kisspeptin targets expressing endogenous GPR54 (Castaño *et al.*, 2009).

1.11.1 Kisspeptin and Puberty

The connection between the kisspeptin/KISS1R system and pubertal development was revealed in 2003 when two groups independently reported the presence of inactivating mutations of KISS1R in patients with hypogonadotrophic hypogonadism (de Roux *et al.*, 2003, Seminara *et al.*, 2003); a condition characterized by the absence of sexual maturation and decreased levels of sex hormones and gonadotrophins. Numerous studies provide convincing arguments for a crucial role of kisspeptin in development, puberty and adult function of the hypothalamic–pituitary–gonadal axis (reviewed by (Colledge 2004, Crown *et al.*, 2007, Roa *et al.*, 2008). The link between kisspeptin activation and onset of puberty was confirmed following the description of the phenotype of Kiss1r-knockout mice which closely paralleled that of human hypogonadotrophic hypogonadism (Funes *et al.*, 2003, Seminara *et al.*, 2003). Mice lacking the KISS1R receptor failed to undergo puberty and mutant males were

sterile with very small genitalia and lacked secondary sexual characteristics (Funes *et al.*, 2003, Seminara *et al.*, 2003). Similarly, mutant female mice also failed to undergo sexual maturation; the uterine horns from mutants were thread-like and the ovaries significantly smaller than normal. In addition, the ovaries contained primary and secondary follicles but large antral (Graafian) follicles or corpora lutea were never found. The phenotype of Kiss1r-null mice was consistent with a lack of sex steroid production and serum testosterone and oestradiol levels were lower than normal in these animals (Seminara *et al.*, 2003). It has also been reported that mice lacking the Kiss1 gene exhibited abnormal timing of puberty (d'Anglemont de Tassigny *et al.*, 2007, Lapatto *et al.*, 2007), although their reproductive phenotypes were not as severe as the Kiss1r-knockout mice. These animals also have impaired sexual maturation, low gonadotrophin levels and abnormal gametogenesis, but the phenotype of Kiss1-knockout mice appears to be more variable, with some animals being less severely affected, and indeed, some females having larger gonadal weight and persistent vaginal cornification (Lapatto *et al.*, 2007).

In support of a role for kisspeptin as a gatekeeper of puberty, a gain-of-function mutation that activates KISS1R signalling has recently been described in an 8-year old girl who presented with idiopathic central precocious puberty (Teles *et al.*, 2008). In vitro studies demonstrated that the substitution of proline for arginine at amino acid 386 (Arg386Pro) leads to prolonged activation of intracellular signaling pathways in response to kisspeptin (Teles *et al.*, 2008). KISS1R agonists have therapeutic potential in initiating puberty in cases of pubertal delay and kisspeptin antagonists or desensitization with agonists may find application in precocious puberty (Reynolds *et al.*, 2009).

1.12 Aim

The aim of the present study was to investigate in sexually immature male rats, the effect of a range of kisspeptin doses on testicular tissue, seminal vesicle and prostrate following the subchronic intraperitoneal administration of mammalian kisspeptin-10 (KP-10) alone and after a pretreatment with GnRH antagonist, acyline.

1.13 Objectives and plan of work

Following were the objectives of the present study:

- To investigate the effect of kisspeptin and acyline treatment on the HPG axis.

This was achieved through the estimation of plasma gonadotropins and testosterone through radioimmunoassay.

- Is spermatogenesis affected by kisspeptin and acyline treatment?

Spermatogenesis was studied by counting the each type of germ cells at stage VII of the spermatogenic cycle. Number of elongated spermatid heads (g^{-1} testis wt.) and daily sperm production (g^{-1} testis wt. day^{-1}) were also calculated.

- To investigate the effect on histomophology of testicular tissue and accessory sex glands

Histomorphometry was done to evaluate cellular architecture through light and electron microscopy. Epithelial height of seminiferous tubules and epithelial height of secretary acini of seminal vesicles and prostate were also measured.

- To investigate the effect on DNA parameters

DNA damage was measured by DNA Ladders assay and DNA Fragmentation assay.

MATERIALS AND METHODS

MATERIALS AND METHODS

2.1 Animals and maintenance

To investigate the role of puberty/reproduction regulating peptide "kisspeptin" in prepubertal male rats one hundred and ninety, five weeks old (postnatal day, PND 35) prepubertal male rats with an average weight of 100±10g were purchased from the National Institute of Health, Islamabad and maintained in the animal house facility of Quaid-i-Azam University, Islamabad, during the experimental period. To minimize crowding stress, five rats were housed per cage (15″ × 11″ × 9″, steel mesh cages) under standard conditions of 12L: 12D hrs photoperiod, 25±2°C temperature controlled with automatic timers and adjustable controls for heating and cooling. Standard rat diet and water were provided *ad libitum.*

All animal handling and subsequent sacrifice were done according to the guidelines provided by the "Ethics Committee" of the Department of Animal Sciences, Faculty of Biological Sciences, Quaid-i-Azam University, Islamabad, for humane use of animals for scientific research. Animal handling was also in accordance with European Union guidelines for use of laboratory animals.

2.2 Experimental design

Two sets of experiments were conducted. In the first, kisspeptin doses were administered subchronically for 12 days, while in the second, kisspeptin action was indirectly blocked with a pretreatment of acyline, a potent GnRH antagonist, and the experiment was carried out for 12 days with kisspeptin treatment.

2.2.1 Experiment 1: Effect of alone kisspeptin treatment on testes, seminal vesicle and prostate tissues.

2.2.1.1 Dosage and treatment

Kisspeptin (metastin 45-54 or kisspeptin-10; 1mg lyophilized powder) was purchased from Calbiochem (EMD Biosciences, Inc. La Jolla, CA) and was dissolved in 1 ml dimethylesulphoxide (DMSO) to give a stock solution of 1 mg ml^{-1} that was

diluted further with distilled water (dH_2O) and was administered intraperitonealy (i.p.). Kisspeptin doses were selected according to Tovar *et al.* (2006).

Rats were arranged randomly to twenty four groups each comprising seven rats (n=7). Control non-treated rats received 0.9% w/v physiological saline (DMSO was added to saline at the same rate as it was added to kisspeptin stock, and was diluted further to concentration equivalent to the experimental doses), while the experimental groups received three different doses of kisspeptin-10: 10 pg, 1 ng and 1μg equivalent to15 pmol, 1.5 nmol and 1.5 μmol doses. Saline and kisspeptin were administered i.p. twice daily after every 12 hr for 12 days to control and experimental rats respectively. Seven rats each from control and treated groups were sacrificed 3 hr after the last dose of kisspeptin after 2, 4, 6, 8, 10 and 12 days of kisspeptin treatment. Experimental days on which sampling was done correspond to age of rats as 37, 39, 41, 43, 45, 47 days (postnatal), respectively.

This sub-chronic treatment of 12 days was designed because the germ cells advance within the seminiferous epithelium, in a specific 12 to 13-day cycle that begins with mitotic division of spermatogonia and proceeds through meiosis and finally ends with the release of sperms (Leblond and Clermont, 1952).

2.2.2 Experiment 2: Effect on testes, seminal vesicle and prostate tissues following indirect blockade of endogenous kisspeptin action with GnRH antagonist acyline

2.2.1.1 Dosage and treatment

In an other set of experiments, to indirectly block the action of endogenous kisspeptin, (n=20) rats were pretreated with a single subcutaneous (s.c.) dose of a GnRH antagonist, acyline, (kind gift of Prof. Dr. M. Shahab, Animal Sciences Department, Quaid-i-Azam University, Islamabad), given 1 day prior to kisspeptin treatment (day 0) at the rate of 300 μg kg^{-1} b.w. Acyline dose was selected according to Herbst *et al.* (2004) who showed that a single 300 μg kg^{-1} b.w. dose of acyline suppressed gonadotropins and testosterone release to castrate levels for 15 days. Blood was drawn from the tail vein, at day 1 of the experiment to determine the

plasma LH, FSH and testosterone levels post-acyline exposure. Soon after the required suppression of hormone concentrations was achieved; of these twenty rats, ten constituted the acyline group and were injected saline only, while the other ten were injected with 1 μg kisspeptin dose exactly as described for experiment 1. In the second experiment only one kisspeptin dose of 1 μg was selected because a significant effect on hormones concentrations and cellular populations was obtained at this dose in the first experiment. Kisspeptin and saline treatments were continued twice daily for 12 days.

2.2.2 Collection of blood and tissue samples

Animals were anesthetized (sodium pentobarbital: 60-80 mg kg^{-1} b.w. i.p.); blood was collected in EDTA vaccutainers directly from the left ventricle of heart. Blood was allowed to stand for 1 hr and plasma was extracted by a 10 min centrifugation at 1258 ×*g* at 4°C (Eppendorff centrifuge 5810 R, Germany). Plasma samples of control and treated rats were aliquoted and stored at –20 °C until assayed for hormone concentrations.

For light microscopy, one of the testes, seminal vesicles and prostate tissues from control and kisspeptin treated rats were excised, weighed, rinsed in phosphate buffered saline (PBS) and fixed in freshly prepared 4 % paraformaldehyde (PFA) solution prepared in PBS. For electron microscopy, the tissues were fixed in 5 % glutaraldehyde (BDH, Germany) solution prepared in pipes buffer.

For the determination of elongated spermatid head count and daily sperm production (DSP), the testes of control and kisspeptin treated rats were snap frozen in liquid nitrogen and stored at -70°C. They were later homogenized and processed.

Similarly for investigation of the DNA fragmentation and concnetration, the testes, seminal vesicle and prostate tissues were frozen in liquid nitrogen and stored at -70°C, to process at a later stage.

Testes were weighed. Gonadosomatic index percent (GSI %) was determined according to the formula:

$$GSI\,(\%) = \frac{Testes\ weight}{Body\ weight} \times 100$$

..... (1)

Testis length and width were determined using the digital vernier callipers. Testis volume was estimated from the equation of an ellipsoid according to Pochran and Wright (2002):

$$Testis\ volume\ (mm^3) = 4/3 \times \pi \times L \times W^2$$

..... (2)

Where L is length, and W is width of the testis. The volumes of the left and right testis were then averaged.

2.3 Light microscopy

2.3.1 Reagents and solutions

See Appendix I for reagent composition and preparation of solutions.

2.3.2 Tissue processing and staining

Tissue samples were fixed overnight at 4°C, in freshly prepared in 4% PFA (pH=7.2), dehydrated in ascending grades of ethanol, cleared in xylene, and embedded in paraplast. Thick sections (5 μm) were cut on a rotary microtome (Shandon Finesse 325, Italy).

Testicular sections were stained with Periodic acid Schiff (PAS) and Harris's hematoxylin, while seminal vesicle and prostate tissues were stained with Harris's hematoxylin and eosin. Staining procedure was as under:

For hematoxylin and eosin staining, sections were dewaxed in xylene, rehydrated in descending alcoholic grades, washed in running tap water and rinsed in dH_2O. They were stained with Harris's hematoxylin for 5 min, dipped in acid alcohol, washed in running tap water for 5 min, counterstained with eosin and again washed

for 2 min in running tap water. Sections were dehydrated in ascending grades of ethanol, cleared in xylene and finally mounted in DPX (BDH, Germany) mountant medium.

For PAS staining, sections were dewaxed, hydrated in descending alcohol grades, and finally rinsed in dH_2O. They were oxidized in 1% periodic acid for 5 min, rinsed in dH_2O, washed in running tap water for 1 min, and again rinsed in dH_2O. Next they were treated with Schiff's reagent for 15 min, rinsed in dH_2O and washed for 5 min in running tap water. They were counterstained with Harris's hematoxylin for 1 min and rinsed in running tap water for 5 min, dehydrated, cleared and mounted as above. Sections were observed and photographed under a Nikon Optiphot BH 2 research microscope (Japan) using Fuji color 100 ASA films. Photographic panels were prepared using the Adobe Photoshop Software (Version 7, Inc. Chicago, Illinois, USA).

2.4 Stereology and morphometry

Quantitative study of spermatogenesis was carried out by counting the number of each variety of germ cells at stage VII of the seminiferous cycle. Stage VII was selected for quantitative analyses of spermatogenesis as the androgen receptor protein expression is highest in stage VII in case of rat, providing support to the contention that mid-spermatogenic stages are androgen responsive. In rats androgen receptor mRNA and immunoexpression is maximal in the midspermatogenic stages VII–VIII, with a clear-cut downregulation during stage VIII (Donnel *et al.*, 2006).

Type-A spermatogonia (Asg), preleptotene spermatocytes (PlSc), pachytene spermatocytes (PSc) and stage VII spermatids (7Sd), were counted according to the method of Leblond and Clermont (1952). The nuclei of different germ cells were counted in 100 round tubules per treatment group (of ten selected slides, five sections from each were taken for counting). Two notes were obtained from each transverse section, considering as the representative measurement of the mean of both. All the counts (crude counts) of germ cells were corrected for section thickness and differences in the nuclear or nucleolar diameter according to the method of Abercrombie (1946) using the following formula:

$$P = A\frac{M}{L+M}$$

..... (3)

Where P = the average number of nuclear points per section, A = the crude count of nuclei in the section, M = section thickness (μm) and L = the average diameter (μm) of the nuclei. The results are expressed as cell number per cross section of seminiferous tubule. Ratios as mentioned below were obtained from the corrected counts according to the method described by Segatelli, (2004):

$$Coefficient\ of\ efficiency\ of\ spermatogonial\ mitosis = \frac{Pachytene\ spermatocytes}{Type\ A\ Spermatogonia}$$

..... (4)

$$Rate\ of\ germ\ cell\ loss\ during\ meiosis\ (meiotic\ index) = \frac{Round\ spermatids}{Pachytene\ spermatocytes}$$

..... (5)

$$Sertoli\ efficiency = \frac{Round\ spermatids}{Sertoli\ cell\ nuclei}$$

..... (6)

$$Total\ \text{sup}\ port\ capacity\ of\ each\ Sertoli\ cell = \frac{Total\ number\ of\ germ\ cells}{Sertoli\ cell\ nuclei}$$

..... (7)

The diameter of seminiferous tubules and germ cells was measured with an ocular micrometer calibrated with a stage micrometer, while sections were observed under oil to count Sertoli and germ cell nuclear profiles. Epithelial cell height of the seminal vesicle and prostate mucosa was measured using an ocular micrometer scale. Due to the variability in the epithelial cell shape, the epithelial cell height was measured at a place where the epithelial cells stood erect on the basement membrane.

2.5 Cells identification and grouping

Sertoli and germ cells were readily identified by the appearance of their nuclei in conjunction with the stage of the cycle of the seminiferous epithelium according to the descriptions of Clermont and Leblond (1952), Clermont (1972) and Hess (1990). Stage VII of seminiferous epithelium was recognized by the acrosome system which covers nearly one third of the step 7 spermatid nucleus and type B spermatogonia had been replaced by small preleptotene spermatocytes. Sertoli and germ cells were grouped as follows:

Sertoli Cells-The nuclei of these cells were distinguished from germ cells by irregular shapes, paler chromatin pattern, and a single nucleolus. Their cytoplasm extended from basal lamina to the tubular lumen.

Type A Spermatogonia-These cells were located on the basement membrane and had a nucleus with diffuse, finely granulated chromatin and one or two nucleoli associated with the nuclear membrane.

Preleptotene Spermatocytes-The nuclei of these cells were characterized by threadlike clumps of chromatin and were located on the basement membrane.

Pachytene Spermatocytes-The nuclei of these spermatocytes were larger and positioned closer to the tubule lumen than preleptotene spematocytes and their chromatin had a mottled appearance.

Step 7 Spermatids-They were identified on the basis of their position (close to the tubule lumen), size (smaller than spermatocytes), lack of heterochromatin, presence of an acrosome covering one-third or greater of the round spermatid nucleus.

2.6 Testicular spermatid head count

2.6.1 Reagents and solutions

See Appendix II

2.6.2 Preparation of the tissue

Frozen testes were thawed for 2-3 min. A shallow incision was made in the tunica albuginea to remove the tunica and associated blood vessels.

2.6.3 Homogenization

Only one testis was transferred to homogenizer at a time and 12.5 ml DMSO/saline solution was added. Homogenization was done for 1 min at 1000×*g*. The contents were poured into a flask. The homogenizer was washed twice with 12.5ml, and then with 25ml DMSO/saline. Both washes were added to the flask. Homogenization vessel and rotor were washed three times with deionized water. The vessel and rotor were dried with lint-free wipe before homogenizing another sample.

2.6.4 Staining spermatid heads

250 µl of 0.1 % trypan blue were added into flasks containing sample (50.5 ml). The flasks were covered with parafilm and vortexed for 5 sec at 2000 rpm. Samples were stained for ≥1 min.

2.6.5 Counting spermatid heads

Spermatid head suspension was vortexed for 10 sec and 10 µl suspension was loaded onto an improved Neubaur's chamber. Spermatid heads were allowed to settle for 5 min before counting. Two notes were taken for each animal and the mean of both was considered as representative measurement. Each chamber of the hemacytometer is designed to hold 0.1 µl of solution in its tertiary square. The tertiary square is divided into 25 secondary squares. Thus each secondary square contained 0.004 µl of suspension. As spermatid heads were counted in 10 secondary squares, 0.04 µl of suspension was used per chamber. The total volume of rat testis suspension

was 50.5 ml. The total number of spermatid heads in a rat testis was calculated as described by Seung *et al.* (2003) using the following formulae:

$$Total\ number\ of\ spermatid\ heads = \frac{mean\ count\ of\ spermatid\ heads}{0.00004\ ml} \times 50.5\ ml$$

..... (8)

$$Elongated\ spermatids\ per\ gram\ of\ tastis\ weight = \frac{Total\ number\ of\ spermatids\ heads}{testis\ weight}$$

..... (9)

Daily sperm production (DSP) was calculated as:

$$Daily\ sperm\ production\ per\ gram\ testis\ weight\ per\ day = \frac{Total\ number\ of\ spermatid\ heads\ per\ gram\ of\ testis\ weight}{6.10\ (time\ divisor)}$$

..... (10)

2.7 Hormone analyses

Plasma was separated by centrifugation at 1258 × *g* for 10 min and stored at -20^{O}C until assayed for LH, FSH and testosterone.

2.7.1 Determination of FSH

Serum FSH concentration was assayed using rat-specific IRMA kit (Biocode-Hycel, rue E, Solvay, Liege Belgium). Assays were done according to the manufacturers instructions.

2.7.1.1 Principle of the assay

The rat FSH IRMA is a single step solid phase immunoradiometric assay. It provides high affinity and specificity for two different epitopes on FSH. A first monoclonal anti-FSH antibody bound to a polystyrene tube will capture the FSH of the plasma or serum sample in the presence of a second ^{125}I labeled monoclonal anti-FSH antibody. The single step solid phase-FSH-^{125}I labeled monoclonal antibody sandwich is formed following the incubation. The tube is then washed to remove excess of unbound labeled antibody. The radioactivity of the sandwich is directly proportional to the concentration of FSH present in the sample. Sample concentrations are read from a calibration curve and the results are expressed in ng/ml.

2.7.1.2 Procedure of the assay

Serum samples from treated and control rats (100 µl each) were pipetted into corresponding tubes and 50 µl MAb FSH I^{125} antiserum was added to each tube. Tubes were vortexed and incubated for 90 min at room temperature. 100 µl of rat LH I^{125} tracer was added to each tube and incubated overnight at room temperature. Supernatants were carefully aspirated the following day, 2 ml of washing solution was added to each tube and the tubes were decanted for 1 min, washing step was repeated and finally the radioactivity was counted for at least 60 sec in a 16-channel Gamma counter (Oakfield Sourcerer RIA counter, No. 238, Type SD 16, UK). Mean sensitivity of the assay was 0.2 ng/ml. Intra and inter-assay co-efficient of variations were found below or equal to 2.9 % and 7.6 % respectively. All the plasma samples were run in duplicate.

2.7.1.3 Data processing

Mean count rate was determined for each of the duplicate tubes. The ratio B/BO was calculated using the following equation:

$$\frac{B}{BO}\% = \left[\frac{cal\ or\ sample\ cpm}{T\ cpm}\right] \times 100$$

A standard curve was drawn on a semilogarithmic paper by plotting the ratio B/BO % (linear scale), obtained for each calibrator, versus its respective concentration expressed in ng/ml (logarithmic scale).

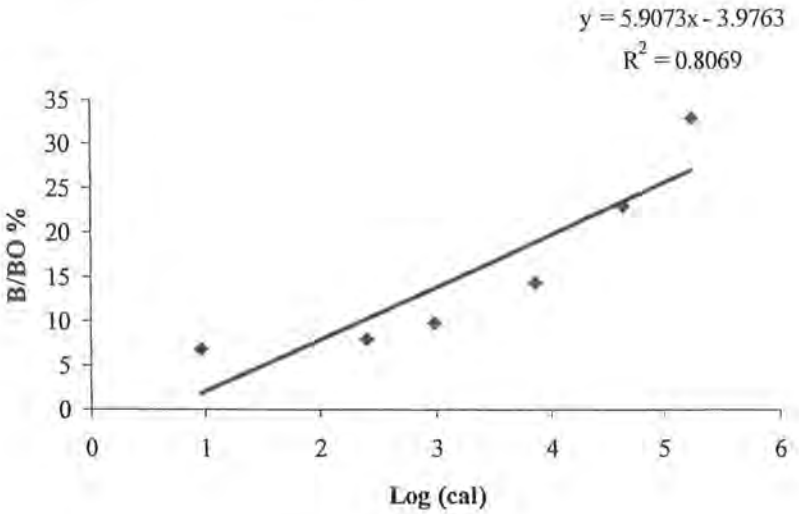

Standard Curve for FSH (IRMA)

2.7.2 Determination of LH

Plasma LH concentration was assayed using rat specific RIA kit (Biocode-Hycel, rue E, Solvay, Liege Belgium).

2.7.2.1 Principle of the assay

The rat LH assay is based on competition between a ^{125}I-labelled rat LH tracer and the LH contained in the rat sample for binding to a highly specific rabbit polyclonal antibody (Ab) according to the following equation:

rLH rLH-Ab

Free { +Ab, bound {

^{125}I-rLH ^{125}I-rLH-Ab

As the concentrations of ^{125}I-rLH and Ab are constant, the status of the above mentioned equation depends on the concentration of rat LH in the sample. Samples are incubated with antiserum and tracer. The separation of bound LH from free is accomplished by a second antibody (mouse monoclonal anti rabbit Ig) coupled to magnetic particles. The radioactive bound fraction is precipitated by magnetic separation or centrifugation and counted in a gamma counter. Sample LH concentrations are read from a calibration curve and the results are expressed in ng/ml.

2.7.2.2 Procedure of the assay

Samples were brought to room temperature just before use. 25 µl each of sample and control were pipetted into corresponding tubes to which 100 µl of antiserum (Ab rat LH) was added. Tubes were vortexed and incubated at 37°C for 3 hr. 100 µl of rat LH ^{125}I tracer was added to each tube and incubated overnight at room temperature. The magnetic particles (SORB Ab Fc) were vortexed and 200 µl of these were added to each of the tubes. The tubes were again vortexed and incubation was done for 1 hr at room temperature without further mixing. Tubes were centrifuged at 1500 ×*g* for 20 min. Supernatants were carefully aspirated and, finally the radioactivity was counted for at least 60 sec in a Gamma counter as above. Mean sensitivity of the assay was 0.14 ng/ml. Intra and inter-assay co-efficient of variations were found below or equal to 12.0 % and 22.4 % respectively. All the plasma samples were analyzed in duplicate.

2.7.2.2 Data processing

Mean count rate for each of the duplicate tubes was determined. The ratio B/BO was calculated according to the following equation:

$$\frac{B}{BO}\% = \left[\frac{cal\ or\ sample\ cpm}{BO\ (cal\ 0)\ cpm}\right] \times 100$$

A standard curve was drawn on a semilogarithmic paper by plotting the ratio B/BO % (linear scale) obtained for each calibrator versus its respective concentration expressed in ng/ml (logarithmic scale).

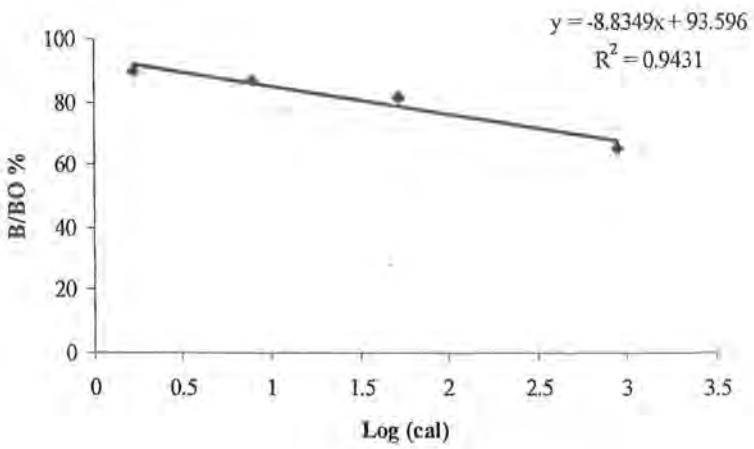

Standard Curve for LH (RIA)

2.7.3 Determination of plasma testosterone

Plasma testosterone levels were determined using the solid phase radioimmunoassay method using a commercially available kit (Immunotech, France).

2.7.3.1 Principle of the assay

This assay is based on competition between the unlabelled testosterone and a fixed quantity of ^{125}I-labelled testosterone for a limited number of binding sites on testosterone specific antibody bound to the tubes, allowing to react a fixed amount of tracer and antibody with different amounts of unlabelled ligand. The bound reactivity is then counted in a gamma counter. The amount of tracer bound by the antibody will be inversely proportional to the concentration of unlabelled ligand. Sample testosterone concentrations are read from a calibration curve and the results are expressed in ng/ml.

2.7.3.2 Procedure of the assay

Samples and reagents were brought to room temperature. Tubes were labeled in duplicate for total counts, standards, control and samples. All reagents and samples were mixed thoroughly before use. 50 µl each of standard, control and samples were taken in antibody coated tubes to each of which 500 µl of tracer was added and mixed. The tubes were covered and incubated for 3 hr at 37°C in a water-bath with constant shaking (350 rpm). The tubes were decanted and the bound cpm and total cpm were counted in a 16-channel Gamma counter as above. All the plasma samples were analyzed in duplicate. The calibrator range was 0 - 20 ng/ml (first calibrator at 0.1 ng/ml). The mean sensitivity of the assay was 0.025 ng/ml and the mean intra and inter-assay coefficient of variations were equal to 14.8 % and 15 % respectively.

2.7.3.3 Data processing

Standard curve was plotted by taking B/BO (%) on vertical axis and log of the calibrators of testosterone on the horizontal axis (ng/ml). Testosterone concentration of samples was obtained from the standard curve by interpolation.

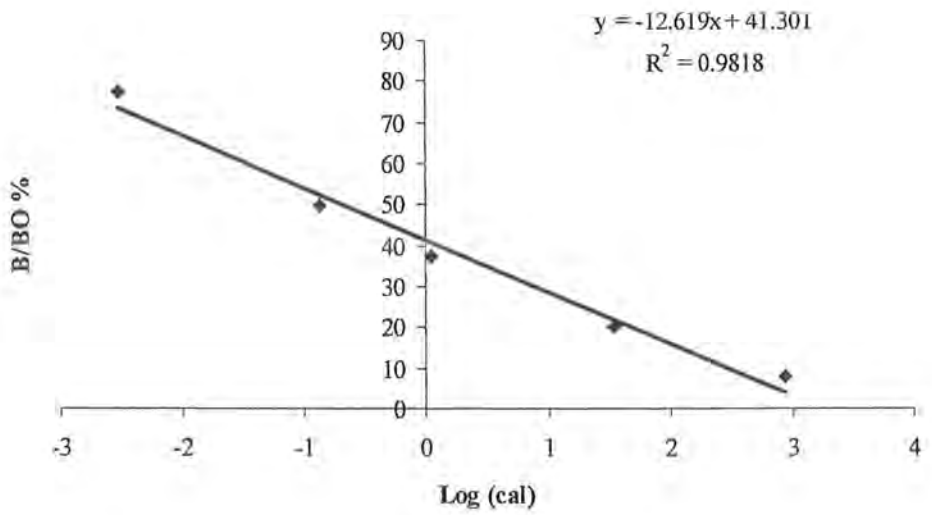

Standard Curve of Testosterone (RIA)

2.8 DNA Ladder Assay

2.8.1 Reagents and solutions

See Appendix III for reagent composition and preparation of solutions.

2.8.2 DNA extraction

Tissues stored at -70^{O}C were brought to room temperature. DNA was isolated according to the method of Bin Wu *et al.* (2005) and Gilbert *et al.* (2007). At least 30 mg testicular, seminal vesicle and prostate tissues were washed twice with 1 ml TE buffer (pH 7.5). They were ground and 300 µl lysis buffer and 240 µl 10 % SDS were added. Contents were vortexed gently and then incubated overnight at 45°C in a water bath. 200 µl of phenol was then added, shaken vigorously for 5 min, and the contents were centrifuged for 5 min at 3000 rpm. Supernatant was pipetted out into a new tube to which 200 µl of phenol and 200 µl chloroform/isoamyl alcohol (24:1) were added, shaking vigorously for 5 min, and then centrifuged for 5 min at 3000 rpm. The supernatant was pipetted out into a new tube and 25 µl of 3 M sodium acetate (pH 5.2) and 5 ml of ice cold 100 % ethanol were added and tubes were kept overnight at -20°C and then centrifuged for 30 min. The supernatant was aspirated gently to avoid disturbance to the DNA. DNA was washed in 70 % ethanol and dried in oven at 30°C. Finally, 20- 50 µl TE buffer (pH 8.0) and 2 µl RNase were added.

2.8.3 Gel electrophoresis

DNA samples from control and treated testis, seminal vesicle and prostate were analyzed on 2 % agarose resolving gel prepared by melting 1 g of agarose in 50 ml 1 X TBE buffer (pH 8.3) in a microwave oven. 5 µl of ethidium bromide (0.5 µg ml^{-1} final concentration) was added.

5 µl of DNA samples were mixed with loading dye (0.25 % bromophenol blue with 40 % sucrose) and loaded onto the wells. 100 bp DNA ladder was loaded alongside the DNA samples to identify the size of the DNA fragment. Electrophoresis was performed for 45 min at 100 V (80 mA) in 1 × TBE buffer. The gel was viewed under Gel Doc system (BIORAD, Germany) and photographed.

2.9 Quantification of DNA fragmentation

DNA quantification was done according to the method of Boraschi and Maurizi (1998). 30 mg each of frozen testis, seminal vesicles and prostrate tissues were ground in 1 ml TTE solution (pH 7.4) to make cell suspension and kept overnight at 37 °C. Cells were centrifuged at 2000 rpm for 10 min. Supernatants were transferred carefully to new tubes labeled "S". To the pellet in tubes "B", 1.0 ml TTE solution was added and thoroughly vortexed. To separate fragmented DNA from intact chromatin, tubes B were centrifuged at 20,000 × *g* for 10 min at 4°C. Supernatants were transferred carefully to new tubes labeled "T". To the small pellet in tubes B, 1.0 ml TTE solution was added. 1.0 ml of 25% TCA was added to tubes T, B and S and vortexed vigorously. Precipitation was allowed to proceed overnight at 4°C. After the incubation, precipitated DNA was recovered by pelleting for 10 min at 20,000 × *g* at 4°C. Supernatants were aspirated and DNA was hydrolyzed by adding 160 µl of 5% TCA to each pellet and heated for 15 min at 90°C in a heating block. A blank with 160 µl of 5% TCA alone was prepared. To each tube, 320 µl of freshly prepared diphenylamine (DPA) solution was added, vortexed and allowed to develop color for about 4 h at 37°C or overnight at room temperature. Optical density at 620 nm was read on a UV-visible spectrophotometer (HP8453, Agilent Technologies, USA). The percentage of fragmented DNA was calculated using the formula:

$$\% \ Fragmented \ DNA = \frac{T \times 100}{T + B}$$

2.10 Transmission electron microscopy (TEM)

Electron microscopy was conducted to observe ultrastructural changes in testicular, seminal vesicle and prostate tissues.

2.10.1 Reagents and solutions

See appendix IV for reagent composition and solutions.

2.10.2 Procedure

Small pieces of approximately $1mm^3$ control and kisspeptin treated rat testicular, prostate and seminal vesicle tissues were immersed in 5% glutaraldehyde (prepared in 0.2 M pipes buffer). These were subjected to vacuum in order to draw the fixative into the cells and vessels. Fixation took place in 18 hr by placing the samples on a 55^0 fixed angle specimen rotator at 5 rpm at room temperature. Rinsing of samples to remove the fixative was performed in 0.2 M pipes buffer (pH 6.8) for three times with an interval of 15 min each. Post fixation was achieved with 1 % osmium tetraoxide for 18 hr at room temperature. The tissues were again washed with autoclaved dH_2O twice for 15 min and then shifted to 5 % uranyl acetate solution for 16-18 hr. The tissues were again washed with dH_2O twice for 15 min and then dehydrated in ascending grades of ethanol keeping in each grade for 15 min except the 100 % grade in which they were kept for overnight. The tissues were transferred to absolute acetone twice for 15 min as transitional solvent because the ethanol does not mix well with spur resin. Tissues were infiltrated with a mixture of Spur embedding media. The ratio of resin to acetone was 1:3 for 18 hr followed by 1:1 and 3:1 for another 18 hr each. A 100 % resin mixture was added to the samples and vacuum infiltration was carried overnight. The samples were oriented in moulds and resin cured at 70 °C for 48 hr.

The polymerized resin blocks were trimmed and faced with fine scalpel blade and glass knife. Ultrathin serial sections of approximately 120 nm were cut with an ultramicrotome (RMC MT 7000, Japan) and placed onto 200 mesh nickel grids. Sections were stained with 5% uranyl acetate for 30 min and then washed twice with dH_2O and stained with lead citrate for 15 min in NaOH chamber. Sections were examined with a Transmission Electron Microscope (JEOL JEM1010, Japan) operating at 80 kv available at the National Institute for Biotechnology and Genetic Engineering (NIBGE) Faisalabad.

2.11 Statistical Analysis

Results were expressed as mean ± SE. The results obtained were analyzed and compared by one way ANOVA followed by post hoc Tukey's adjustment using the

Statistical Package for Social Sciences (SPSS, version 16, Inc, Chicago, Illinois, USA). $p < 0.05$ was considered to be statistically significant. Data have presented as mean and standard error of mean (SEM).

RESULTS

SECTION I

RESULTS

3.1 Testes

Experiment 1: Effect on testicular tissue, plasma gonadotropins and testosterone concentrations following treatment with kisspeptin alone at variable doses.

3.1.1 Body weight and testicular parameters

No change occurred in body weight, testicular weight, testes volume and gonadosomatic index (%) at any of the kisspeptin doses (Fig. 3.1 and 3.2).

Regression analysis showed a linear increase in body weight (g), testes weight (g), testes volume (ml) and gonadosomatic index (%) with increasing age for control and kisspeptin treated rats (Table 1).

3.1.2 Seminiferous tubular diameter and epithelium height

No effect was observed on seminiferous tubular diameter at any of the treatment doses. Compared to control, seminiferous tubular epithelium height decreased after 12 days of treatment at 1 ng and 1 μg doses ($p < 0.01$; $p < 0.001$ respectively), while no effect was observed at 10 pg dose (Fig. 3.3).

Regression analysis showed a linear increase in seminiferous tubular diameter (μm) and seminiferous tubular epithelium height (μm) with increasing age for control as well as treatment with variable kisspeptin doses (Table 2).

3.1.3 Plasma gonadotropins and testosterone

Plasma FSH levels remained unaffected throughout the experiment (Fig. 3.4).

LH concentration increased significantly at 1 μg and 1 ng doses ($p < 0.01$) after 4 days of treatment but thereafter decreased gradually approaching significant level at 1 μg ($p < 0.01$) and 1 ng doses ($p < 0.05$) after 12 days of treatment as compared to the control, while remaining nonsignificantly different from control at 6, 8 and 10^{th} treatment days. No significant difference was observed at 10 pg dose during the experimental period (Fig. 3.5).

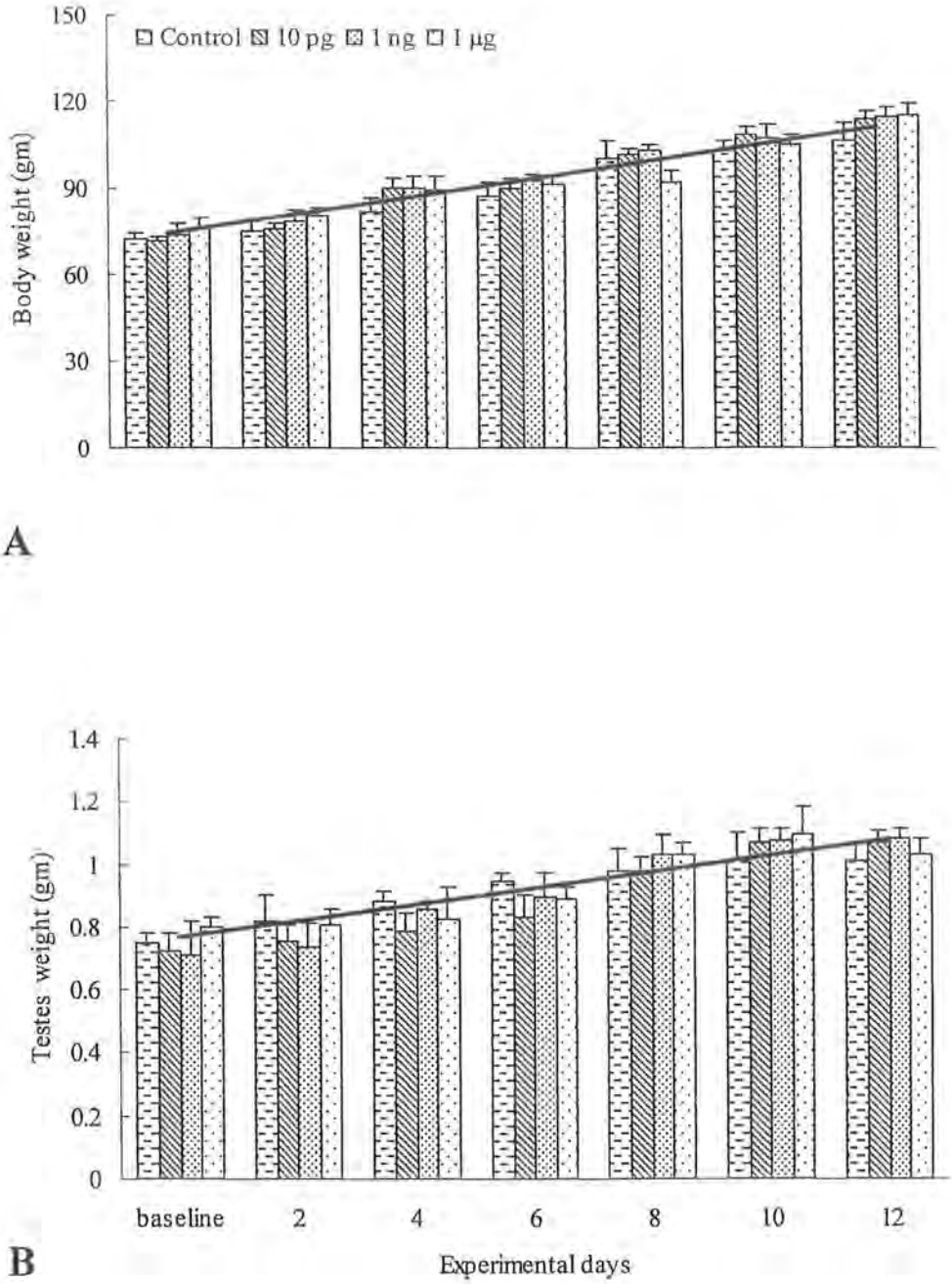

Figure 3.1 Body weight (A) and testis weight (B) after 2, 4, 6, 8, 10 and 12 days of alone kisspeptin treatment (10 pg, 1 ng, and 1 µg doses). No difference was observed at any dose or treatment day. The trend line shows a linear increase in body weight and testis weight throughout the experimental days irrespective of the treatment. Trend line is shown only for 1 µg dose. Values are expressed as mean ± SE.

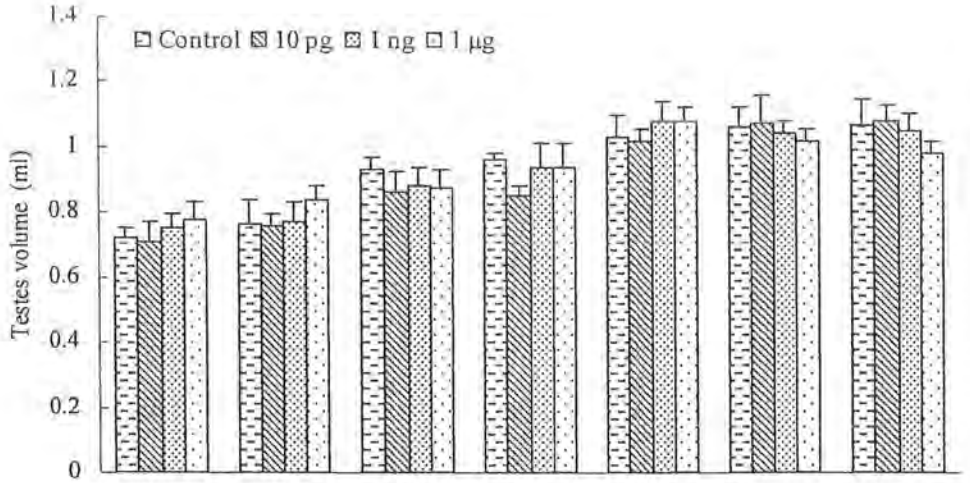

A

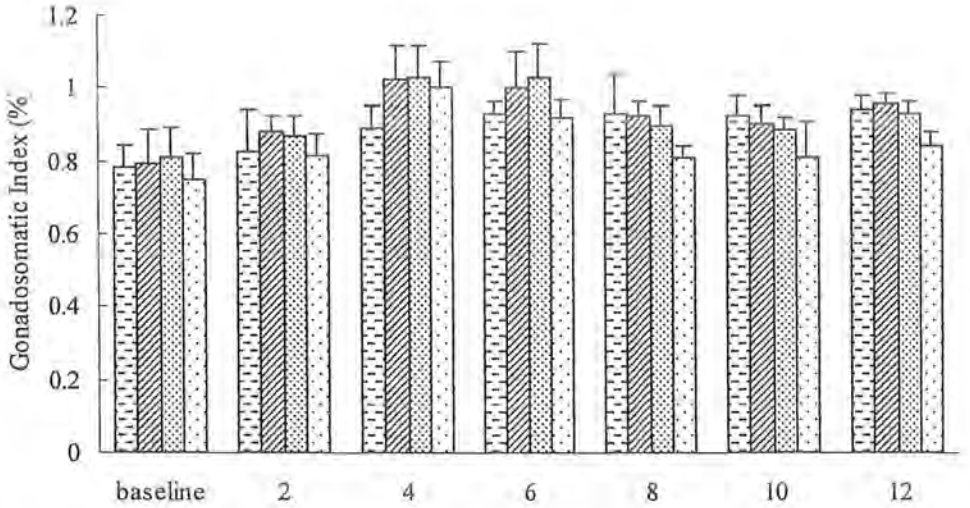

B

Figure 3.2 Testis volume (A) and gonadosomatic index (%) (B) after 2, 4, 6, 8, 10 and 12 days of alone kisspeptin treatment (10 pg, 1 ng, 1µg doses). No significant effect was observed at any of the treatment doses on testis volume and gonadosomatic index (%). Values are expressed as mean ± SE.

Table 1 Regression analysis indicating increase in mean body weight and testicular parameters against variable doses of kisspeptin (KP).

Parameter	Treatment	R^2
Body weight	Control	0.97
	KP 10 pg	0.97
	KP 1 ng	0.99
	KP 1 µg	0.93
Testes weight	Control	0.93
	KP 10 pg	0.93
	KP 1 ng	0.93
	KP 1 µg	0.85
Testes volume	Control	0.90
	KP 10 pg	0.94
	KP 1 ng	0.88
	KP 1 µg	0.73
Gonadosomatic index	Control	0.78
	KP 10 pg	0.19
	KP 1 ng	0.06
	KP 1 µg	0.004

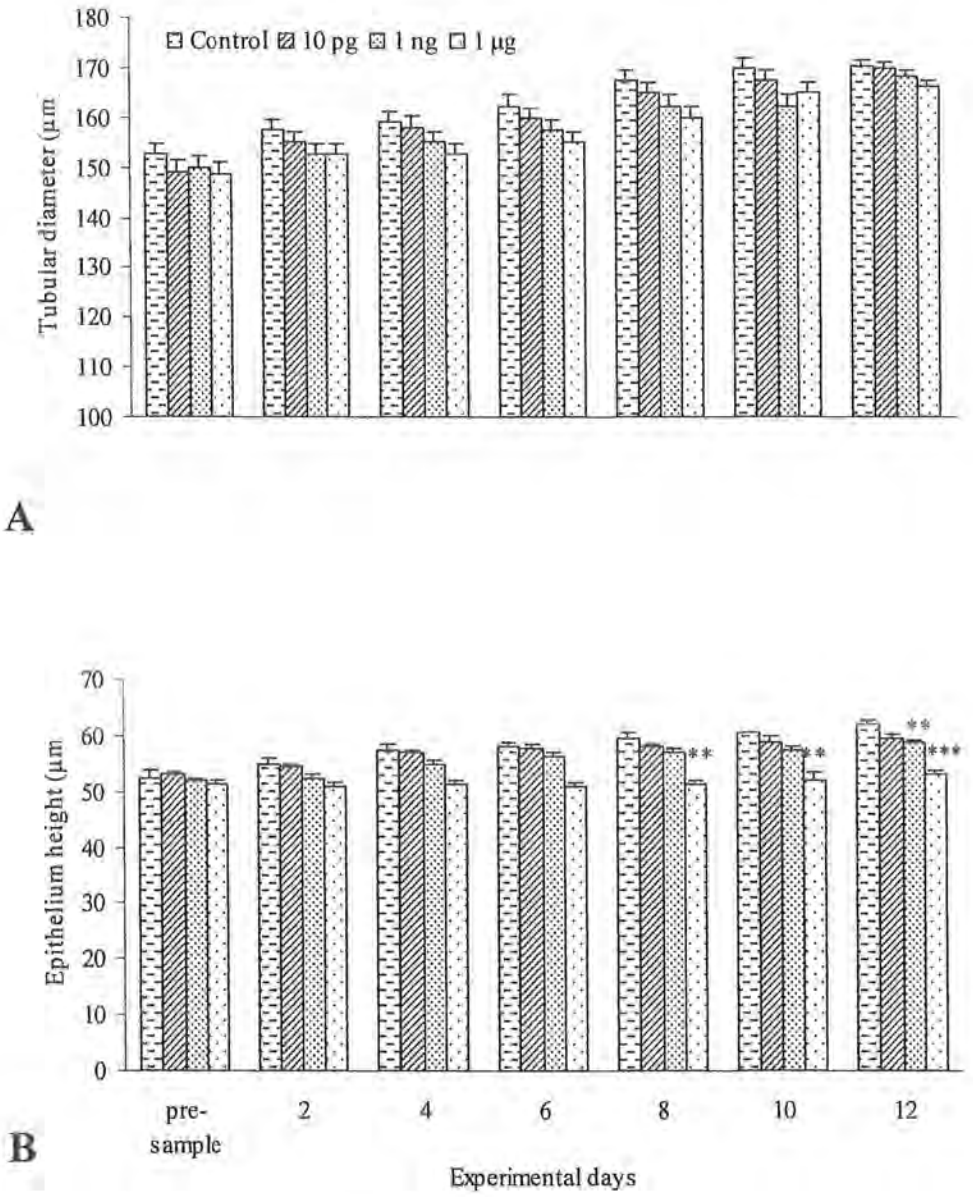

Figure 3.3 Seminiferous tubular diameter (µm) (A) and epithelium height (µm) (B) after 2, 4, 6, 8, 10 and 12 days of alone kisspeptin treatment (10 pg, 1 ng, 1µg doses). Kisspeptin (1 µg) significantly decreased epithelium height after 8, 10 and 12 days treatment, 1 ng dose significantly decreased epithelium height after 12 days treatment while no effect was observed with 10 pg dose. Values are expressed as mean ± SE. $^{**}p < 0.01$, $^{***}p < 0.001$.

Table 2 Regression analysis indicating decrease in seminiferous tubular diameter and epithelium height against variable doses of kisspeptin (KP).

Parameter	Treatment	R^2
Seminiferous tubular diameter	Control	0.97
	KP 10 pg	0.98
	KP 1 ng	0.97
	KP 1 μg	0.95
Seminiferous tubular epithelium height	Control	0.96
	KP 10 pg	0.92
	KP 1 ng	0.95
	KP 1 μg	0.53

Testosterone levels remained unaltered at 10 pg dose. At other doses, no change was observed in plasma testosterone concentration after 2 and 4 days of treatment, but a nonsignificant decrease ($p < 0.074$) was noticeable after 6 days. The decrease continued and approached significant levels after 8, 10 and 12 days of treatment at 1 ng dose ($p < 0.05$) and ($p < 0.01$) at 1 µg dose (Fig. 3.6).

3.1.4 Quantitative data on spermatogenic cells

Type A spermatogonia decreased only after 12 days of treatment at both 1 ng and 1 µg kisspeptin doses ($p < 0.05$; $p < 0.01$ respectively), while remaining unaltered at 2, 4, 6, 8, 10 days of treatment. No significant effect was observed at 10 pg dose (Fig. 3.7).

Preleptotene spermatocytes decreased significantly ($p < 0.05$) at both 1 ng and 1 µg kisspeptin doses but only after 12 days of treatment. The dose of 10 pg remained ineffective (Fig. 3.8).

Pachytene spermatocytes decreased significantly at 1 ng and 1 µg kisspeptin doses after treatment day 4 ($p < 0.01$), day 6 ($p < 0.001$; $p < 0.01$ respectively), day 8 ($p < 0.01$; $p < 0.001$ respectively), day 10 ($p < 0.05$; $p < 0.001$ respectively), and day 12 ($p < 0.01$; $p < 0.001$ respectively). No effect was observed with 10 pg dose (Fig. 3.9).

Step 7 spermatids decreased significantly at 1 ng and 1 µg doses after day 4 ($p < 0.05$; $p < 0.01$ respectively), day 6 ($p < 0.05$; $p < 0.01$ respectively), day 8 ($p < 0.01$; $p < 0.001$ respectively), day 10 ($p < 0.05$; $p < 0.001$ respectively), and day 12 ($p < 0.001$) of kisspeptin treatment. At 10 pg dose, the decrease could be detectable only after 12 days of treatment ($p < 0.05$) (Fig. 3.10).

3.1.5 Elongated spermatid heads and daily sperm production

Elongated spermatid heads (g^{-1} testis wt.) showed significant decrease at 1 ng and 1 µg doses after 8, 10 and 12 days of treatment ($p < 0.001$). The decrease also occurred at 10 pg dose after 8, 10 and 12 days of treatment ($p < 0.01$; $P < 0.05$; $p <$

0.05 respectively). Only a few spermatids were observed before 41 day of age (Fig. 3.11).

Daily sperm production (g^{-1} testis weight day^{-1}) was significantly decreased at 1 ng and 1 μg doses after 8, 10 and 12 days of kisspeptin treatment ($p < 0.001$). A significant decrease was also noticeable at 10 pg dose after 8, 10 and 12 days ($P < 0.001$; $p < 0.01$; $p < 0.05$ respectively). The decrease was greater at higher kisspeptin doses (1 ng and 1 μg) while comparatively less significant at 10 pg dose (Fig. 3.12).

3.1.6 Cell ratios from the corrected counts

Coefficient of efficiency of spermatogonial mitosis increased significantly in 1 ng and 1μg dosage groups ($p < 0.01$), while no difference was observed in the 10 pg group as compared to control rats (Fig. 3.13 A). Rate of germ cell loss during meiosis (meiotic index) decreased only at 1 μg ($p < 0.05$) kisspeptin dose, but remained unaltered at 10 pg and 1 ng doses (Fig. 3.13 B).

Sertoli efficiency decreased at all kisspeptin doses, $p < 0.01$ at 10 pg and $p < 0.001$ at 1 ng and 1 μg doses (Fig. 3.13 C). Total support capacity of each Sertoli cell also decreased significantly ($p < 0.001$) in all the treatment groups (Fig. 3.13 D).

3.1.7 Correlation Analysis

A positive correlation ($r = 0.55$, $p < 0.01$) existed between LH and testosterone concentrations. In contrast a significant negative ($r = -0.317$, $p < 0.01$) correlation existed between FSH and LH concentration.

A significant positive correlation existed between type A spermatogonia and preleptotene spermatocytes ($r = 0.41$, $p < 0.01$), type A spermatogonia and pachytene spermatocytes ($r = 0.37$, $p < 0.01$), type A spermatogonia and step 7 spermatids ($r = 0.35$, $p < 0.01$). Number of preleptotene spermatocytes correlated positively with pachytene spermatocytes ($r = 0.50$, $p < 0.01$) and step 7 spermatids ($r = 0.47$, $p < 0.01$). A positive correlation was observed between pachytene spermatocytes and step 7 spermatids ($r = 0.35$, $p < 0.01$). A positive correlation was found between FSH levels and Sertoli cell number ($r = 0.10$).

A positive correlation existed between elongated spermatid head count and daily sperm production (r = 0.12). Similarly, a strong positive correlation existed between testosterone and elongated spermatid head count (r = 0.57, $p < 0.01$), and also between testosterone and daily sperm production (r = 0.48, $p < 0.01$).

3.1.8 Histomorphology of seminiferous tubules

Control Testes

Light microscopic examination of control saline treated testicular sections showed normal seminiferous tubules with intact epithelia and evenly spaced type A spermatogonia and primary spermatocytes. Dark stained small size preleptotene spermatocytes were arranged at the periphery, while pachytene spermatocytes containing large size nuclei were present next to these. Round spermatids and elongated spermatids, as characterized by the acrosome, were present further toward the lumen (Fig. 3.14 a-b and 3.15 a).

Testes from rats treated with 10 pg kisspeptin

At 10 pg dose of kisspeptin, degeneration of seminiferous tubules was evidenced by intraepithelial vacuolizations in some tubules. Germ cells were regressed, atrophied and mildly necrotic. Tubular lumen was filled with necrotic tissue. Round and elongated spermatids had abnormal acrosome (Fig. 3.14 c-d).

Testes from rats treated with 1 ng kisspeptin

At 1 ng dose, further degeneration of seminiferous tubules was observed. Intraepithelial vacuolizations and multinucleated giant cells were frequently found. Interstitial spaces were enlarged while tubular epithelium was irregular shaped. Spermatogonial cells were highly regressed and atrophied. Luminal space was filled with necrotic tissue. Round and elongated spermatids were scarce and had abnormal acrosome (Fig. 3.14 e-f).

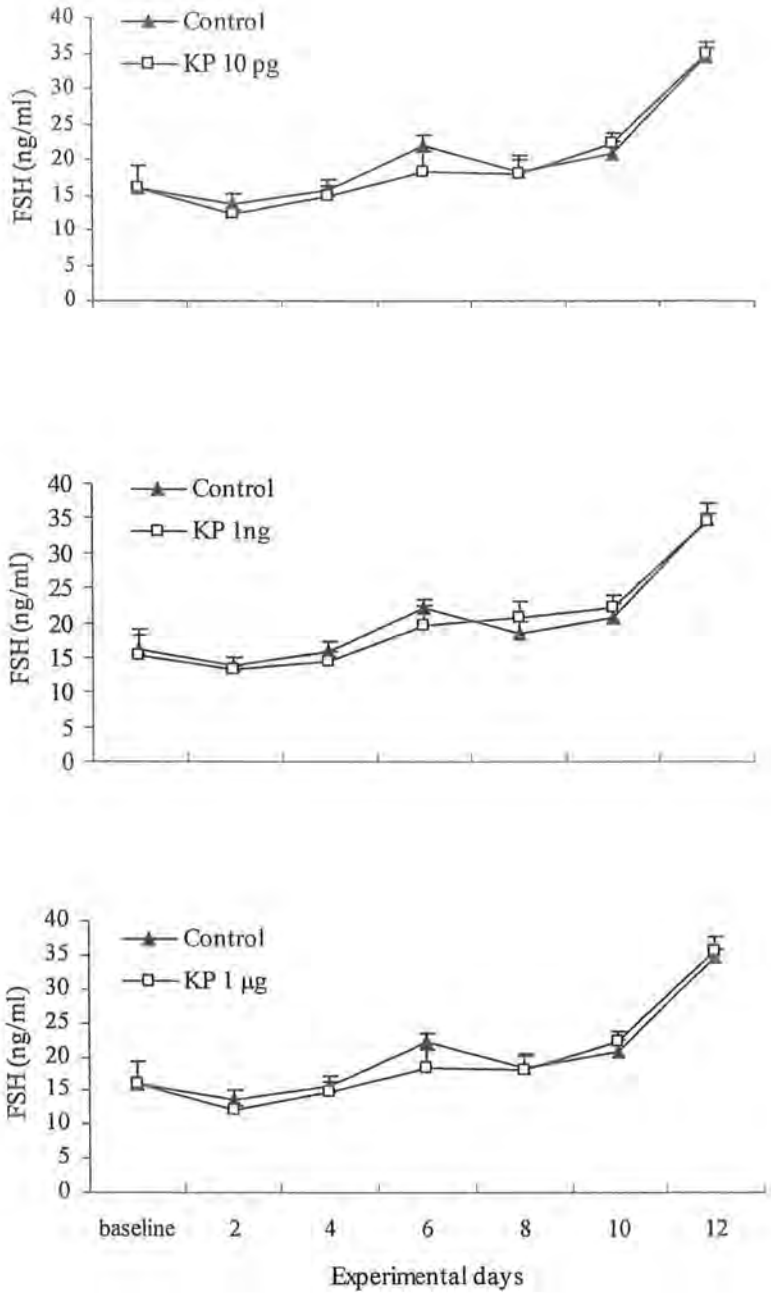

Figure 3.4 Plasma FSH concentration following treatment with 10 pg (A), 1 ng (B) and 1 µg (C) doses after 2, 4, 6, 8, 10 and 12 days of alone kisspeptin treatment. FSH levels remained unaltered throughout the experiment. Values are expressed as mean ± SE.

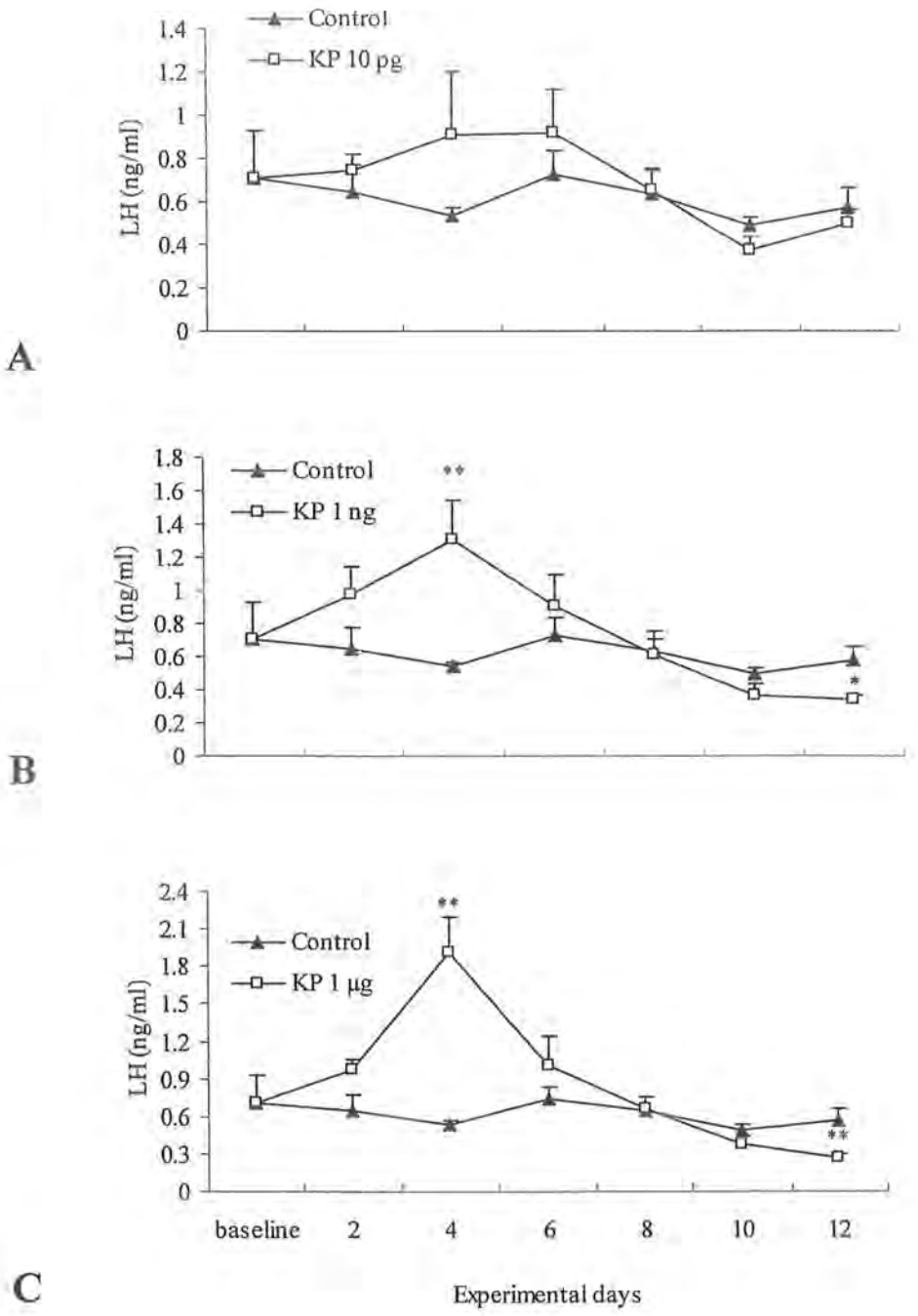

Figure 3.5 Plasma LH concentration following treatment with 10 pg (A), 1 ng (B) and 1 µg (C) doses after 2, 4, 6, 8, 10 and 12 days of alone kisspeptin treatment. LH levels increased significantly after 4 days of treatment at 1 ng and 1 µg doses but decreased afterwards. The decrease was significant after 12 days of treatment. The levels remained unaltered at 10 pg dose as compared to control throughout the experiment. Values are expressed as mean ± SE. $^{*}p < 0.05$, $^{**}p < 0.01$.

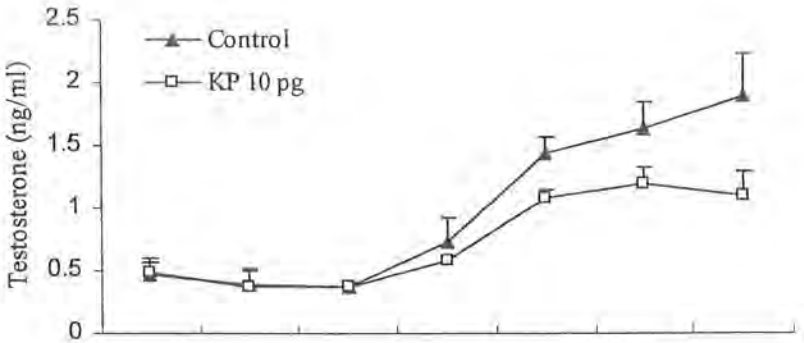

A

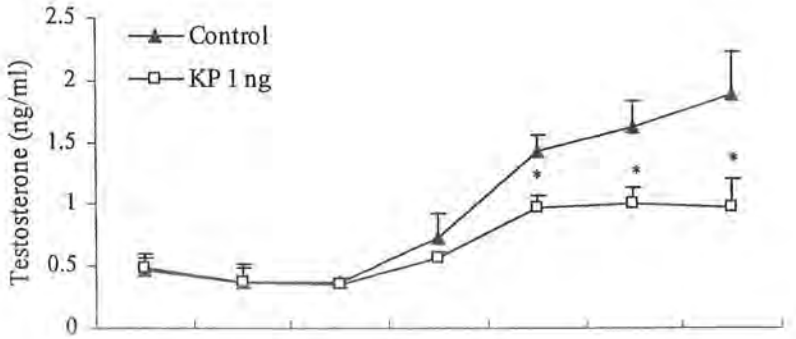

B

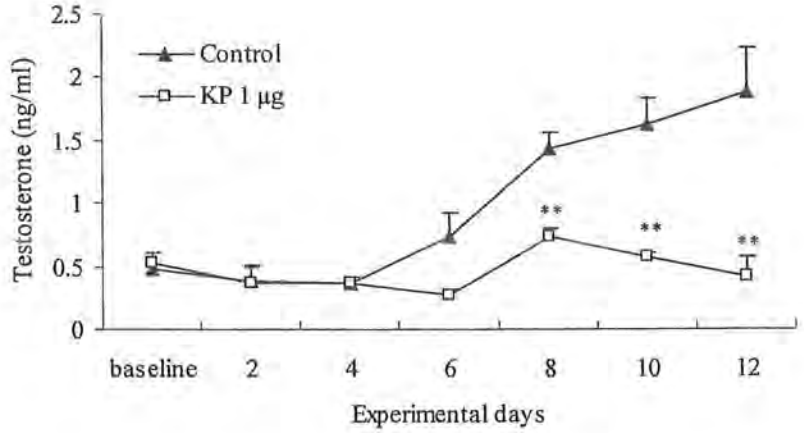

C

Figure 3.6 Plasma testosterone concentration following treatment with 10 pg (A), 1 ng (B) and 1 µg (C) doses after 2, 4, 6, 8, 10 and 12 days of kisspeptin treatment. Testosterone concentrations remained unaltered untill 4 days of treatment but decreased significantly thereafter. Values are expressed as mean ± SE. $^{*}p < 0.05$, $^{**}p < 0.01$.

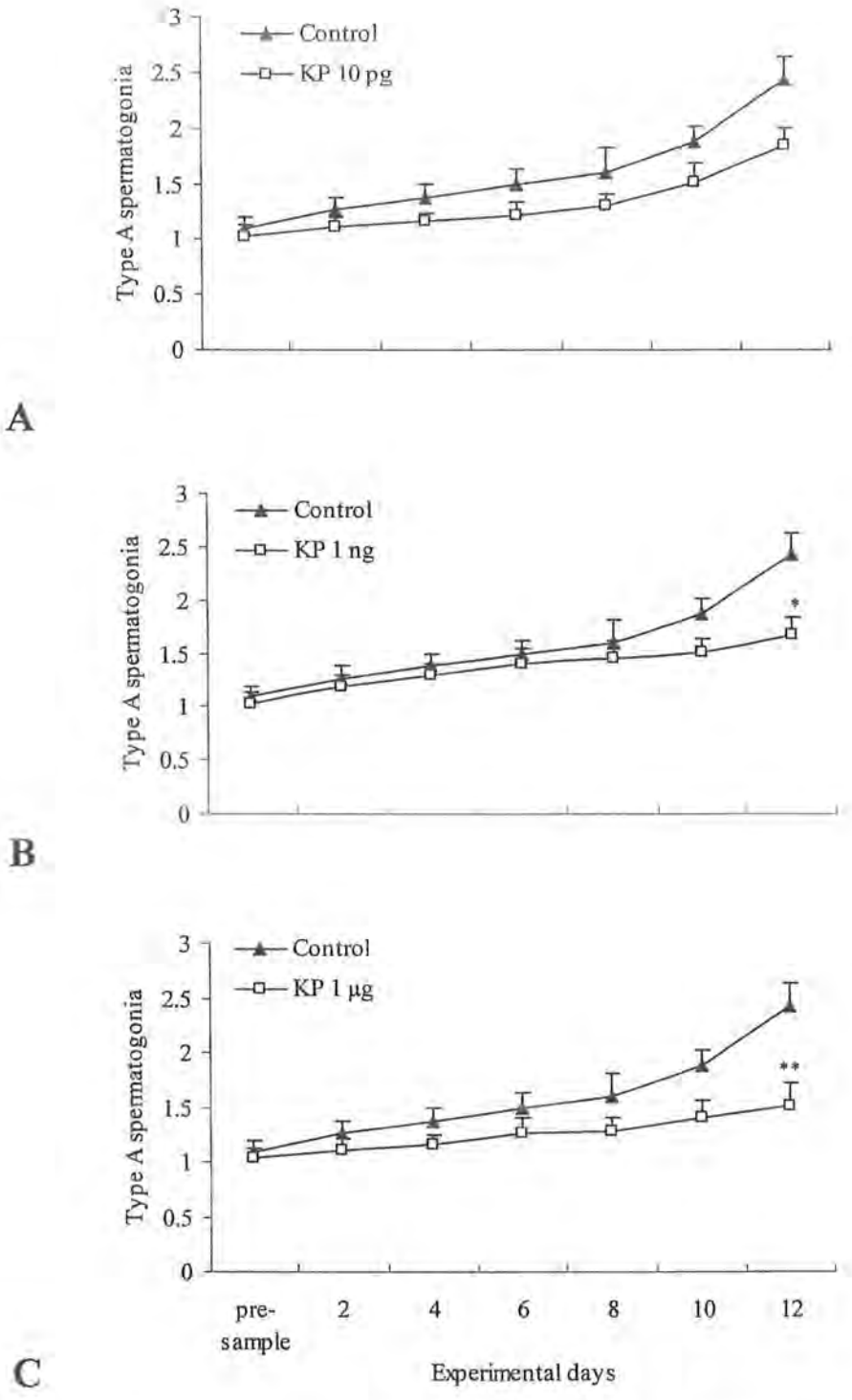

Figure 3.7 Number of type A spermatogonia following 10 pg (A), 1 ng (B) and 1 µg (C) doses after 2, 4, 6, 8, 10 and 12 days of alone kisspeptin treatment. Type A spermatogonia decreased significantly in 1 ng and 1 µg treatment groups only after 12 days of treatment. Values are expressed as mean ± SE. $^{*}p < 0.05$, $^{**}p < 0.01$.

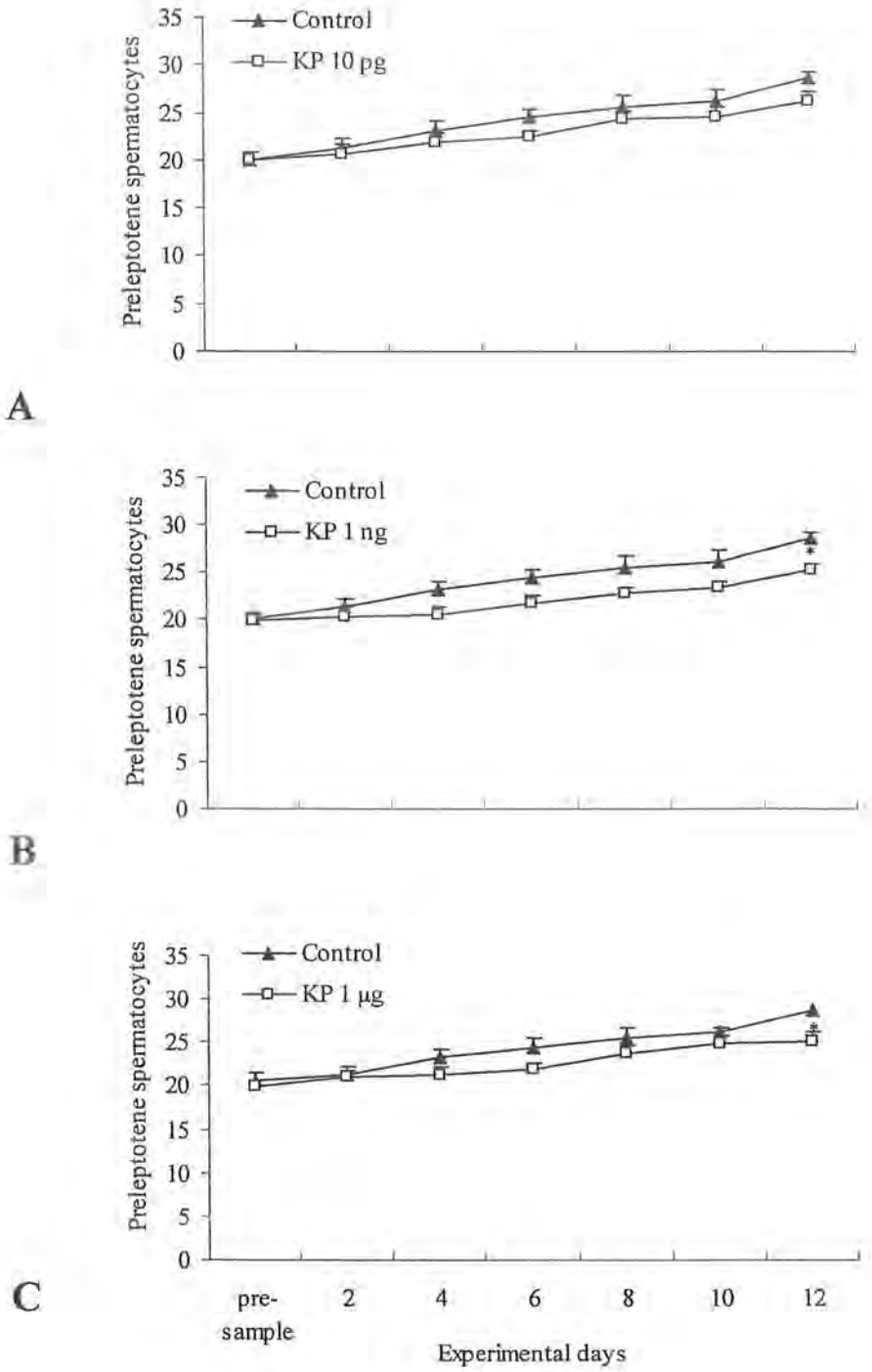

Figure 3.8 Number of preleptotene spermatocytes following 10 pg (A), 1 ng (B) and 1 µg (C) doses after 2, 4, 6, 8, 10 and 12 days of alone kisspeptin treatment. Preleptotene spermatocytes decreased significantly only after 12 days of treatment at 1 ng and 1 µg treatment doses only. They remained unalterted at 10 pg dose. Values are expressed as mean ± SE. $^{*}p < 0.05$.

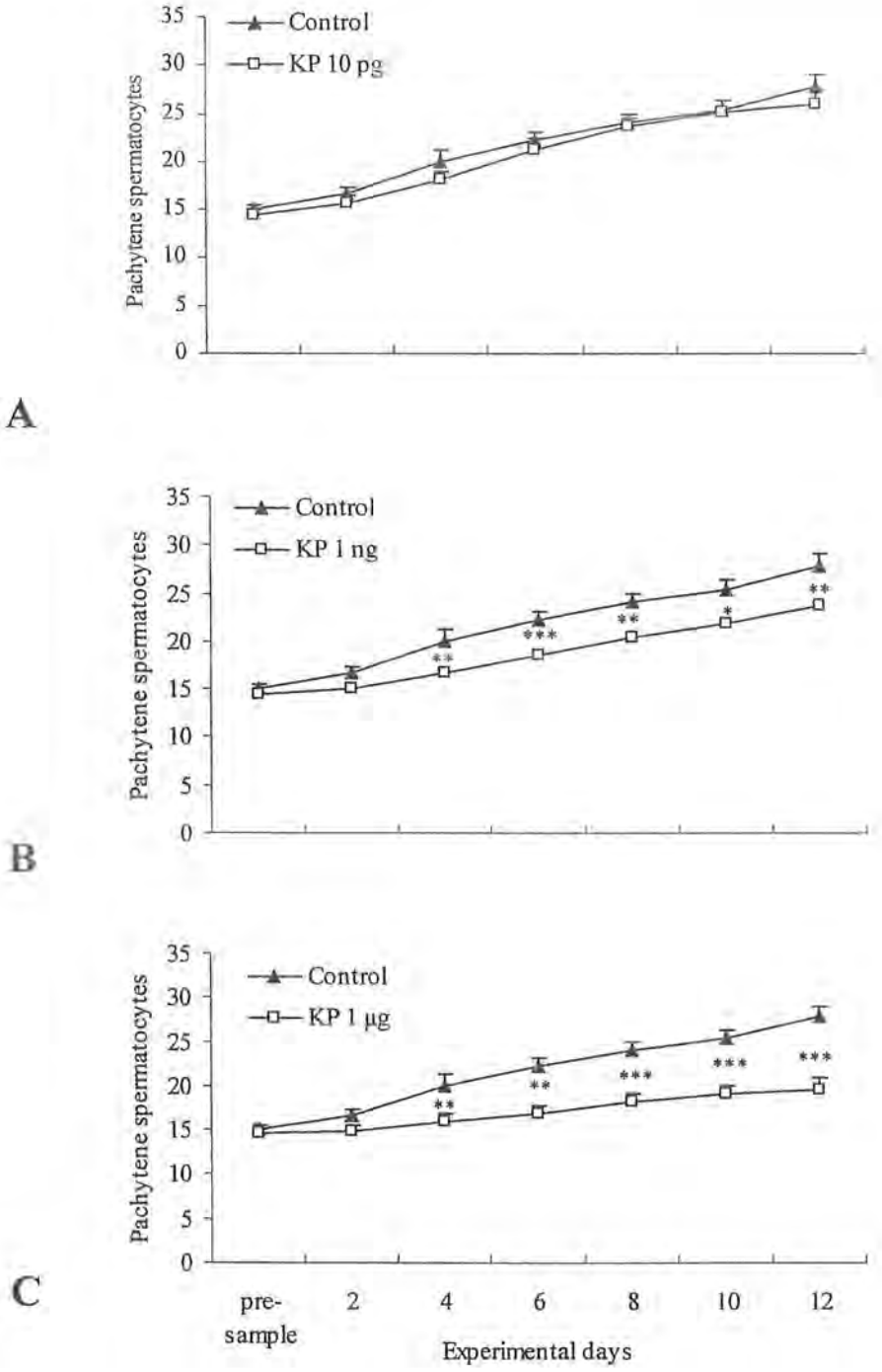

Figure 3.9 Number of pachytene spermatocytes following 10 pg (A), 1 ng (B) and 1 µg (C) doses after 2, 4, 6, 8, 10 and 12 days of alone kisspeptin treatment. Significant decrease occurred in pachytene spermatocytes at 1 ng and 1 µg kisspeptin doses after 4 days of treatment, which continued to 12 days. No effect was observed at 10 pg kisspeptin dose throughout the experiment. Values are expressed as mean ± SE. $^{*}p < 0.05$, $^{**}p < 0.01$, $^{***}p < 0.001$.

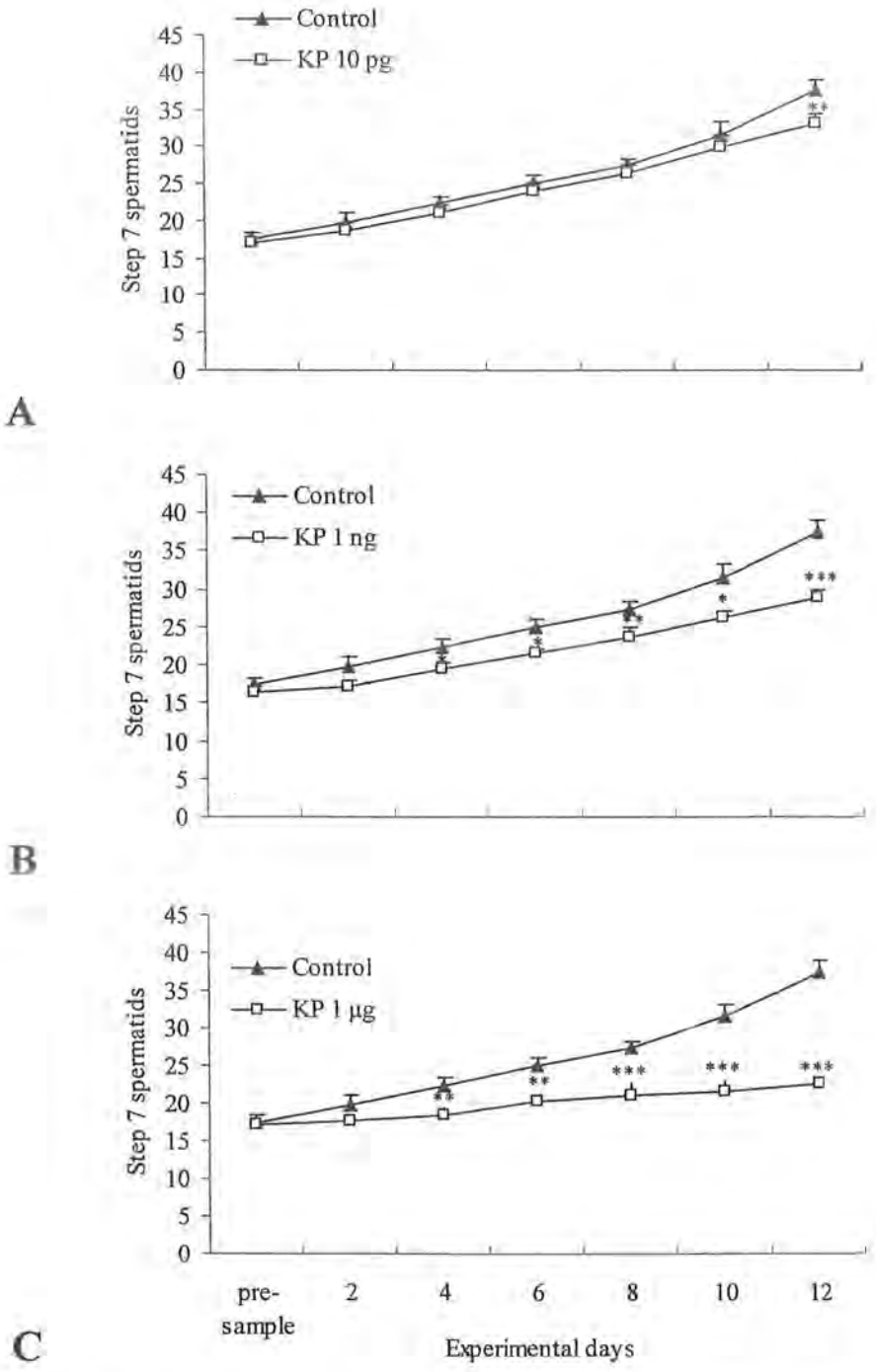

Figure 3.10 Number of step 7 spermatids following 10 pg (A), 1 ng (B) and 1 µg (C) doses after 2, 4, 6, 8, 10 and 12 days of alone kisspeptin treatment. Step 7 spermatids decreased significantly in 1 ng and 1 µg treatment groups after 4 days of treatment and thereafter, decreased gradually upto 12 days. 10 pg dose of kisspeptin caused a decrease in step 7 spermatids only after 12 days of treatment. Values are expressed as mean ± SE. $^{*}p < 0.05$, $^{**}p < 0.01$, $^{***}p < 0.001$.

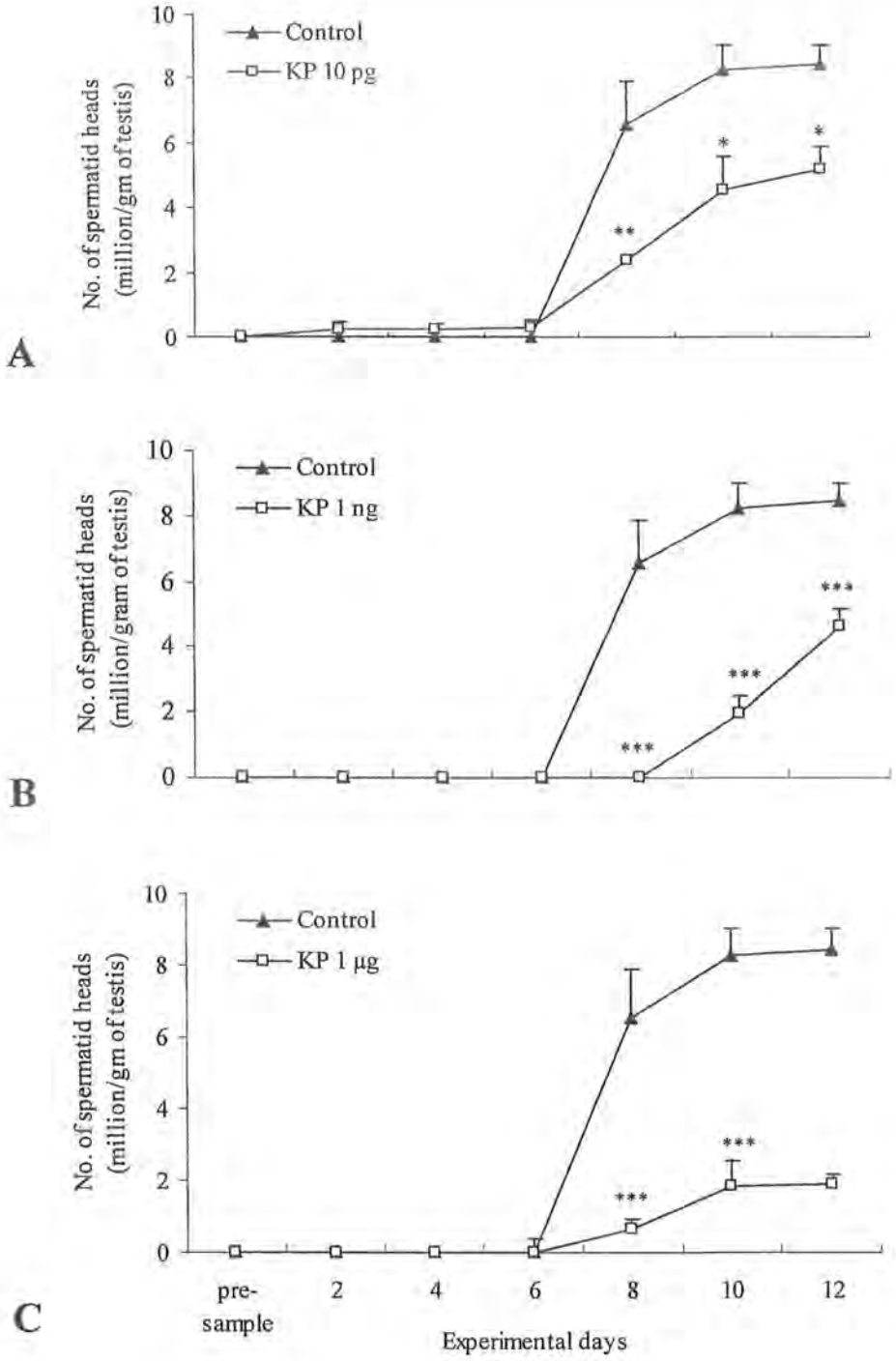

Figure 3.11 Number of elongated spermatid heads per gram of testis following 10 pg (A), 1 ng (B) and 1 µg (C) doses after 2, 4, 6, 8, 10 and 12 days of alone kisspeptin treatment. A few elongated spermatids were observed before 41 days i.e. at 6 days of kisspeptin treatment. Elongated spermatids decreased significantly at all doses. Values are expressed as mean ± SE. $^{*}p < 0.05$, $^{**}p < 0.01$, $^{***}p < 0.001$.

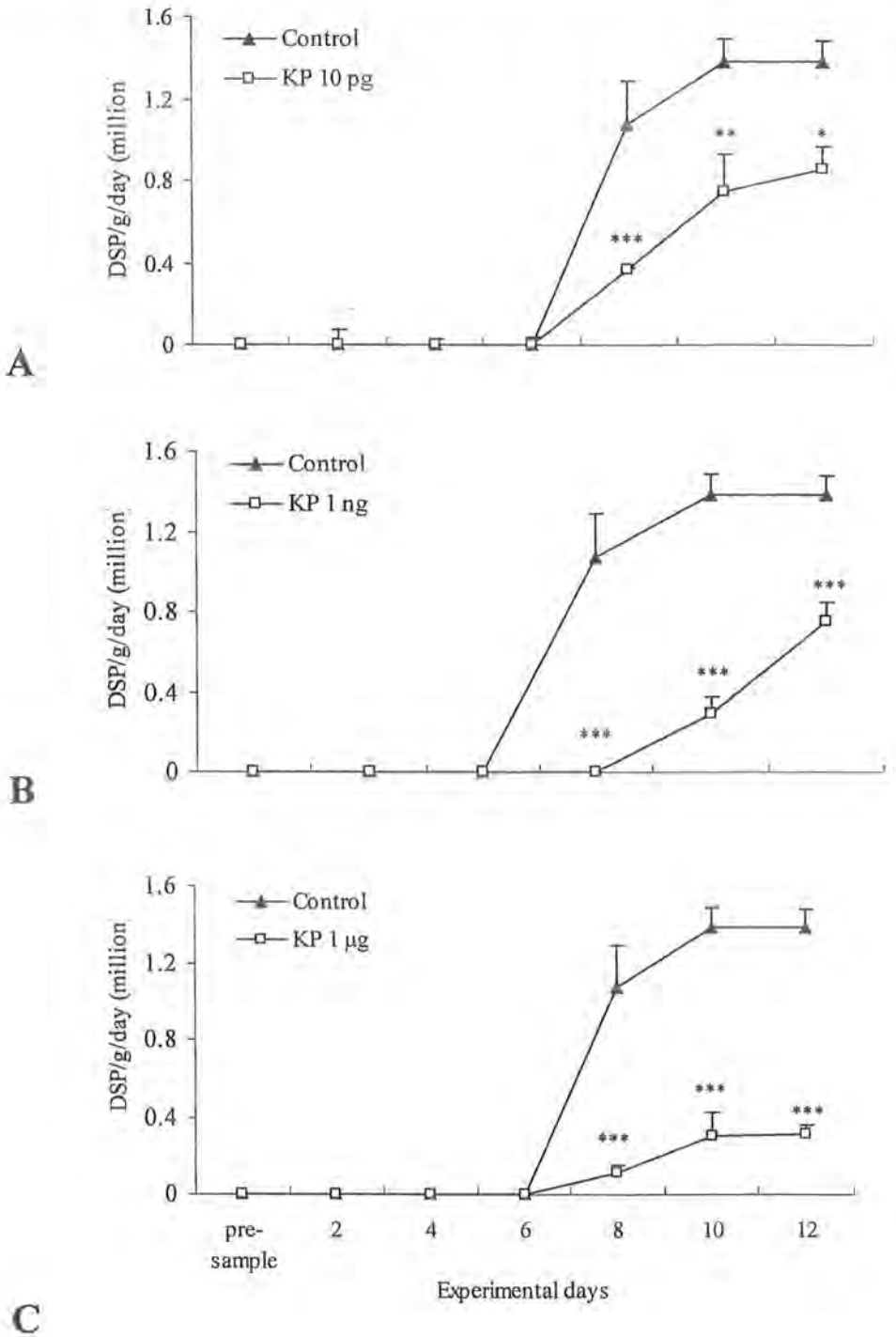

Figure 3.12 Daily sperm production per gram of testis per day following 10pg (A), 1 ng (B) and 1 µg (C) doses after 2, 4, 6, 8, 10 and 12 days of kisspeptin treatment. Daily sperm production decreased significantly at all kisspeptin doses after 8, 10 and 12 days of treatment. Values are expressed as mean ± SE. $^{*}p < 0.05$, $^{**}p < 0.01$, $^{***}p < 0.001$.

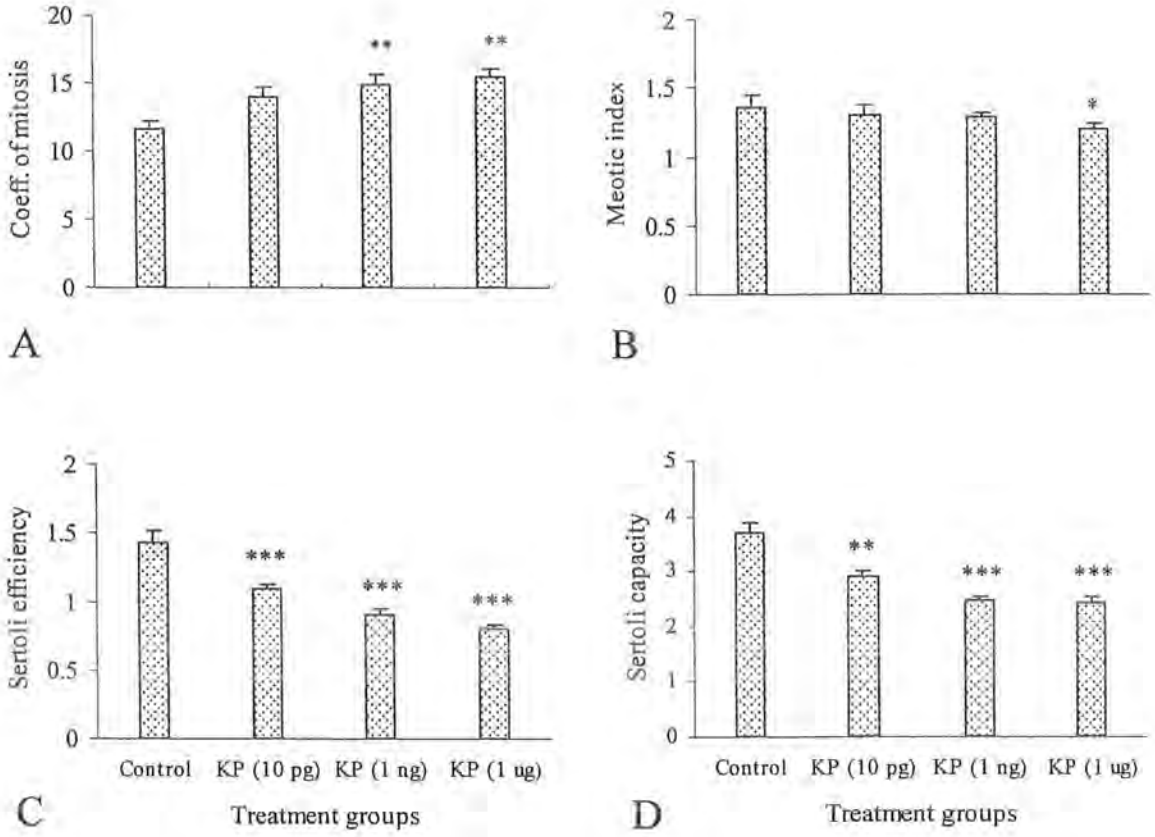

Figure 3.13 Cell ratios from corrected counts after 12 days of kisspeptin treatment.

A Coefficient of efficiency of spermatogonial mitosis increased at 1 ng and 1 μg doses, while at 10 pg it remained similar to control.

B Rate of germ cell loss during meiosis (meiotic index) decreased at 1 μg dose only.

C Sertoli efficiency decreased highly significantly at all kisspeptin doses.

D Total support capacity of each Sertoli cell (Sertoli capacity) decreased highly significantly at all treatments. Values are expressed as mean ± SE.

$^{*}p < 0.05$, $^{**}p < 0.01$, $^{***}p < 0.001$.

Testes from rats treated with 1 µg kisspeptin

At 1 µg kisspeptin dose, marked degeneration of seminiferous tubules was evident. Leydig cell aggregations with loss of contact with the seminiferous tubules were frequent. Spermatogonia were regressed and hyperchromatic. Pachytene spermatocytes were deshaped and showed cellular and nuclear elongations. Spermatocytes indicated necrosis, nuclei were pyknotic. Round and elongated spermatids were scanty indicating maturation arrest. Luminal space was increased while the epithelial height decreased (Fig. 3.14 g-h). Intraepithelial vacuolizations were also evident. Many tubules contained multinucleated giant cell formation and atrophied germinal epithelium (Fig. 3.15 b-c).

3.1.9 Electron microscopic examination

Control testes

The spermatogonia were recognized as ovoid cells situated at the periphery of the seminiferous tubules. These were characterized by large ovoid nuclei containing finely granular nucleoplasm. The nuclei were situated with their long axis parallel to the boundary tissue, the chromatin was homogenous and the cytoplasm was granular (Fig. 3.16 a). The primary spermatocytes had spherical nuclei with finely granular nucleoplasm and chromatin accumulation. The secondary spermatocytes were rarely seen among the germinal cells. They were smaller in size than the late primary spermatocytes. The nuclei were spherical with centrally located clumps of chromatin substance (Fig. 3.17 a). The early spermatids were round with large spherical nuclei which contained chromatin clumps against a lightly stained cytoplasm (Fig. 3.18 a).

Sertoli cells were recognized by the cytoplasm that extended from the basal lamina to the lumen of the seminiferous tubules and enveloped the adjacent germinal elements. Sertoli cell nuclei were infolded, had irregular shapes but the nucleoplasm was homogenous. The cytoplasm contained abundant endoplasmic reticulum, ovoid Golgi apparatus and spherical or cylinder shaped mitochondria (Fig. 3.16 a).

Leydig cells were present in the intestitium. Their nuclei were eccentrically placed within the cell and usually displayed a round or irregular cell shape. They were

recognized by the heterochromatin associated with the inner nuclear envelope (Fig. 3.18 a).

Testes from rats treated with 10 pg kisspeptin

At 10 pg kisspeptin dose, the seminiferous tubules showed a cellular architecture more or less similar to that found in the control groups. Spermatogonia were least affected, the cytoplasm of these cells was more or less electron dense. Primary spermatocytes and Sertoli cells also contained vacuolated mitochondria. The spermatids however showed changes even at this low dose. The cytoplasm was of moderate electron density. The nuclei were reduced in size with coarse granular chromatin distributed within the karyoplasms. The acrosome showed involutions towards the nucleus and the outline was highly irregular. A few step 7 spermatids had normal acrosome (Fig. 3.17 b). Leydig cell nuclei were irregular shaped with nuclear membrane invaginations. The cytoplasmic organelles were dilated (Fig. 3.18 b).

Testes from rats treated with 1 ng kisspeptin

In addition to the above mentioned changes, testes showed enlarged intercellular spaces. The basal laminae were not laminated and appeared thin (Fig. 3.16 b). Step 7 spermatids contained abnormal acrosome (and 3.17 c). Leydig cell nuclei demonstrated massive nuclear envelop invaginations. Nuclear sizes were greatly reduced (Fig. 3.18 c).

Testes from rats treated with 1 µg kisspeptin

At 1 µg kisspeptin dose, the seminiferous tubules showed exaggerated features of focal areas of spermatogenic arrest depicted by degenerative changes in the germinal cells. The Sertoli cells had massive cytoplasmic vacuolations. Dilatation of the endoplasmic reticulum was frequent (Fig. 3.16 c and 3.17 d). Leydig cells were prominently defective and vacuolated (Fig. 3.18 d).

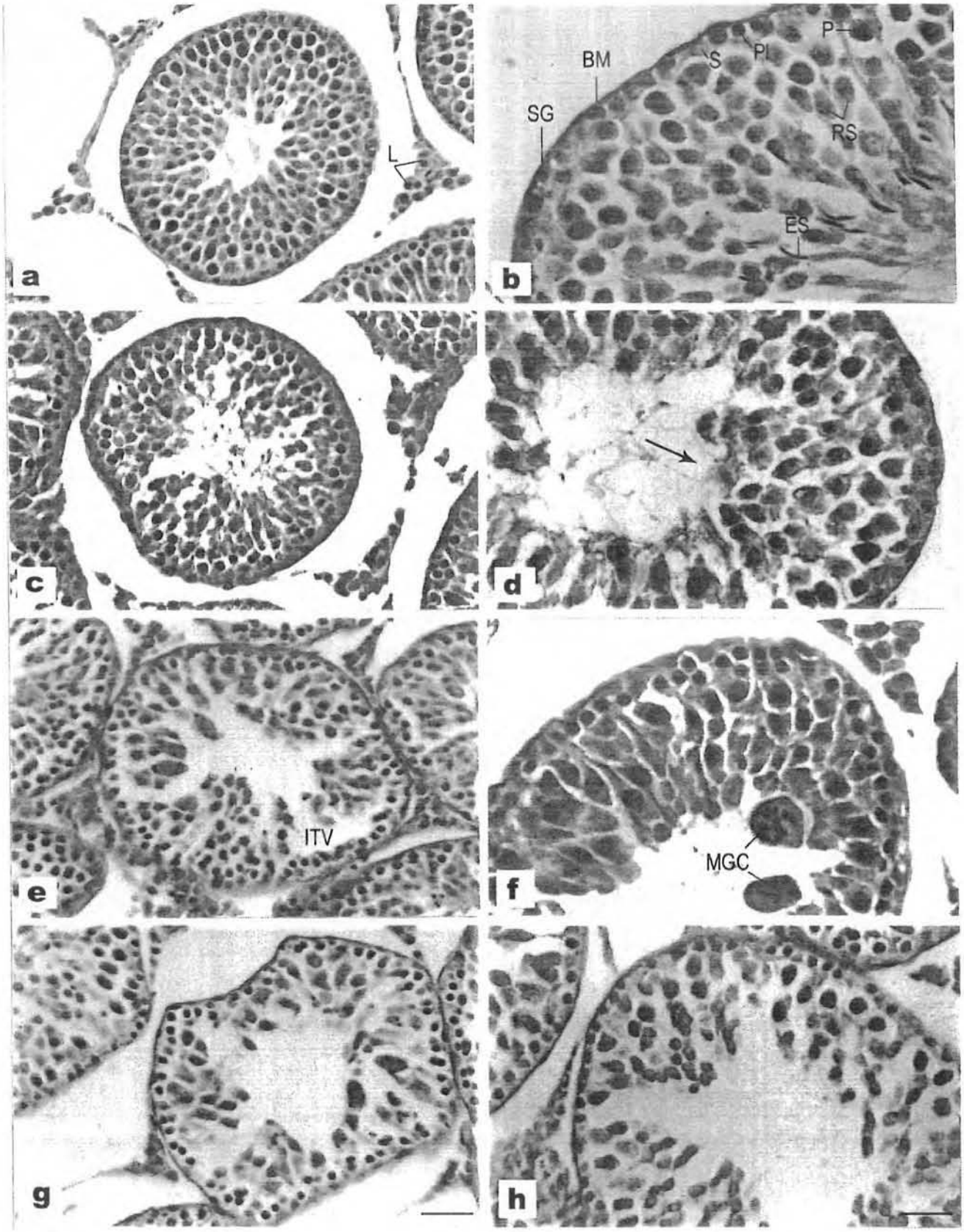
a
L
b
BM
SG
S
Pl
P
RS
ES
c
d
e
ITV
f
MGC
g
h

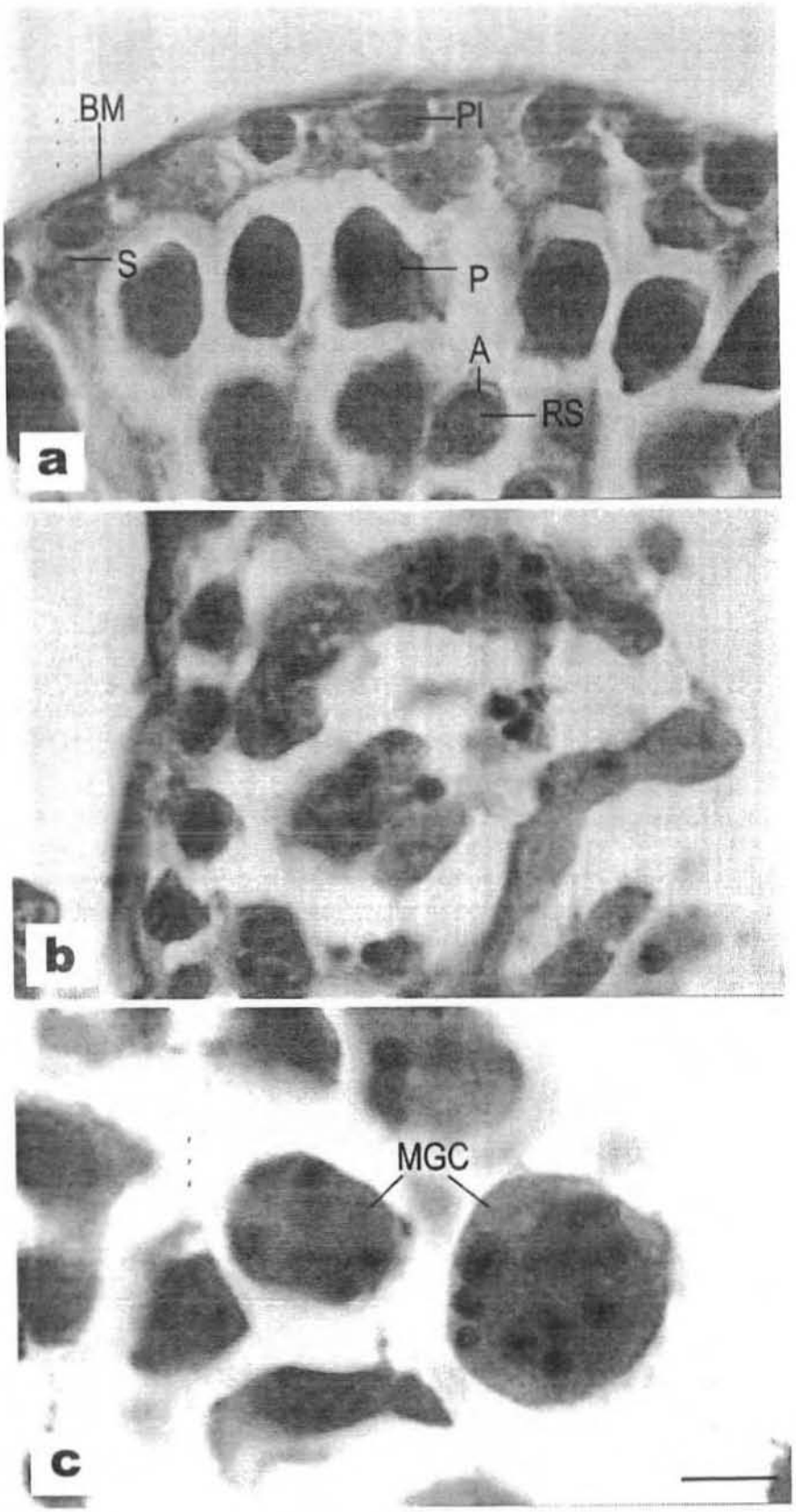
BM
Pl
S
P
A
RS
a
b
MGC
c

a: Seminiferous tubule from control rat showing the basement membrane (BM), Sertoli cell nucleus (S), type A spermatogonia (A) and pachytene spermatocytes (P).

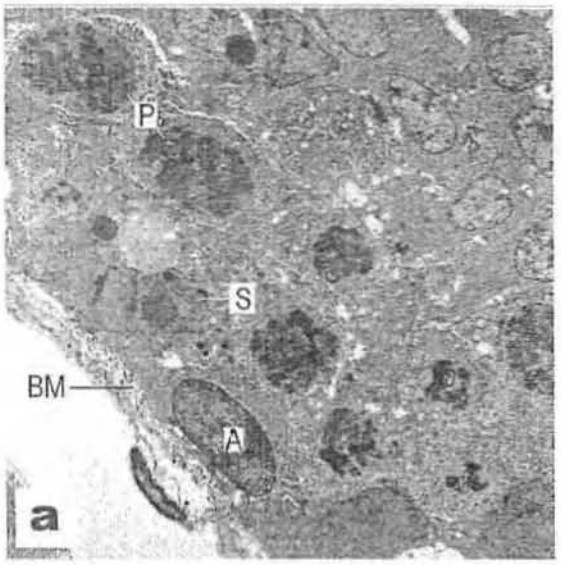

b: Seminiferous tubule from rats treated with 1 ng kisspeptin. Note pachytene spermatocytes, abnormal step 7 spermatids (arrow) and enlarged intercellular spaces (*). Basement membrane is thin and irregular.

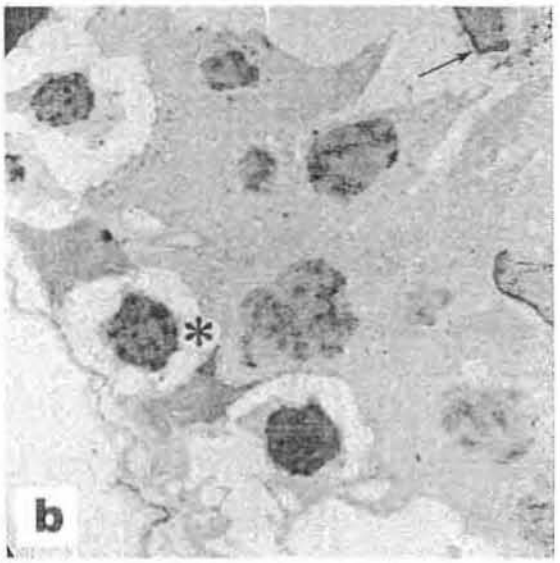

c: Seminiferous tubule from rats treated with 1 μg kisspeptin, showing abnormal spermatogonia, vacuolated Sertoli cells, spermatocytes and spermatids. Tubular organization appears deranged with enlarged intracellular spaces.

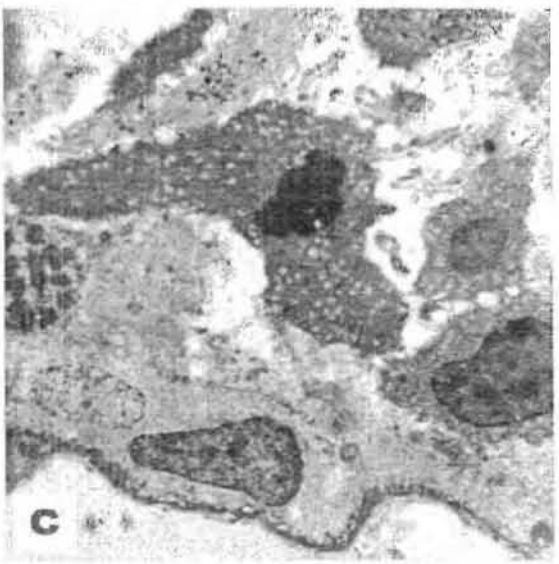

Figure 3.16 Electron micrographs of testicular tissue of control and kisspeptin treated rats. Magnification a-c = ×3000.

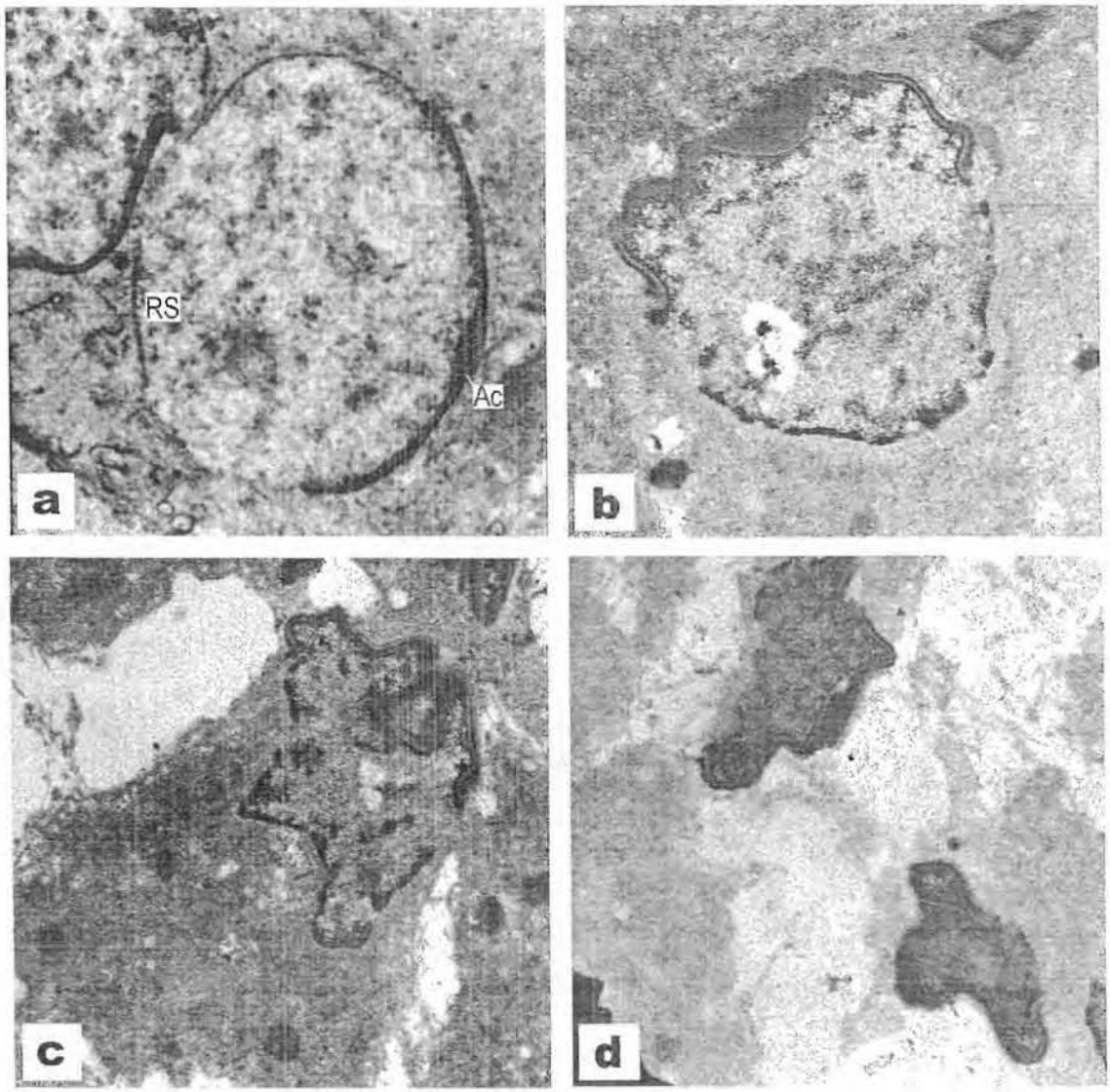

Figure 3.17 Electron micrographs of control round spermatids and treated with kisspeptin alone at variable doses.

a: The spermatids (RS) in control rats appear round cells with large spherical nuclei. The acrosome system (Ac) covers nearly one-third to one-half of the step 7 spermatid nucleus.

b: The spermatids showed less morphplogical alterations at 10 pg dose. The acrosome inverted towards the nucleus and its outline is irregular, both the acrosomal granule and vesicle are detached from the nuclei. The acrosome was not electron-dense and had an enlarged acrosomal vesicle.

c: Note excessive damage to spermatids after treatment with 1 ng dose. Spermatids show electron dense cytoplasm with prominent vacuolations. The nuclear membranes appear highly distorted and ruptured in some areas. The intercellular spaces were enlarged.

d: Cellular damage is more pronounced at 1 μg kisspeptin treatment. The intercellular spaces are greatly enlarged.

Magnification a-d = ×12,000.

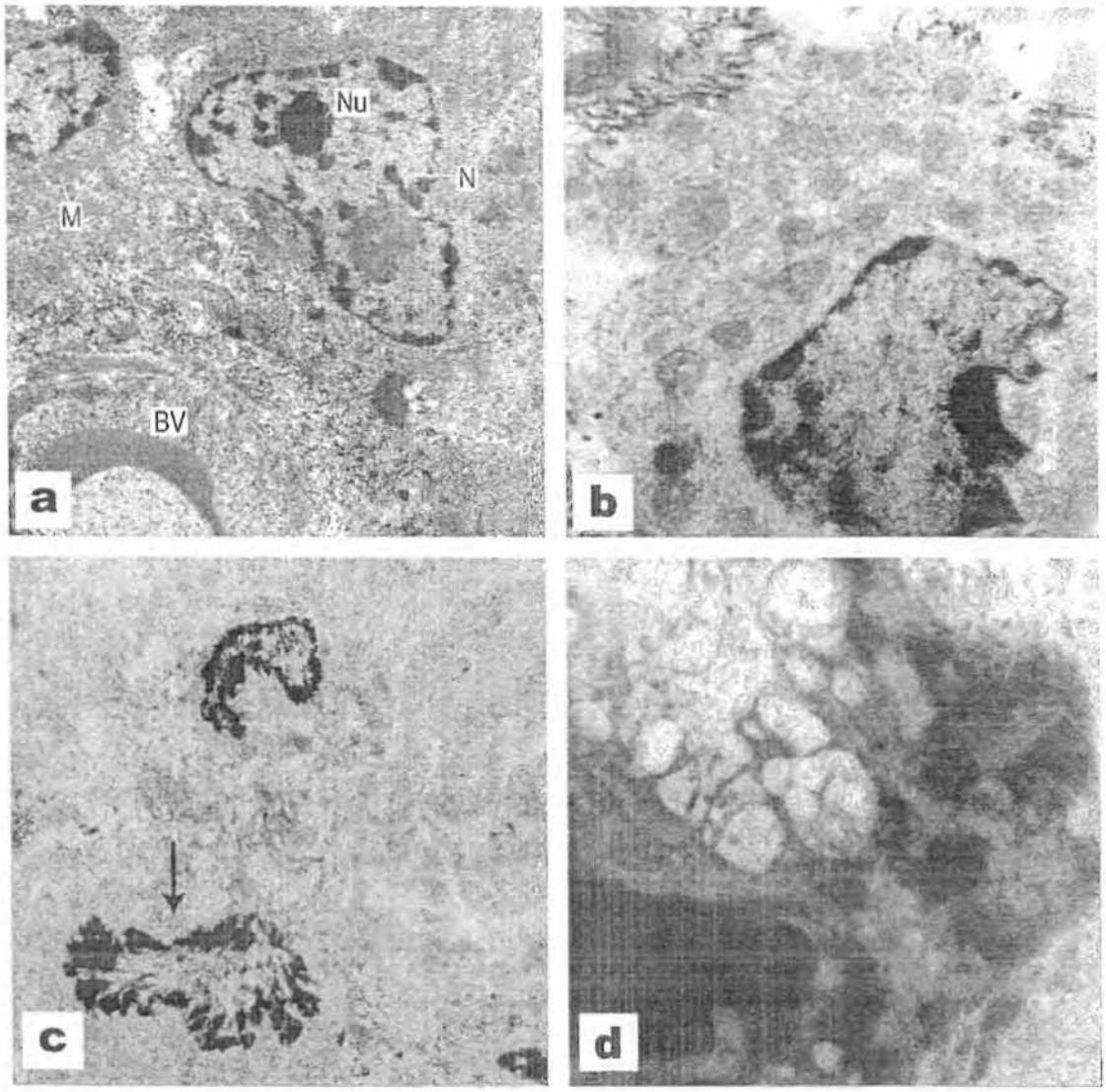

Figure 3.18 Electron micrographs of Leydig cell from rats treated with kisspeptin alone at variable doses.

a: A Leydig cell from a control rat shows nucleus (N) with conspicuous nucleolus (Nu). In the cytoplasm, elongated mitochondria (M) containing tubular cristae are present. A blood vessel (BV) is also evident. ×12,000.

b: At 10 pg dose, Leydig cell nucleus appears deshaped, shrunken and heterochromatic indicating decline of activity. The chromatin is clumped at some places with in the karyoplasm. ×20,000.

c: At 1 ng dose of kisspeptin, Leydig cell nuclei were reduced greatly in size with clear invagination of the nuclear envelop (arrow). ×12, 000.

d: Note excessive degeneration in the Leydig cells structure at 1 μg kisspeptin dose. Cytoplasm is electron dense and vacuolated. ×20,000.

3.1.10 DNA fragmentation

Ladder assay demonstrated DNA fragmentation in the testicular tissue. Fragments of 180-bp subunits and 400-bp subunits were observed at 10 pg kisspeptin, while high dose of 1 ng and 1 μg kisspeptin produced 180, 400, 650-bp and 780-bp DNA subunits. DNA fragmentation was scarcely visible in control testicular tissue (Fig. 3.19A).

To quantify the dose dependent characteristics of DNA fragmentation, the ratio of fragmented DNA relative to total DNA was determined in all the treatment groups as well as control testes after 12 days of treatment. Percent DNA fragmention gradually increased at the highest tested dose of kisspeptin. The % DNA fragmention increased significantly in 10 pg treatment group ($p < 0.05$) while it increased significantly at 1 ng and 1 μg dose groups ($p < 0.001$) as compared to control (Fig. 3.19B).

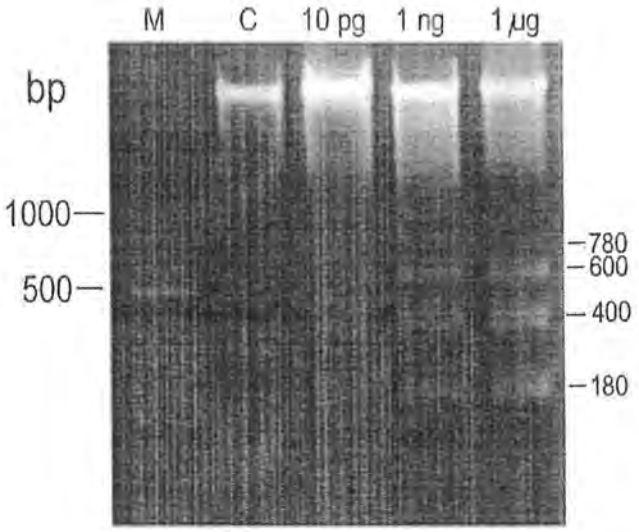

A

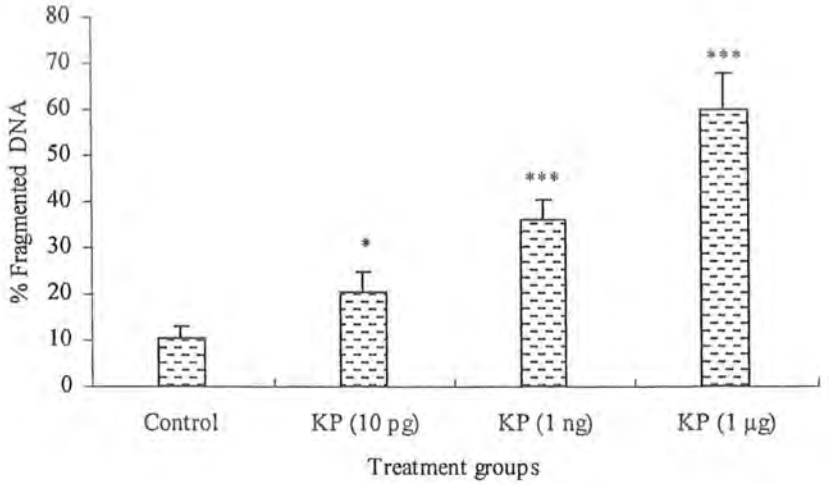

B

Figure 3.19 A) DNA ladder assay of rat testis showing 180, 400, 600 and 780 bp bands of fragmented DNA, at 1 ng and 1 µg kisspeptin doses. Weaker fragments were also visible in the 10 pg dose. Control DNA was intact (lane C). M= 100-bp DNA ladder.

B) DNA fragmentation assay. Percentage of fragmented DNA relative to total DNA increased significantly at all kisspeptin doses. Values are expressed as mean ± SE. $^{*}p < 0.05$, $^{***}p < 0.01$ compared to control rat testes DNA.

Experiment 2: Indirect blockade of endogenous kisspeptin action after pretreatment with acyline, a GnRH antagonist

3.1.11 Body weight and testicular parameters

No difference was found in body weight, testicular weight, testis volume, Gonadosomatic index (%) and epididymes weights between control, kisspeptin, saline (acyline pretreated) and kisspeptin (acyline pretreated) (Table 3).

3.1.12 Seminiferous tubular diameter and epithelium height

Seminiferous tubular diameter was not effected at any of the treatment doses (Table 1). Seminiferous tubular epithelial height decreased highly significantly ($p < 0.001$) in treated groups as compared to control. Intergroup comparison showed no difference between kisspeptin (acyline pretreated) and alone kisspeptin treatment, whereas, it increased highly significantly ($p < 0.001$) in kisspeptin (acyline pretreated) group as compared to saline treated (acyline pretreated) group (Table 3).

3.1.13 Plasma hormone levels

Following acyline administration, a significant decrease was observed in plasma FSH ($p < 0.001$) (Fig. 3.20 B), LH ($p < 0.001$) (Fig. 3.20 E) and testosterone levels ($p < 0.001$) (Fig. 3.20 H), at day 1 of the experiment.

After 12 days of treatment, following kisspeptin alone challenge, plasma FSH levels were unaltered. They decreased highly significantly ($p < 0.001$) in the saline (acyline pretreated) and kisspeptin (acyline pretreated) treated groups as compared to the control nontreated rats (Fig. 3.20 C).

Plasma LH levels decreased significantly ($p < 0.01$) in kisspeptin alone and saline (acyline pretreated) treated groups. In contrast LH concentration decreased further in kisspeptin (acyline pretreated) group ($p < 0.001$). On intergroup comparison, LH concentration showed non-significant decrease in kisspeptin (acyline pretreated) treated group as compared to the saline (acyline pretreated) control (Fig. 3.20 F).

Table 3 Effect of kisspeptin (KP) on testicular parameters in different experimental groups of prepubertal male n=10 rats. Mean±SD.

	Control	Kisspeptin alone	Saline (Acyline pretreated)	KP (Acyline pretreated)
Body weight (g)	108.41 ± 18.98	115.54 ± 11.96 ^{ns}	122.00 ± 20.54^{ns}	120.20 ± 31.49^{ns}
Testis weight (g)	1.02 ± 0.18	1.03 ± 0.16 ^{ns}	1.05 ± 0.10 ^{ns}	1.04 ± 0.07 ^{ns}
Testis volume (mm^3)	1.06 ± 0.25	0.96 ± 0.13 ^{ns}	1.01 ± 0.08 ^{ns}	1.04 ± 0.07 ^{ns}
Gonadosomatic Index (%)	0.93 ± 0.13	0.85 ± 0.13 ^{ns}	0.88 ± 0.19 ^{ns}	0.91 ± 0.19 ^{ns}
Epididymus weight (g)	319.20 ± 27.41	275.6 ± 36.28 ^{ns}	308.00 ± 64.18 ^{ns}	296.4 ± 66.36^{ns}
Epithelium height (μm)	63.06 ± 7.97	53.25 ± 5.69^{a***}	42.54 ± 5.79^{a,b***}	54.58 ± 5.43^{a,c***}
Seminiferous tubular diameter (μm)	170.52 ± 12.16 ^{ns}	167.37 ± 10.33 ^{ns}	169.24 ± 10.24 ^{ns}	169.24 ± 10.24 ^{ns}

Difference from Control = $^{*}p < 0.05$, $^{**}p < 0.01$, $^{***}p < 0.001$

a=difference from control group,

b= difference from kisspeptin (KP) group,

c= difference between saline (pre-treated with acyline) and kisspeptin (pre-treated with acyline) group.

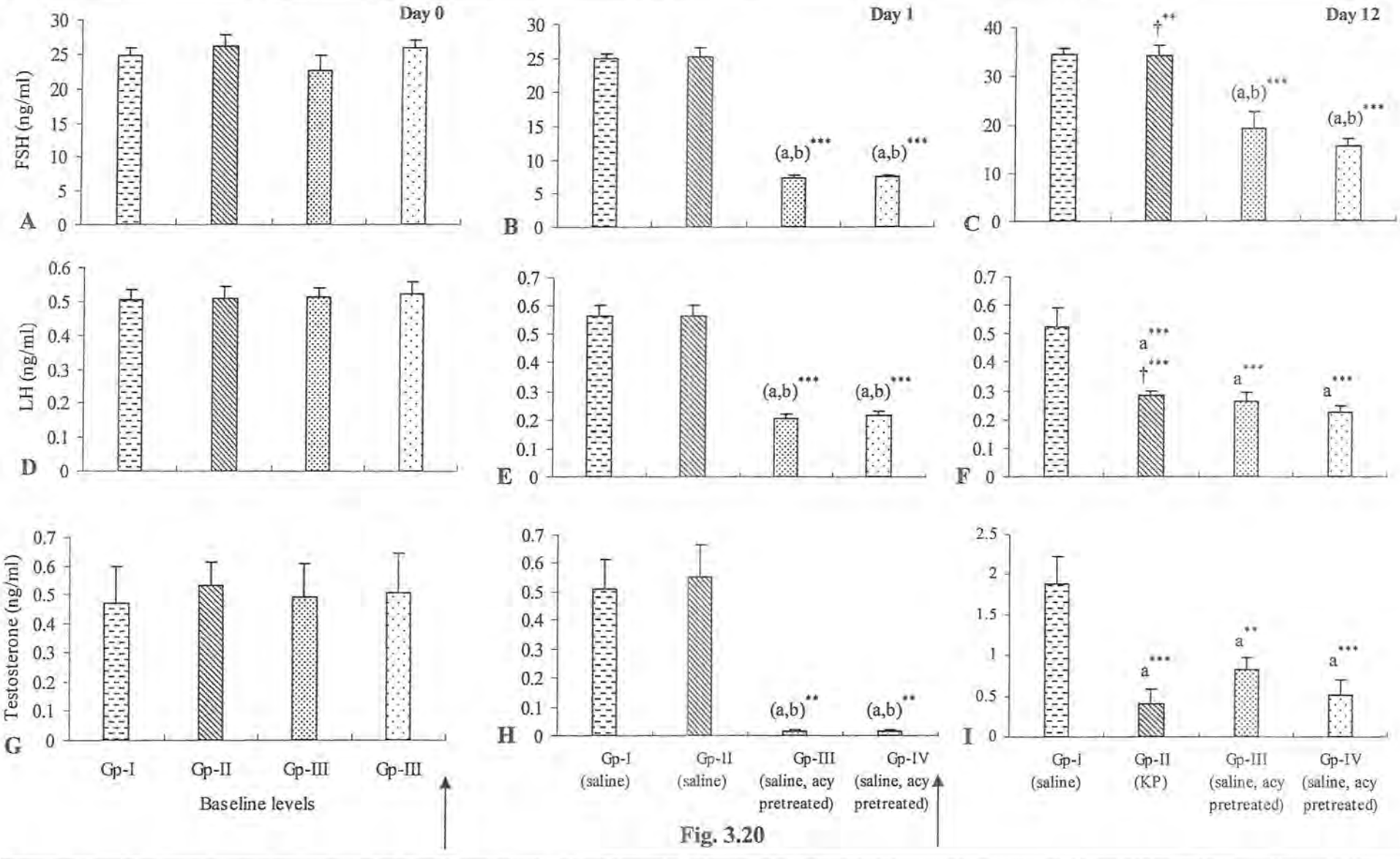
Day 0
Day 1
Day 12
FSH (ng/ml)
LH (ng/ml)
Testosterone (ng/ml)
A
B
C
D
E
F
G
H
I
(a,b)***
(a,b)**
a***
a**
†**
†***
Gp-I
Gp-II
Gp-III
Gp-III
Baseline levels
Gp-I (saline)
Gp-II (saline)
Gp-III (saline, acy pretreated)
Gp-IV (saline, acy pretreated)
Gp-II (KP)

Fig. 3.20

Plasma testosterone concentration decreased highly significantly ($p < 0.001$) with the kisspeptin alone treatment and where kisspeptin was given after acyline pretreatment ($p < 0.01$) than the saline treated rats. Between group comparisons showed no difference in the kisspeptin (acyline pretreated) and saline (acyline pretreated) groups (Fig. 3.20 I).

3.1.14 Quantitative data on spermatogenic cells

Type A spermatogonia decreased highly significantly ($p < 0.001$) in all treatment groups versus control. Intergroup comparison showed that compared to kisspeptin alone and saline (acyline pretreated) group, they increased highly significantly ($p < 0.001$) in kisspeptin (acyline pretreated) group although not approaching control values (Fig. 3.21 A).

Preleptotene spermatocytes decreased ($p < 0.001$) in the kisspeptin alone and in saline (acyline pretreated) groups ($p < 0.05$), whereas kisspeptin (acyline pretreated) group showed unremarkable difference as compared to control. On intergroup comparison, it was found that preleptotene spermatocytes increased significantly ($p < 0.01$) in the kisspeptin (acyline pretreated) group as compared to both the saline (acyline pretreated) and kisspeptin alone groups. Compared to saline (acyline pretreated) group preleptotene spermatocytes decreased ($p < 0.01$) in the alone kisspeptin treatment group (Fig. 3.21 B).

Pachytene spermatocytes decreased highly significantly in both the kisspeptin alone ($p < 0.001$) and saline (acyline pretreated) ($p < 0.01$) treated groups, while no significant difference was observed between the kisspeptin (acyline pretreated) treated group than the control. When intergroup comparisons were made, compared to saline (acyline pretreated) treated group, significant increase was found ($p < 0.001$) in the kisspeptin (acyline pretreated) treated group (Fig. 3.21 C).

A highly significant decrease ($p < 0.001$) was found in step 7 spermatids in kisspeptin alone and saline (acyline pretreated) treated groups. In contrast, kisspeptin (acyline pretreated) treated group showed no difference from saline treated rats. Intergroup comparison showed highly significant ($p < 0.001$) increase in step 7

spermatids in kisspeptin treated (acyline pretreated) group as compared to the saline (acyline pretreated) treated group. Alone kisspeptin treatment led to a significant decrease ($p < 0.001$) in step 7 spermatids from saline treated control rats (Fig. 3.21D).

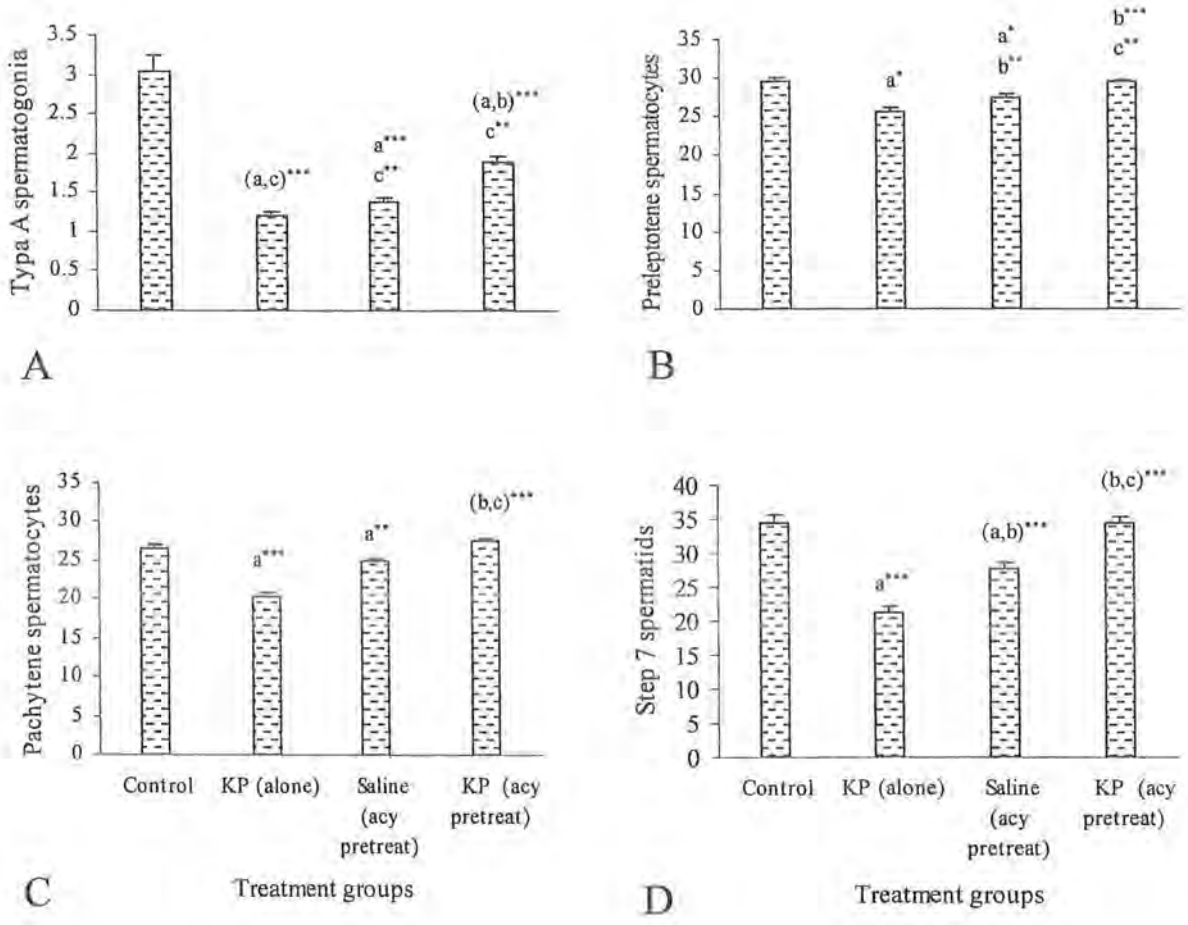

Figure 3.21 Number of germ cells per 100 round seminiferous tubules at stage VII of spermatogenesis. Type A spermatogonia (A), preleptotene spermatocytes (B), pachytene spermatocytes (C) and step 7 spermatids (D) decreased significantly in saline (acyline pretreated) group. With kisspeptin (acyline pretreated) they increased as compared to saline treatment (acyline pretreatment). a= difference from control group, b= difference from kisspeptin group, c= difference between saline (acyline pretreated) group and kisspeptin (acyline pretreated) group. Values are expressed as ± SE. $^{**}p < 0.01$, $^{***}p < 0.001$.

3.1.15 Elongated spermatid heads and daily sperm production

Elongated spermatids (g^{-1} testis wt.) and daily sperm production (g^{-1} of testis weight day^{-1}) both decreased significantly ($p < 0.01$) in the kisspeptin alone and saline (acyline pretreated) treated groups but in the kisspeptin (acyline pretreated) group, compared to control, no significant difference was found. Both elongated spermatids and daily sperm production increased significantly ($p < 0.01$) in the kisspeptin (acyline pretreated) treated group as compared to the saline (acyline pretreated) treatment (Fig. 3.22).

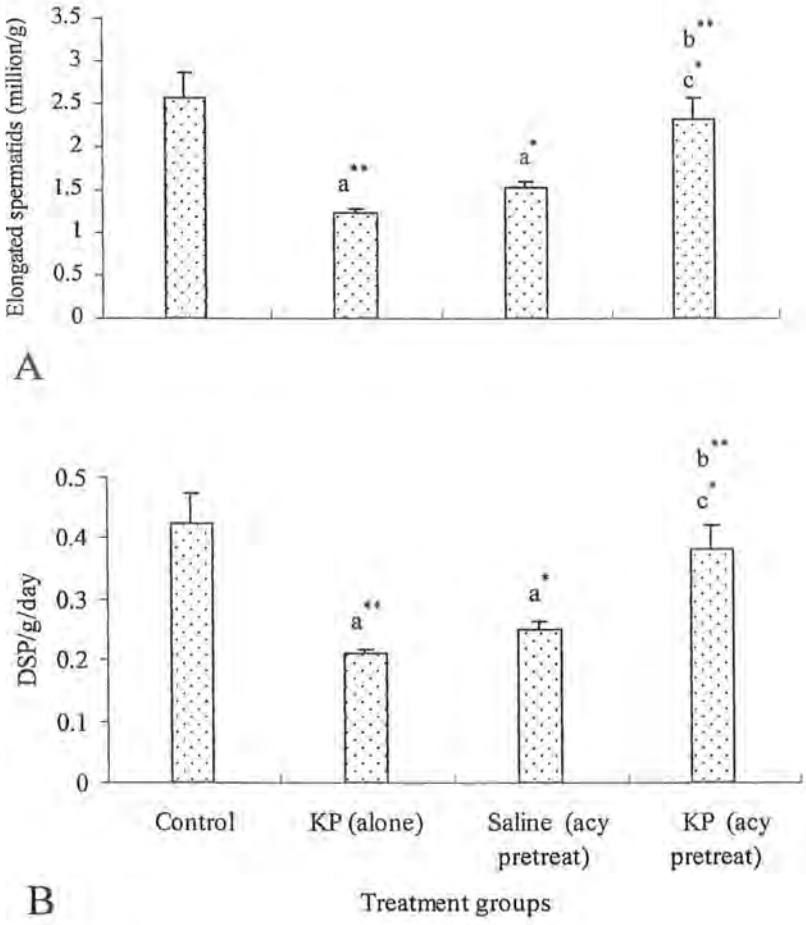

Figure 3.22 Elongated spermatid heads per gram of testis (A) and daily sperm production (DSP) (B) after treatment with saline, kisspeptin alone, saline (acyline pretreated) and kisspeptin (acyline pretreated). a= difference from control group, b= difference from kisspeptin group, c= difference between saline (acyline pretreated) group and Kisspeptin (acyline pretreated) group. Values are expressed as ± SE. $^{*}p < 0.05$, $^{**}p < 0.01$.

3.1.16 Cell ratios from the corrected counts

Coefficient of efficiency of spermatogonial mitosis increased highly significantly in all treatment groups ($p < 0.001$) as compared to control. Intergroup comparison showed significantly ($p < 0.001$) decreased coefficient of efficiency of spermatogonial mitosis in the kisspeptin (acyline pretreated) treated group as compared to the saline (acyline pretreated) treated group (Fig. 3.23 A).

Meiotic index (rate of germ cell loss during meiosis) decreased significantly in the kisspeptin alone ($p < 0.01$) and saline (acyline pretreated) ($p < 0.05$) treated groups, while no difference was evident between the kisspeptin (acyline pretreated) treated and control group. Between group comparison demonstrated that meiotic index increased significantly ($p < 0.05$) in kisspeptin (acyline pretreated) group as compared to saline (acyline pretreat) treated group. Saline (acyline pretreated) and kisspeptin alone groups did not differ significantly (Fig 3.23 B).

Sertoli efficiency decreased ($p < 0.001$) in the kisspeptin alone and saline (acyline pretreated) treated groups ($p < 0.01$), while no difference was observed in kisspeptin (acyline pretreated) treated group as compared to control. Sertoli efficiency increased significantly in kisspeptin (acyline pretreated) treated group as compared to the saline (acyline pretreated) treated group when intergroup comparisons were made. A highly significant ($p < 0.001$) increase was observed in saline (acyline pretreated) as compared to kisspeptin alone group (Fig. 3.23 C).

A highly significant decrease ($p < 0.001$) was noticeable in total support capacity of each Sertoli cell in the kisspeptin alone and in saline treated (acyline pretreated) groups while no difference was found in the kisspeptin (acyline pretreated) treated group as compared to control. Intergroup comparison demonstrated an increase ($p < 0.01$) in total support capacity of each Sertoli cell in the kisspeptin (acyline pretreated) treated group as compared to saline (acyline pretreated) treated group. A highly significant ($p < 0.01$) increase was observed in saline (acyline pretreated) treated as compared to alone kisspeptin treatment (Fig. 3.23 D).

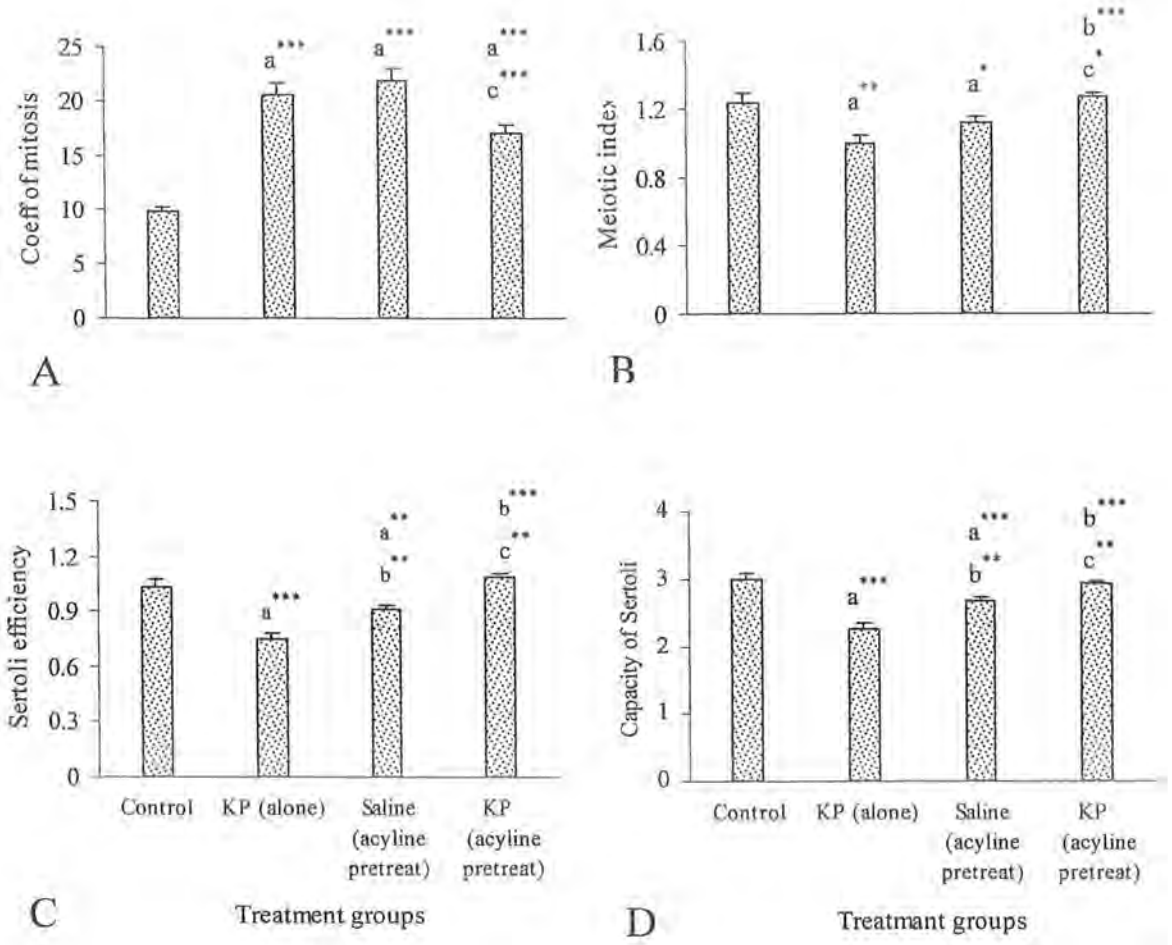

Figure 3.23 Cell ratios from corrected counts following kisspeptin and acyline administration.

A Coefficient of efficiency of spermatogonial mitosis increased in all treated groups as compared to saline treated controls.
B Meiotic index (rate of germ cell loss during meiosis) decreased in kisspeptin alone and saline (acyline pretreated) group while kisspeptin (acyline pretreated) remained similar to control.
C Sertoli efficiency decreased in kisspeptin alone and saline (acyline pretreated) group while kisspeptin (acyline pretreated) remained similar to control.
D Capacity of Sertoli cell decreased in kisspeptin alone and saline (acyline pretreated) group while kisspeptin (acyline pretreated) remained similar to control. a= difference from control group, b= difference from kisspeptin group, c= difference between saline (acyline pretreated) group and KP (acyline pretreated) group. Values are expressed as ± SE. $^{*}p < 0.05$, $^{**}p < 0.01$, $^{***}p < 0.001$.

3.1.17 Effect on histomorphology of seminiferous tubules

Control testes

Light microscopic examination of testicular sections from control saline treated rats showed normal seminiferous tubules with intact seminiferous epithelium (Fig. 3.24 a-b). For details, see section 3.1.8.

Testes from rats treated with kisspeptin alone

With kisspeptin alone treatment, marked degeneration of seminiferous tubules was readily noticeable. Spermatogonia were regressed and hyperchromatic. Spermatocytes were necrosed with pyknotic nuclei. Round and elongated spermatids were scanty indicating maturation arrest. Luminal space was increased while the epithelial height decreased. Many abnormal tubules contained multinucleated giant cells. Atrophy of germinal epithelium was also noticeable (Fig. 3.24 c-d).

Testes from rats treated with saline (acyline pretreated)

Seminiferous tubules showed degenerative changes and intratubular vacuolizations. Germ cells were regressed, atrophied and showed severe necrosis. Loss of germ cells and abnormal cell associations were also evident. Round and elongated spermatids had abnormal acrosome. Tubules were characterized by the secretion of amorphous substance into the lumen and germ cell maturation arrest (Fig. 3.24 e-f).

Testes from rats treated with kisspeptin (acyline pretreated)

Seminiferous tubules of rats treated with kisspeptin (acyline pretreated) revealed partial restoration of spermatogenesis. Close observations at high magnifications showed that preleptotene spermatocytes were ruptured; pachytene spermatocytes were of abnormally large size with larger nuclei containing condensed chromatin. Several round spermatids had abnormally formed acrosome (Fig. 3.24 g-h).

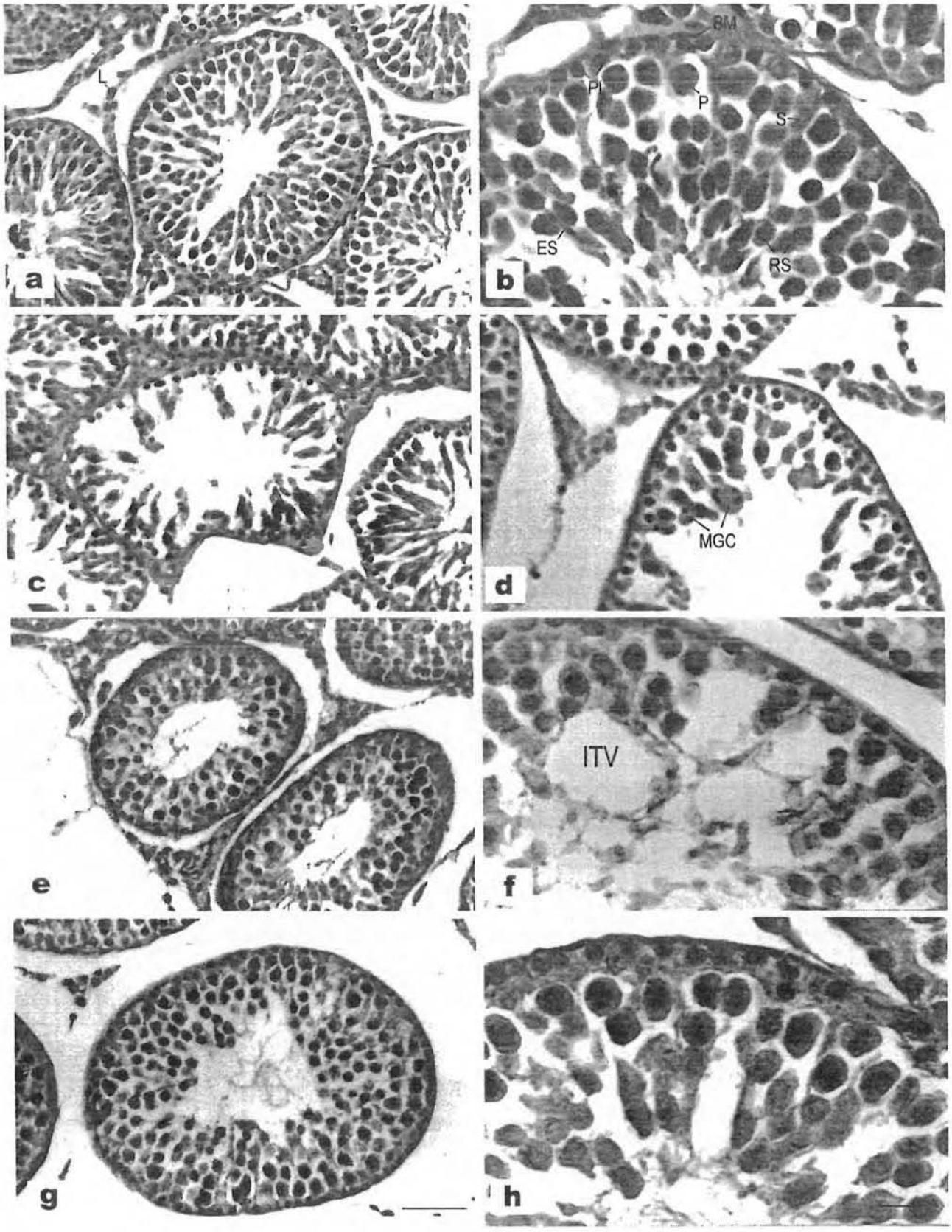
L
a
BM
Pl
P
S
ES
RS
b
c
MGC
d
e
ITV
f
g
h

3.1.18 Electron microscopic examination

Control testes

The spermatogonia located at the boundary tissue of the seminiferous tubules were characterized by large ovoid nuclei containing fine granular nucleoplasm. The nuclei were present with their long axis parallel to the boundary tissue. The primary spermatocytes had spherical nuclei with fine granulated nucleoplasm and chromatin accumulation. Sertoli cells were recognized by the cytoplasm that extended from the basal lamina to the lumen of the seminiferous tubules and enveloped the adjacent germinal elements (Fig. 3.25a). For further details see section 3.1.9.

Testes from rats treated with kisspeptin alone

With alone kisspeptin treatment, the seminiferous tubules showed features of focal spermatogenic arrest depicted by degenerative changes in the germinal cells. The Sertoli cells had massive cytoplasmic vacuolations. Dilatation of the cell organelles was frequent (3.16 c).

Testes from rats treated with saline (acyline pretreated)

After a pretreatment with GnRH antagonist, acyline, the seminiferous tubules showed altered cellular architecture compared to control tubules. Spermatogonia, spermatocytes and Sertoli cells contained vacuolated and swollen mitochondria and germ cells were regressed in shape (Fig. 3.25 b).

Testes from rats treated with kisspeptin (acyline pretreated)

With kisspeptin (acyline pretreated) treatment, the testicular tissue showed recovery. Spermatogonia were normal and basal laminae were intact. Enlarged intercellular spaces were still present. Spermatogonia and spermatocytes still contain vacuolated organelles (Fig. 3.25 c).

a: Seminiferous tubule from control rats showing Sertoli cell nucleus (S) with a prominent nucleolus (Nu), type A spermatogonia (A) and pachytene spermatocytes. ×8, 000.

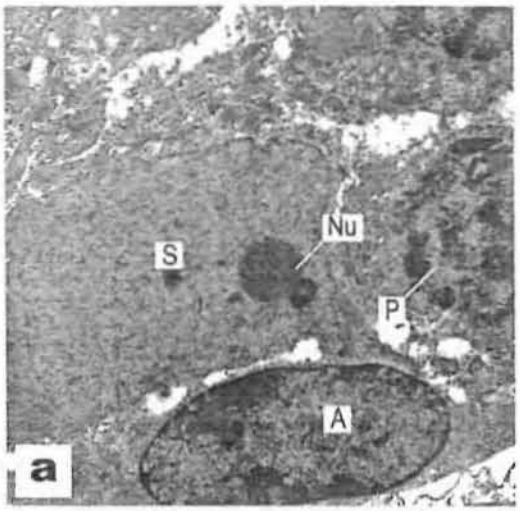

b: Seminiferous tubule of a rat treated with saline (acyline pretreated) showing Sertoli cell and primary spermatocytes containing vacuolated organelles. ×3,000.

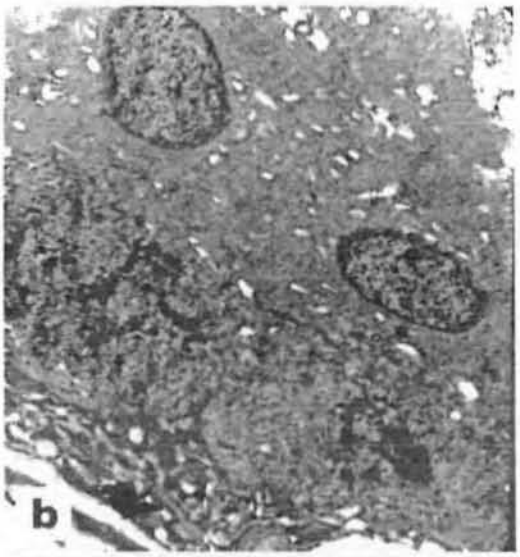

c: Seminiferous tubule of a rat treated with kisspeptin (acyline pretreated) showing recovery in the structure of basement membrane, primary spermatocytes and Sertoli cell cytoplasm. ×5, 000.

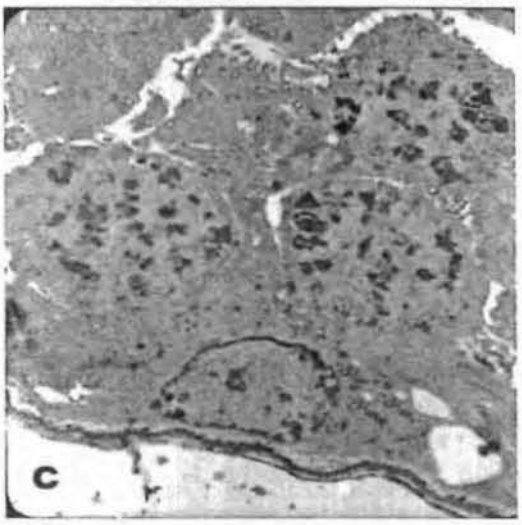

Figure 3.25 Electron micrographs of testicular tissue of control, saline (acyline pretreated) and kisspeptin (acyline pretreated) treated rats.

3.1.19 DNA Fragmentation

DNA ladder assay demonstrated 180-bp and 400-bp fragments in saline (acyline pretreated) treated group, while in the kisspeptin (acyline pretreated) treated group, only 180-bp fragments were recognizable (Fig. 3.26 A).

To quantify the DNA fragmentation, the ratio of fragmented DNA relative to total DNA was determined in treated groups as well as in control testis. The degree of % DNA fragmention increased highly significantly ($p < 0.001$) in kisspeptin alone and saline (acyline prereated) groups as compared to the control. In contrast, it remained similar to control values in the kisspeptin (acyline pretreated) treated group. Intergroup comparison showed a significant increase ($p < 0.001$) in % DNA fragmention in the saline (acyline pretreated) group as compared to kisspeptin (acyline pretreated) group, however compared to kisspeptin alone treatment, the % DNA fragmentation was lower ($p < 0.001$) in all treated groups (Fig. 3.26 B).

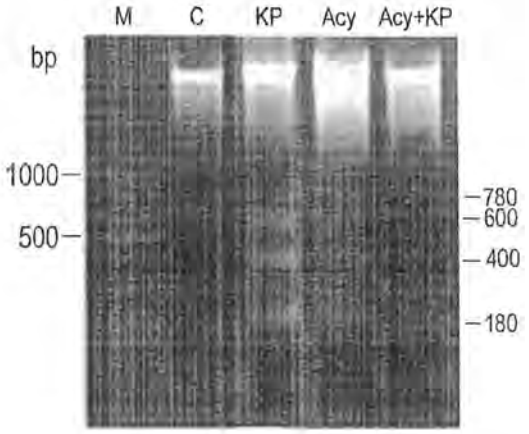

A

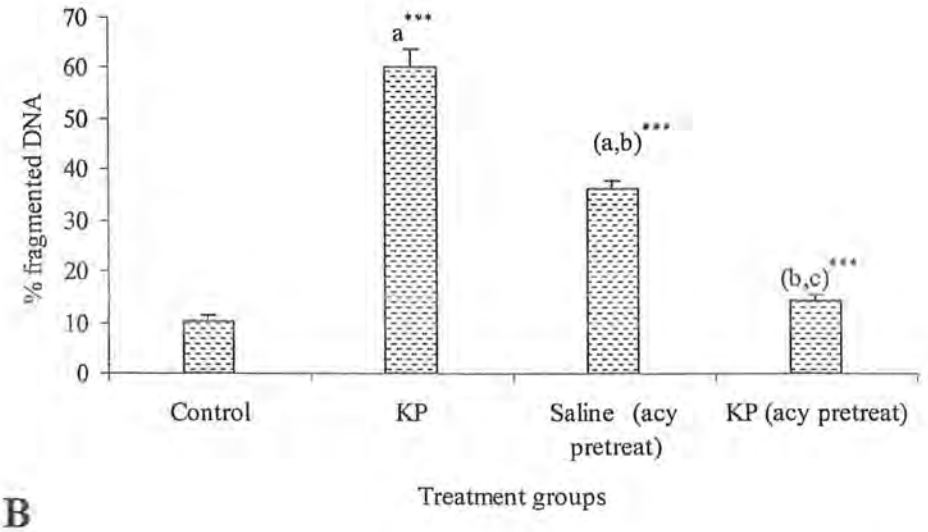

B

Figure 3.26 A) DNA ladder assay showing 180, 400, 600 and 780 bp bands of fragmented DNA, at alone kisspeptin dose, from rat testis. With acyline treatment 400 and 180 bp band were observed. Kisspeptin (acyline pre-treated) treatment demonstrated a single 180 bp fragment. Control testis showed intact DNA. M= 100-bp ladder (DNA size markers), C=control (saline treated), KP= kissprptin alone, Acy= Saline (acyline pre-treated), Acy+KP= Kisspeptin (acyline pre-treated).

B) DNA fragmentation assay. Percentage of fragmented DNA relative to total DNA remained similar to control in acyline pretreatment followed by kisspeptin treatment while it increased significantly in alone kisspeptin and acyline pretreatment followed by saline treatment. Values are expressed as mean ± SE. $^{*}p < 0.05$, $^{***}p < 0.001$ compared with control. a= difference from control, b= difference from alone kisspeptin, c= difference between saline (acyline pre-treated) and kisspeptin (acyline pre-treated).

SECTION II

3.2 Seminal vesicles

Experiment 1: Effect on seminal vesicle tissue following alone kisspeptin treatment at variable subchronic doses

3.2.1 Organ weight

Seminal vesicles weight decreased significantly ($p < 0.01$) at 1 μg kisspeptin dose only but remained nonsignificantly different from control at 10 pg and 1 ng doses (Fig. 3.27).

3.2.2 Epithelial height

Mean epithelial height of secretory acini decreased significantly with kisspeptin treatment. The decrease was more pronounced at I ng and 1 μg doses ($p < 0.001$) than at 10 pg dose ($p < 0.05$) (Fig. 3.28).

3.2.3 Correlation analysis

A positive correlation (r = 0.417) was observed between plasma testosterone concentration and seminal vesicle weight. Epithelial height of secretory acini of seminal vesicles was positively correlated (r = 0.67, $p < 0.01$) with plasma testosterone concentration. Seminal vesicles weight was positively correlated (r = 0.11) with the epithelial height of secretory acini of seminal vesicles.

3.2.4 Histomorphology of seminal vesicles

Control seminal vesicle

The seminal vesicle of the control group was complex and glandular with highly irregular lumen recessed with honeycomb-like features. The mucosa exhibited thin and branched foldings. The epithelia were columnar or pseudostratified columnar. The secretory acini were bounded on their outer periphery by a muscle coat. Pseudostratified epithelium rested on thin basement membrane that was highly folded to form irregular crypts and peaks. The thick muscular coat was formed with smooth muscle fibers containing darkly stained elongated nuclei. Two types of cells were recognized; the principal and basal cells. Principal cells were tall, columnar

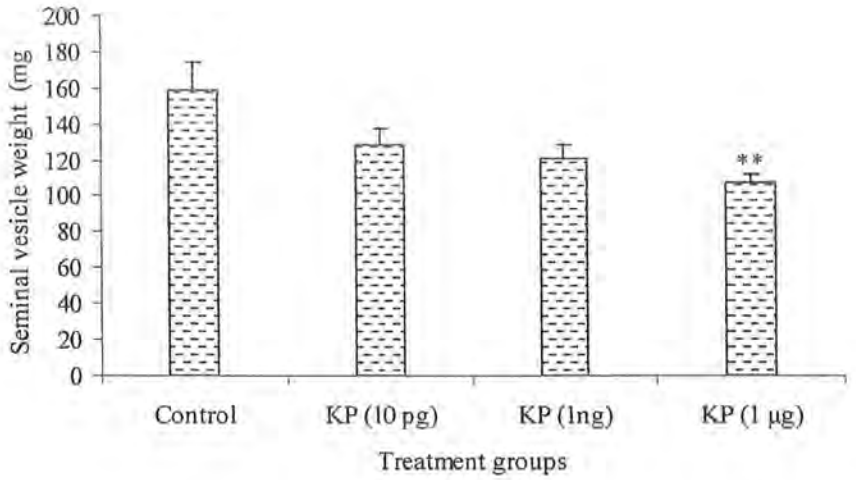

Figure 3.27 Seminal vesicles weight of prepubertal male rats following treatment with 10 pg, 1 ng and 1 µg kisspeptin (KP) doses. The organ weights decreased dose dependently. At 1 µg dose the decrease was more pronounced. Values are expressed as mean ± SE. $^{**}p < 0.01$ vs control.

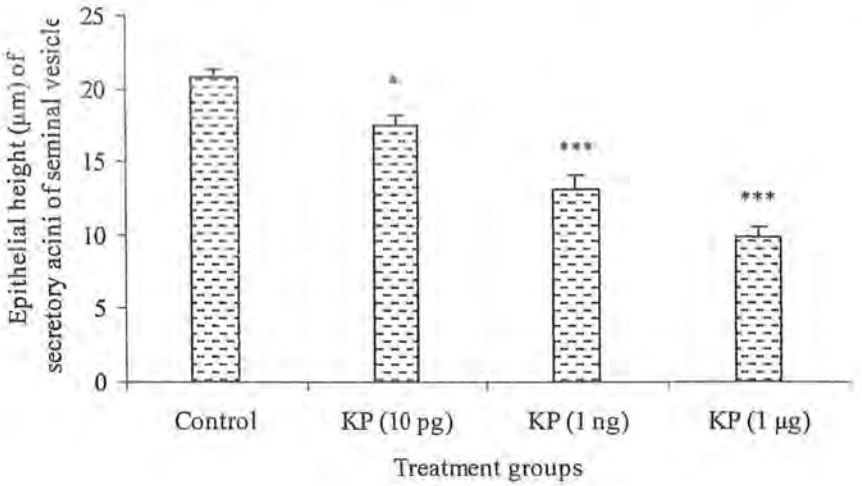

Figure 3.28 Epithelial height of secretory acini of seminal vesicle of prepubertal male rats following treatment with 10 pg, 1 ng and 1 µg kisspeptin (KP) doses. Epithelial height decreased dose dependently. At higher dose the decrease in mean epithelial height of secretory acini of seminal vesicles was more pronounced. Values are expressed as mean ± SE. $^{*}p < 0.05$, $^{***}p < 0.001$ vs control.

contained eosinophilic cytoplasm and round or oval shape nuclei. Basal cells were present on the basal lamina and were sandwiched between principal cells. These cells also contained round or oval shape nuclei (Fig. 3.29 a-b).

Seminal vesicle from rats treated with 10 pg kisspeptin

Luminal space was increased as compared to control, although the epithelium was still lined with columnar cells, but the lumen was irregular (Fig. 3.29 c-d).

Seminal vesicle from rats treated with 1 ng kisspeptin

Seminal vesicle was characterized by the loss of intricate foldings and dilated lumen. The glandular epithelium was nearly abolished and the height of columnar cells was greatly reduced (Fig. 3.29 e-f).

Seminal vesicle from rats treated with 1 µg kisspeptin

At further high dose of 1 µg kisspeptin, the lumen was markedly dilated and folding of the mucosa of seminal vesicles was significantly reduced in comparison to low kisspeptin doses. The mucosal epithelia now contained either cuboid or squamous cells. Luminal space widened to a greater extent (Fig. 3.29 g-h).

3.2.5 Electron microscopic examination

Control seminal vesicle

Secretory epithelium of seminal vesicles had two main types of cells, the principal and basal cells. Principal cells were rich in organelles. They had prominent oval, round or irregular shape nuclei situated at different heights in the epithelium. Nucleoli were prominent. Nuclear bodies of moderate electron density were occasionally visible. Chromatin material was clumped towards the periphery. Mitochondria occupying most of the cytoplasm were located in the perinuclear area. They had spherical or ovoid shapes of variable sizes. The cristae were well developed and tend to traverse the entire breadth of the organelle. The mitochondrial matrices were of low electron density and showed a fine granular appearance. Mitochondrial granules were seldom seen and were inconspicuous. Rough endoplasmic reticulum

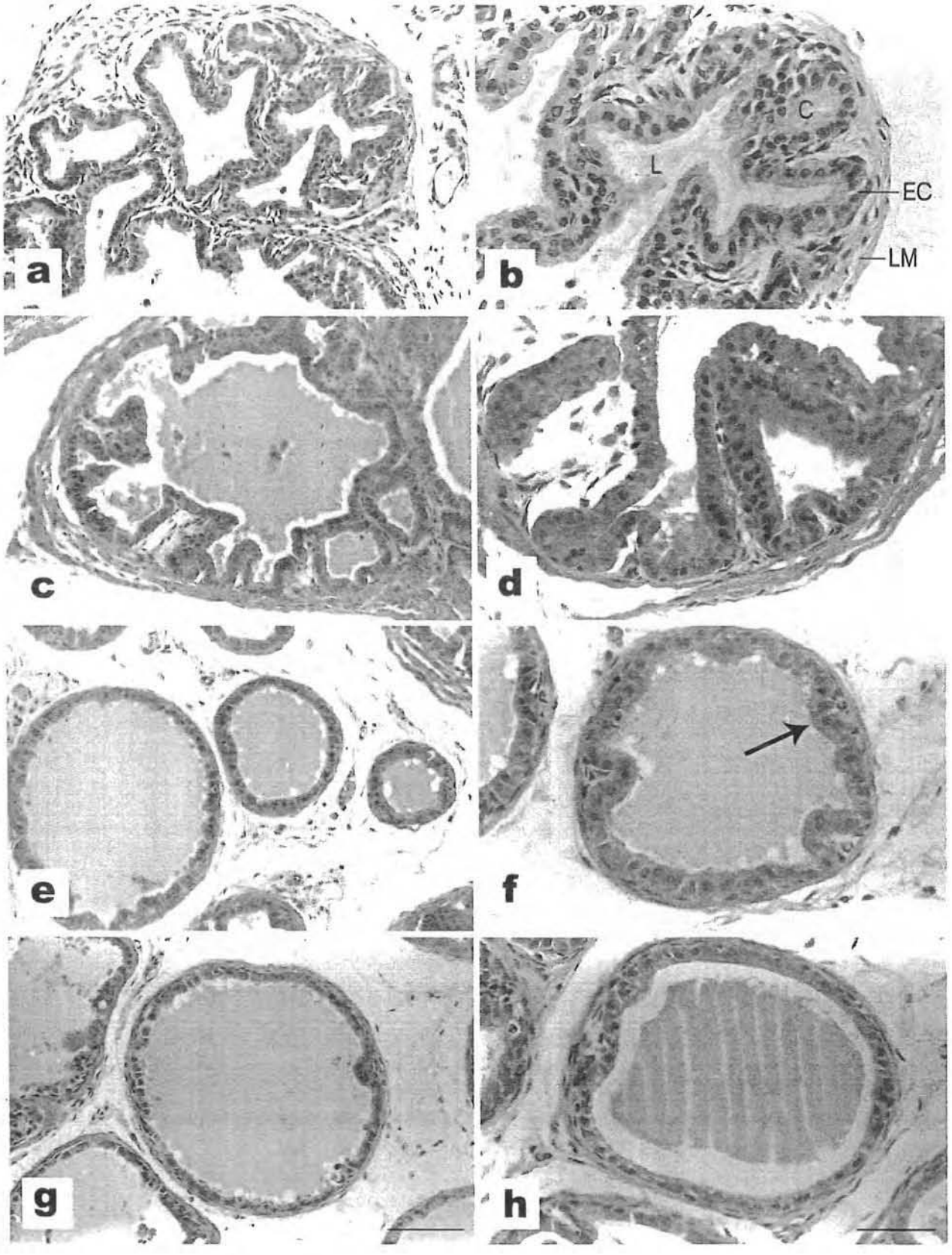
a
b
C
L
EC
LM
c
d
e
f
g
h

was abundant. Golgi apparatus was present in the supranuclear region and occasionally seen in other regions. Usually they formed typical structures consisting of parallel laminae, small vesicles and vacuoles of various sizes. The vacuoles contained dense secretory granules which rarely filled them completely. The interval between the secretory granule and the vacuolar wall varied greatly. In the apical cytoplasm, two or more secretory vacuoles occasionally joined together. Secretory granules were present in significant numbers in the apical portion of principal cells mainly among Golgi apparatus. Lipid droplets and vacuoles were occasionally visible. Ribosomes were free or clustered forming rosette shapes. Twisted and irregular finger shaped microvilli were present, as projections of cytoplasm at luminal border of the principal cells (Fig. 3.30 a and b).

The second type of cells present in the secretory epithelium were basal cells having polygonal shapes with their surfaces separated from the lumen by the apices of the principal cells. These occasionally occupied position between two principal cells. They had compact cytoplasm that contained few organelles, less well-developed Golgi apparatus and rough endoplasmic reticulum, and no inclusions other than lipid droplets. Nucleoli were not recognizable (Fig. 3.30 a and b, Fig 3.31 a).

Seminal vesicle from rats treated with 10 pg kisspeptin

The secretory epithelium of seminal vesicles showed dilatation of rough endoplasmic reticulum and Golgi apparatus, decrease in the number of secretory granules and in cell size. Degenerating as well as normal secretory granules were evident (Fig. 3.31 b).

Seminal vesicle from rats treated with 1 ng kisspeptin

With 1 ng dose, open spaces, lacunae and vacuoles were evident in the cytoplasm. Number of secretory granules was also lower. Endoplasmic reticulum and Golgi complex were disorganized and dilated (Fig. 3.31c).

3.2.4.3 Seminal vesicles from rats treated with 1 μg kisspeptin

Degeneration was excessive in comparison to the low dose treatment. The primary alterations recognizable included irregularity of nuclear shapes with intensive

invaginations of the envelope, small nucleoli and prominent chromatin in the nuclear peripheral portion and around the nucleoli. The tissue appeared heterochromatic indicating low cellular activity. Also noticeable were the granular endoplasmic reticulum and the Golgi complex with dilatation of the cisternae characterizing cellular atrophy and tissue disorganization of the organelles responsible for the secretory process. No secretory granules were evident. Cytoplasm was compact (Fig. 3.31 d).

3.2.6 DNA Fragmentation

Fragments of 180-bp were detected at 10 pg, 1 ng and 1 μg kisspeptin doses. The band intensity was strongest in 1 μg treated group but weaker in 1 ng and 10 pg groups (Fig. 3.32 A).

Percent DNA fragmention gradually increased in rats administered with higher kisspeptin doses. The % DNA fragmention increased at 10 pg dose but did not approach significant levels. It increased significantly ($p < 0.001$) in 1 ng and 1 μg groups as compared to control (Fig. 3.32 B).

a: General view of the seminal vesicle epithelium showing several principal cells; the apical parts of the principal cells which bulge into the lumen (L) contained many secretory granules (SG), especially around the Golgi complex (GC). Many cytoplasmic projections were seen at the apical surface of the principal cells called microvilli (M). They were irregularly spaced along the luminal border. ×3,000.

b: A principal cell containing secretory granules, Golgi complex and endoplasmic reticulum. There were present some lipid droplets (LD), large dense core secretory granules (SG) and ribosomes (R). Twisted, irregular finger shaped microvilli were present at luminal border of principal cells. ×12,000.

c: Principal cells with endoplasmic reticulum, Golgi complex and secretory granules. ×12,000.

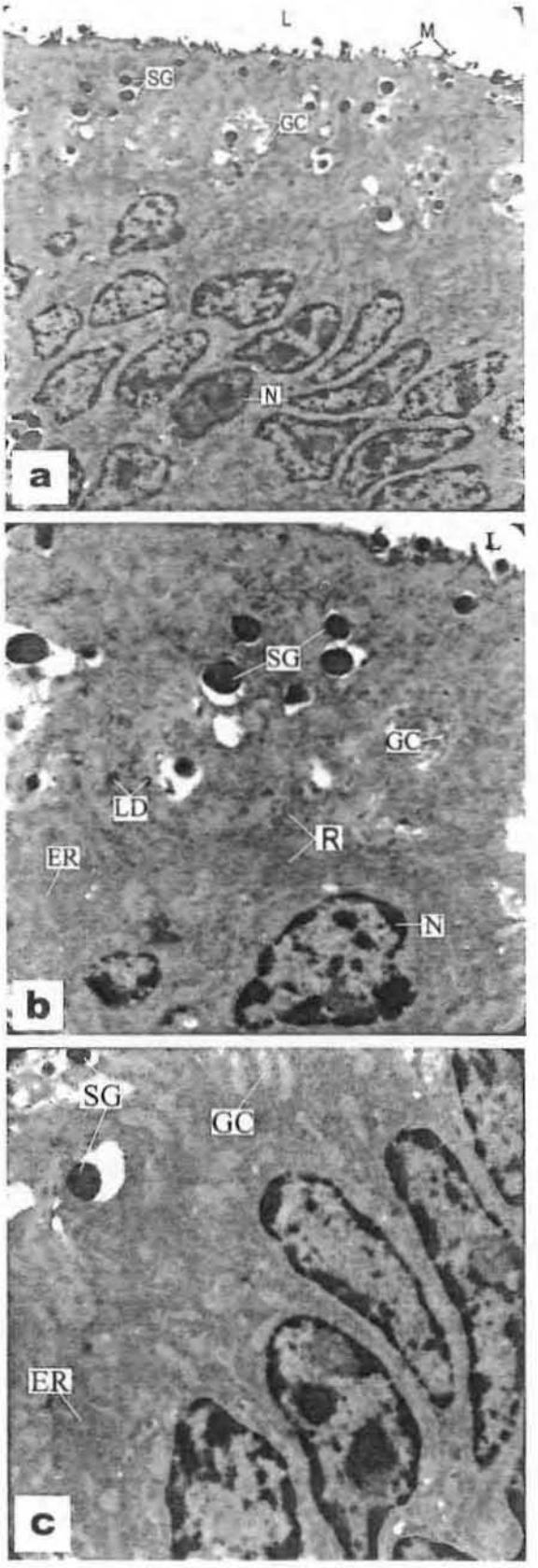

Figure 3.30 Electron micrographs of control seminal vesicle showing principal cells.

a: Seminal vesicle of animals treated with 10 pg kisspeptin. Number of secretary granules is lower. A mild dilatation of Golgi complex and endoplasmic reticulum is evident. ×5,000.

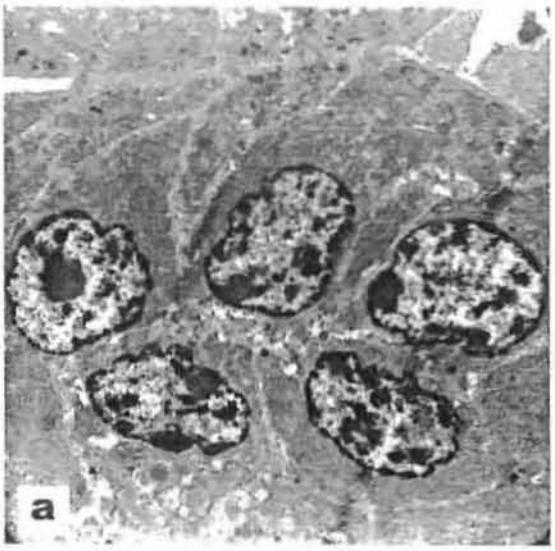

b: Seminal vesicle of animals treated with 1 ng kisspeptin. Number of secretory granules was lower. Endoplasmic reticulum and Golgi apparatus were disorganized and dilated. Large vacuoles were evident. ×12,000.

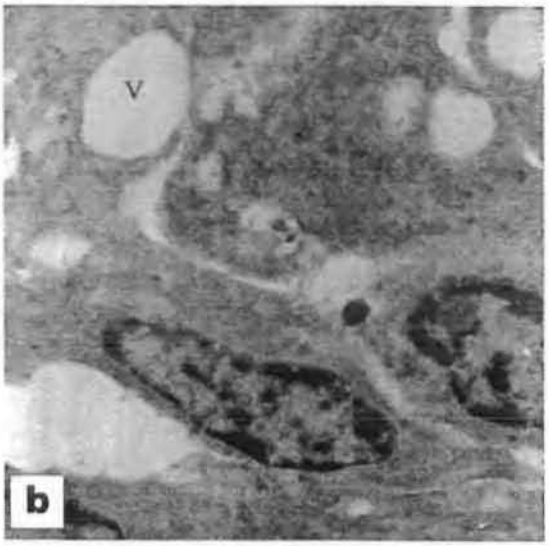

c: Seminal vesicle treated with 1 μg kisspeptin. Degeneration was more severe as compared to the other two treated groups. The alterations noticed were irregularity of nuclear shapes with intensive invagination of the envelope. No secretory granules were evident. ×15,000.

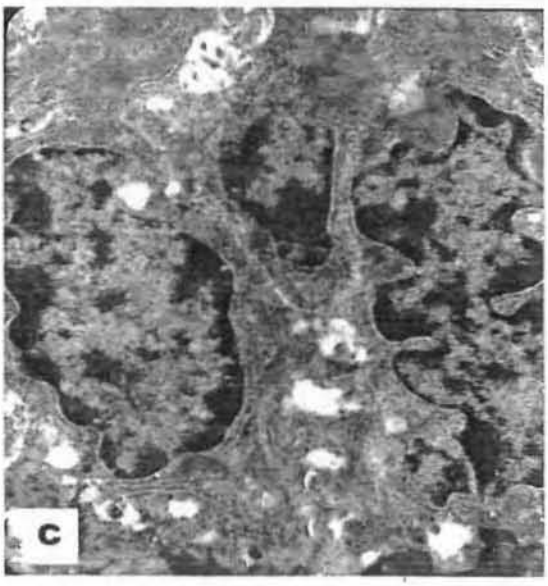

Figure 3.31 Electron micrographs of seminal vesicle of kisspeptin treated rats.

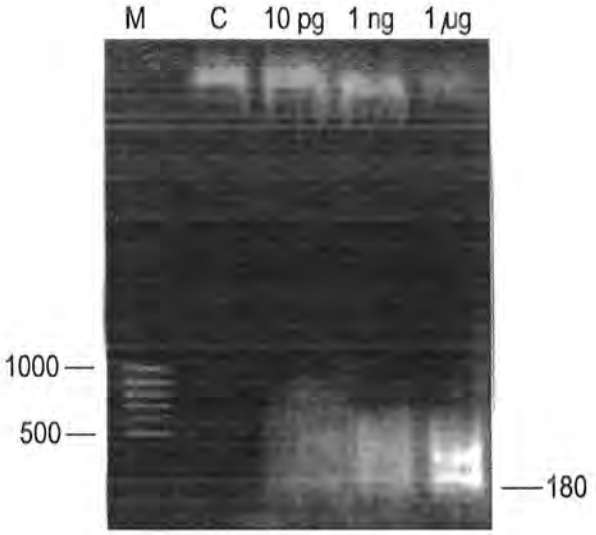

A

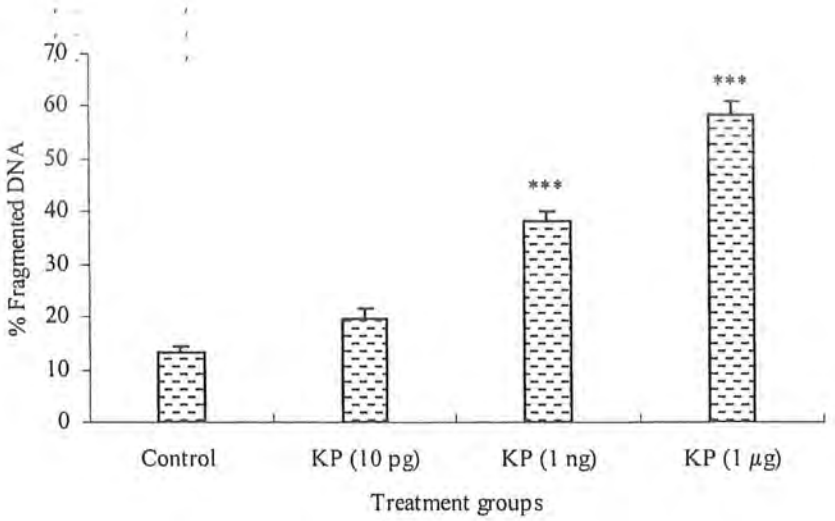

B

Figure 3.32 A) DNA ladder assay showing 180 bp bands of fragmented DNA, at 1 ng and 1 μg kisspeptin doses, from rat seminal vesicles. Faint bands were also visible in the 10 pg dose. Control (lane C) shows intact DNA. M= 100-bp DNA ladder.

B) DNA fragmentation assay. Percentage of fragmented DNA relative to total DNA increased dose dependently with kisspeptin treatment. Values are expressed as mean ± SE. $^{*}p < 0.05$, $^{***}p < 0.001$ compared with control.

Experiment 2: Indirect blockade of endogenous kisspeptin action after pretreatment with acyline, a GnRH antagonist

3.2.7 Organ weight

Seminal vesicle weight decreased nonsignificantly with kisspeptin alone treatment. It increased in saline (acyline pretreated) group and kisspeptin (acyline pretreated) group compared to kisspeptin alone but the increase did not approach significant levels (Fig. 3.33).

3.2.8 Epithelial height

Mean epithelial height of seminal vesicles secretory acini decreased significantly in the kisspeptin alone ($p < 0.001$), saline (acyline pretreated) ($p < 0.05$) and kisspeptin (acyline pretreated) groups ($p < 0.05$). It decreased non-significantly in saline (acyline pretreated) treated group when compared to kisspeptin (acyline pretreated) treated group. Between the kisspeptin alone and kisspeptin (acyline pretreated) groups, it showed significant increase ($p < 0.001$) in kisspeptin (acyline pretreated) group (Fig. 3.34).

3.2.9 Histomorphology of seminal vesicles

Control seminal vesicle

The seminal vesicle from control rats was complex and glandular with highly irregular lumen. The mucosa of the seminal vesicle exhibited thin, branched and anatomizing folds (Fig. 3.35 a). See section 3.2.4 for further details.

Seminal vesicle from rats treated with kisspeptin alone

With kisspeptin alone treatment, the lumen was dilated and the folding pattern of the mucosa of seminal vesicles was significantly reduced. The epithelial cells were no longer columnar. They became either cuboidal or squamous (Fig. 3.35 b).

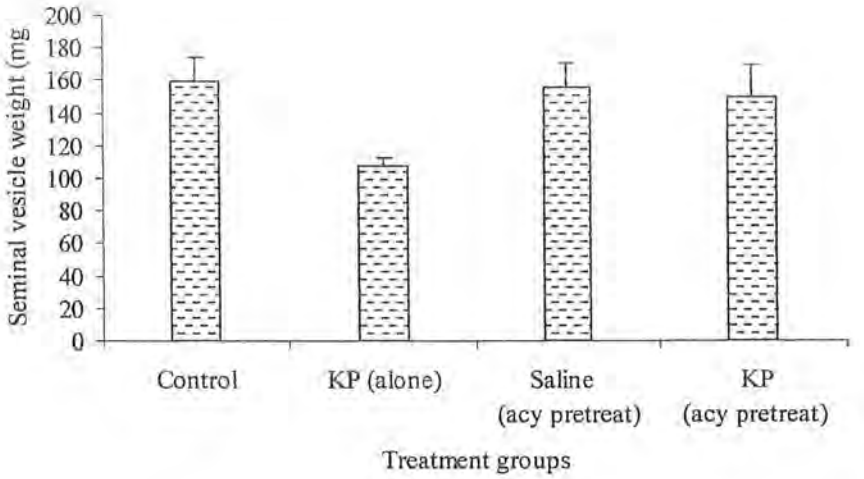

Figure 3.33 Seminal vesicle weight of prepubertal male rats following treatment with kisspeptin, saline (acyline pretreated) and kisspeptin (acyline pretreated). Seminal vesicles weights differed nonsignificantly between the treatment groups. Values are expressed as mean ± SE.

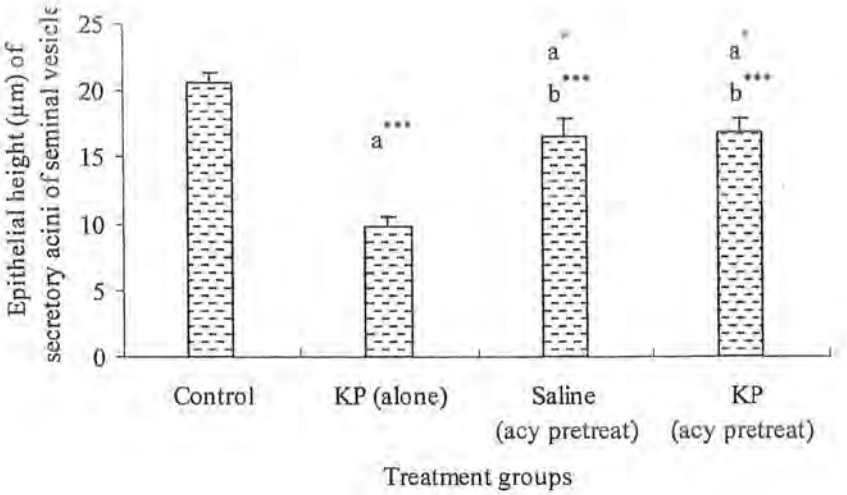

Figure 3.34 Effect of acyline and kisspeptin treatment on mean epithelial height of secretory acini of seminal vesicle of prepubertal male rats. Epithelial height decreased significantly in saline (acyline pre-treat) and kisspeptin (acyline pre-treat). Values are expressed as ± SE. $^{*}P < 0.05$. a= compared with control, b= significance with kisspeptin, c= significance between saline (acyline pretreated) and kisspeptin (acyline pretreated).

Seminal vesicle from rats treated with saline (acyline pretreated)

In seminal vesicle of rats treated with saline (acyline pre-treated), the structure of the tissue was simple and characterized by a loss of intricate foldings and emergence of dilated lumen. The glandular epithelium was not well developed. Columnar cell heights were greatly reduced (Fig. 3.35c).

Seminal vesicle from rats treated with kisspeptin (acyline pretreated)

In rats treated with kisspeptin (acyline pre-treated), the structure appeared nearly restored as folds appeared to reform and were irregular similar to those observed in control. The epithelial height increased as compared to saline (acyline pretreated) treatment and had columnar cells. Luminal sizes were reduced due to folds (Fig. 3.35d).

3.2.10 Electron microscopic examination

Control seminal vesicle

The epithelium of the seminal vesicle was characterized by columnar principal (secretory) cells and basal cells. Some of the nuclei of the secretory cells were irregular while others were oval or spherical. Microvilli were located on the luminal surfaces. Vesicles and vacuoles occurred frequently closer to the Golgi apparatus. Some of the larger vacuoles contained a small, dense, homogeneous granule in the apical cytoplasm. In some cases continuity between the Golgi apparatus and the vacuoles was observed (Fig 3.36a). For further details see section 3.2.5.

Seminal vesicle from rats treated with kisspeptin alone

With kisspeptin alone treatment deep indentation of the nuclear envelope, small size nucleoli and prominent chromatin in the nuclear peripheral portion and around the nucleoli were the primary alterations. Also noticeable were the endoplasmic reticulum and the Golgi complex with dilatation of the cisternae characterizing cellular atrophy and tissue disorganization of the organelles responsible for the secretory process. No secretory granules were evident (Fig. 3.36b).

a: Seminal vesicle from control rats showing complex and glandular structure. The lumen is highly irregular and the epithelia are columnar or pseudostratified columnar.

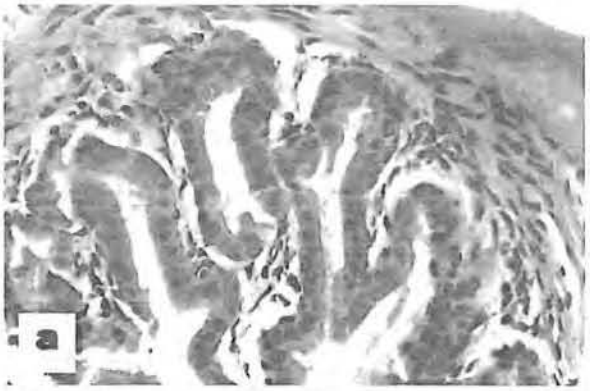

b: The lumen is markedly dilated and the branching of the mucosa of seminal vesicles of rats treated with alone kisspeptin was greatly reduced. In addition, the mucosal epithelia had either cuboid or squamous cells.

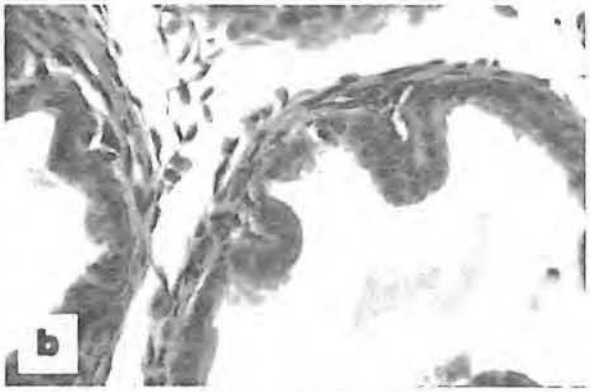

c: Seminal vesicle of rats treated with saline (acyline pre-treated). The structure of the tissue at this dose became simple having no intricate folds, while the lumen was dilated.

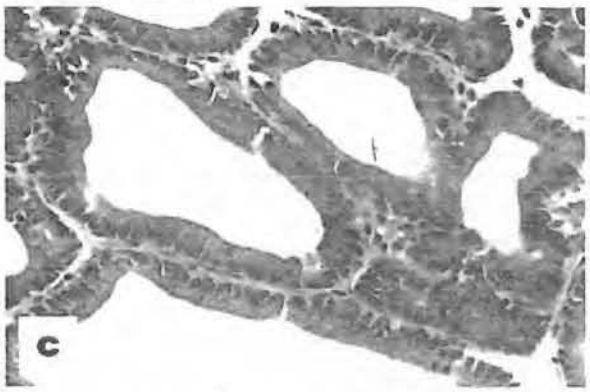

d: Seminal vesicle of rats treated with kisspeptin (acyline pre-treated). The structure was not as complex and irregular as that of control. The epithelium was columnar having irregular lumen.

Scale bar 20 µm

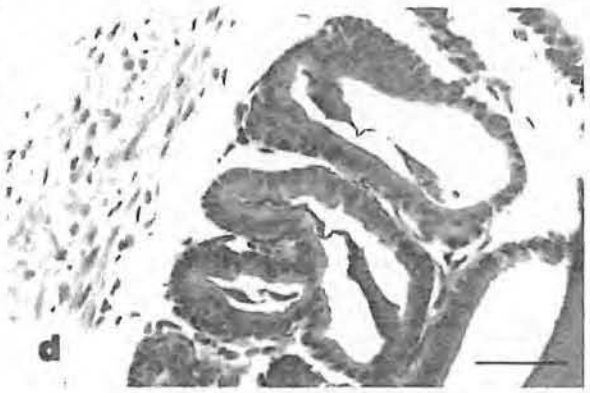

Figure 3.35 Photomicrographs of seminal vesicle of control, kisspeptin alone, saline (acyline pre-treated), kisspeptin (acyline pre-treated) pre-pubertal rats.

Seminal vesicle from rats treated with saline (acyline pre-treat)

Significant changes were noticeable in the secretory epithelium of seminal vesicles of rats treated with saline (acyline pre-treat). These included dilatation of the rough endoplasmic reticulum and Golgi apparatus. No secretory granules were evident and cytoplasm became compact and contained hollow spaces and vacuoles. Intracellular spaces were widened. Nuclei became heterochromatic (Fig. 3.36 c).

Seminal vesicle from rats treated with kisspeptin (acyline pre-treat)

With the kisspeptin (acyline pretreated) treatment the seminal vesicles showed some recovery. Normal as well as degenerating secretory granules were present. Numerous vacuoles were also noticeable. Dilatations of the intercellular space were less obvious. There were no enlarged intercellular spaces. Nuclei were still heterochromatic (Fig. 3.36 d).

3.2.11 DNA Fragmentation

In the normal seminal vesicle tissue, DNA was intact. In the kisspeptin alone group, 180 bp fragment was evident while in saline (acyline pretreated) treated group a faint smear was observed. DNA remained intact in kisspeptin (acyline pretreated) treated group (Fig. 3.37 A).

The degree of % DNA fragmention increased highly significantly ($p < 0.01$) in saline (acyline pretreated) treated group as well as in the ($p < 0.05$) kisspeptin (acyline pretreated) treated group as compared to the control group of rats. it remained similar to control in kisspeptin (acyline pretreated) treated group. Intergroup comparison showed that % DNA fragmention increased non significantly in the saline (acyline pretreated) treated group when compared to kisspeptin treated (acyline pretreated) group (Fig. 3.37 B).

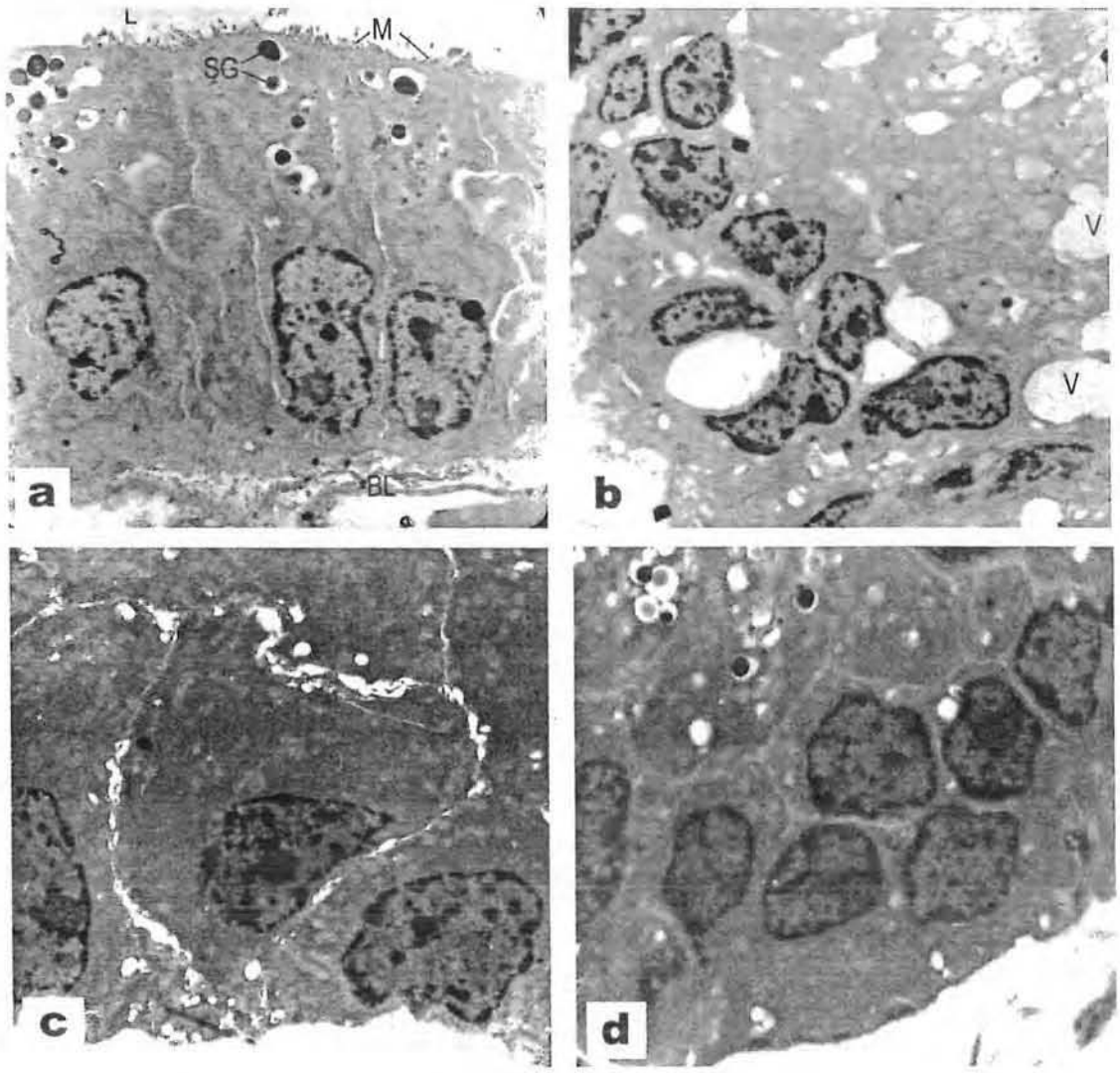

Figure 3.36 Electron micrographs of seminal vesicle of control, kisspeptin alone, saline (acyline pretreated) and kisspeptin (acyline pretreated) rats.

a: Seminal vesicle of control rats showing the principal cells. Secretory granules were present in large numbers in the apical portion of principal cells. ×6000.

b: Seminal vesicle treated with alone kisspeptin. The primary alterations were irregularity of nuclear shape with invagination of the nuclear envelope. No secretory granules were evident. Large vacuoles and intercellular spaces were evident. ×5,000.

c: Seminal vesicle treated with saline (acyline pretreated). The structure appeared electron dense. Enlarged intercellular spaces were noticeable. No secretory granules were evident. ×10, 000.

d: Seminal vesicle treated with kisspeptin (acyline pretreated). Secretory epithelium improved as compared to saline (acyline pretreated). Numerous vacuoles were still noticeable. Number of secretory granules was lower compared to control. ×8,000.

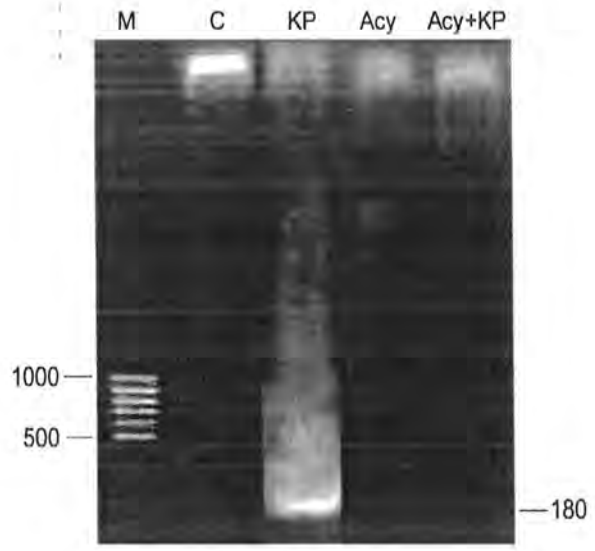

A

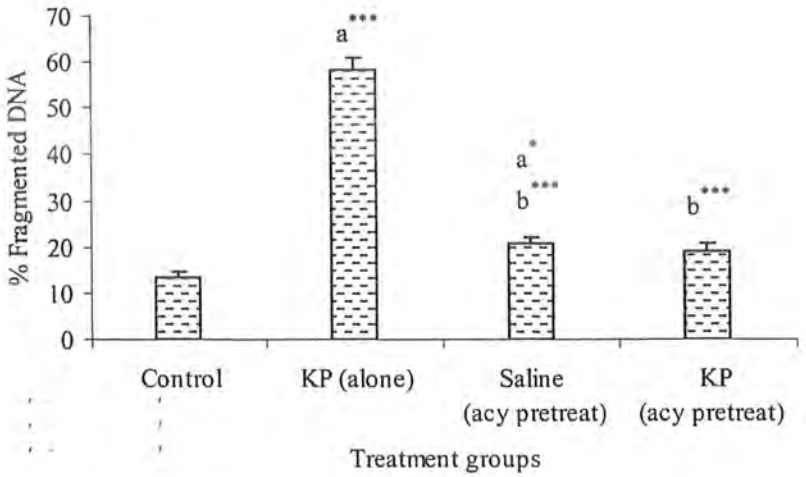

B

Figure 3.37 A) DNA ladder assay showing 180 bp fragment of DNA, at alone kisspeptin dose, from rat seminal vesicle. With acyline treatment a smear was observed while it remained intact with kisspeptin (acyline pretreated) treatment. Control DNA was intact. M= 100-bp ladder (DNA size markers), C=control (saline treated), KP= kissprptin alone, Acy= Saline (acyline pretreated), Acy+KP= Kisspeptin (acyline pretreated).

B) DNA fragmentation assay. Percentage of fragmented DNA relative to total DNA is similar in acyline pretreatment followed by kisspeptin treatment and control. It increased in acyline pretreatment followed by saline treatment and alone kisspeptin treatment. Values are expressed as mean ± SE. $^{*}p < 0.05$, $^{**}p < 0.01$.

SECTION III

3.3 Prostate gland

Experiment 1: Effect on prostate tissue following alone kisspeptin treatment at variable subchronic doses

3.3.1 Organ weight

Prostate weight decreased significantly ($p < 0.05$) at 1 μg kisspeptin dose while the decrease was nonsignificant at 10 pg and 1 ng doses (Fig. 3.38).

3.3.2 Epithelial height

Mean epithelial height of secretory acini of prostate gland decreased significantly at all kisspeptin doses, at 10 pg dose ($p < 0.05$), 1 ng and 1 μg dose ($p < 0.001$) (Fig. 3.39).

3.3.3 Correlation analysis

A positive correlation (r = 0.28) was found between plasma testosterone concentration and prostate weights. Epithelial height of secretory acini of prostate was positively correlated (r = 0.48, $p < 0.01$) with plasma testosterone concentration. Prostate weight was positively correlated (r = 0.29) with epithelial height of secretory acini of prostate.

3.3.4 Histomorphology of prostate gland

Control prostate

Normal non-treated prostate gland contained many tubuloalveolar glands or secretory alveoli lined with a layer of tall columnar epithelial cells. The cells had a high cytoplasm/nuclear ratio. The epithelial cells were irregular shaped due to the papillary projections of mucosa into the lumen of the gland. The lumen was filled with secretory fluid. Periphery of secretory acini was bounded by smooth muscles. The pseudostratified epithelium of secretory acini rested on thin basement memberane that was highly folded to form irregular crypts and peaks. Two types of epithelial cells were recognized, the principal and basal cells. The principal cells were tall, columnar

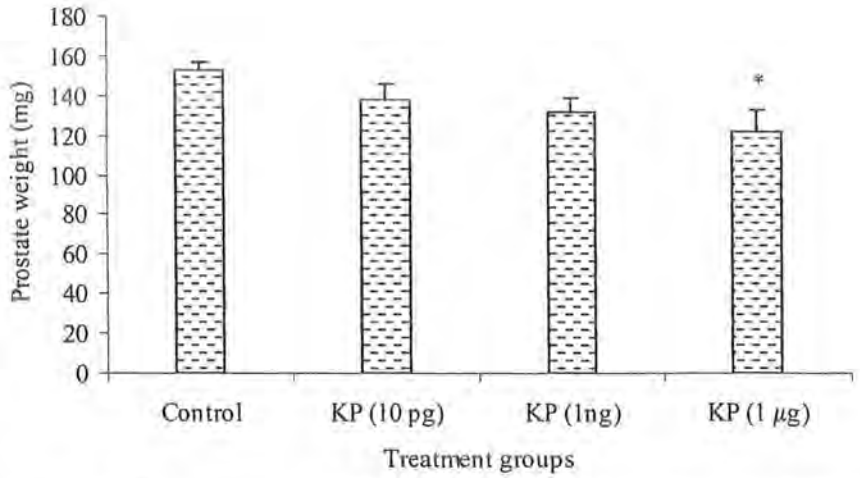

Figure 3.38 Prostate weight of prepubertal male rats following treatment with variable kisspeptin doses. Prostate weight decreased dose dependently. At higher dose the decrease in mean prostate weight was more pronounced. Values are expressed as mean ± SE. $^{*}p < 0.05$ compared with control.

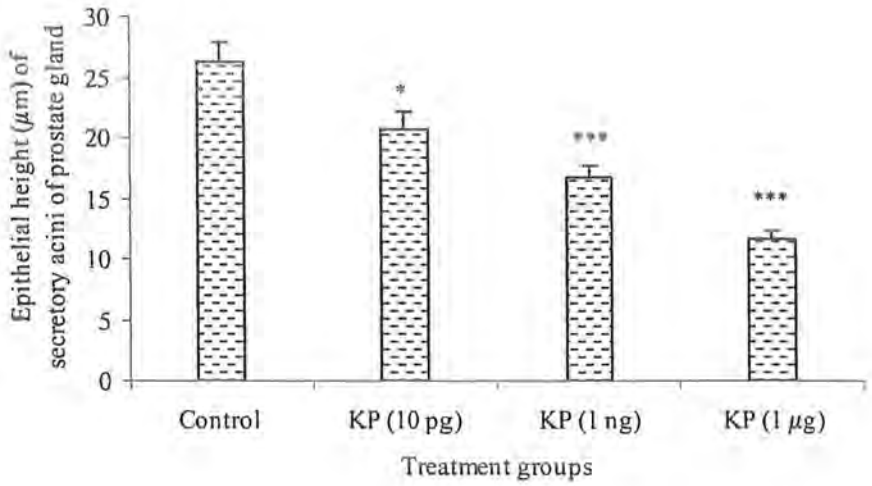

Figure 3.39 Mean epithelial height of secretory acini of prostate gland of prepubertal male rats following increasing doses of kisspeptin. Epithelial height decreased dose dependently. At higher dose the decrease in mean epithelial height of secretory acini of prostate gland was more pronounced. Values are expressed as mean ± SE. $^{*}p < 0.05$, $^{***}p < 0.001$ compared with control.

and contained round or oval nuclei with eosinophilic cytoplasm, while the basal cells contained round or oval shape nuclei. The cellular cytoplasm of principal cells showed a clearly visible supranuclear region, which corresponded to the area of the Golgi complex (Fig. 3.40 a-b).

Prostate gland from rats treated with 10 pg kisspeptin

The folds of prostatic epithelium were decreased in number at 10 pg kisspeptin dose. Epithelial height decreased, while lumen widened (Fig. 3.40 c-d).

Prostate gland from rats treated with 1 ng kisspeptin

A further decrease occurred in foldings of the epithelium, the height of epithelial folds and epithelial cell height at the dose of 1 ng kisspeptin (Fig. 3.40 e-f).

Prostate gland from rats treated with 1 μg kisspeptin

A marked dilatation of the prostatic lumen was induced at 1 μg kisspeptin dose. Epithelial folds were absent, principal cells became cuboidal in shape, basal cells were non conspicuous and the size of lumen was greatly increased (Fig. 3.40 g-h).

3.3.5 Electron microscopic examination

Control prostate

Ultrastructure of control non-treated prostate showed simple secretory epithelium with high columnar cells. The cells had basal nuclei with an intact nuclear envelopes, prominent nucleoli with condensed chromatin were distributed at the nuclear periphery. The contents of nuclei consisted of aggregates of dense granules in a homogeneous matrix. Columnar cells were occasionally intermingled with basal cells located on the basal lamina. In the perinuclear cytoplasm, granular endoplasmic reticulum was observed with parallel and flattened cisternae. The Golgi complex was well developed and located in the supranuclear region with flattened cisternae. Secretory vacuoles at different stages of maturation, were observed in the apical region as well as in the intercellular junctions. The mitochondria were distributed

evenly in the cytoplasm. The basement membrane was intact and well defined (Fig. 3.41 a and 3.42 a).

Treatment with kisspeptin

With kisspeptin treatment, the glandular alterations were decrease in cell height, characterized by cellular atrophy and tissue disorganization of the organelles responsible for the secretory process.

Prostate gland from rats treated with 10 pg kisspeptin

Irregularity of nuclear shapes, and prominent chromatin in the nuclear peripheral portion and around the nucleoli were the primary alterations with 10 pg kisspeptin treatment. Endoplasmic reticulum and Golgi apparatus were less organized with dilated cisternae. Vacuoles and cellular debris were present. In the apical cytoplasm, occasional secretory vacuoles were evident. Intercellular spaces were enlarged (Fig. 3.41 b and 3.42 b).

Prostate gland from rats treated with 1 ng kisspeptin

A greater damage was evident at 1 ng kisspeptin dose. Endoplasmic reticulum and Golgi apparatus were dilated. Large vacuoles, condensed chromatin and cellular debris consisting of more or less degenerated organelles were frequently found (Fig. 3.41 c). Digestive vacuoles were also evident (3.42 c).

Prostate gland from rats treated with 1 μg kisspeptin

The prostate in this group was characterized by marked atrophy, wide intercellular spaces, irregular shape nuclei, and condensed and fragmented chromatin found scattered throughout the nucleoplasm. Digestive vacuoles containing cell remnants were observed in the perinuclear cytoplasm. The cisternae of the Golgi complex were dilatated. The basement membrane was infolded (Fig. 3.41 d and 3.42d).

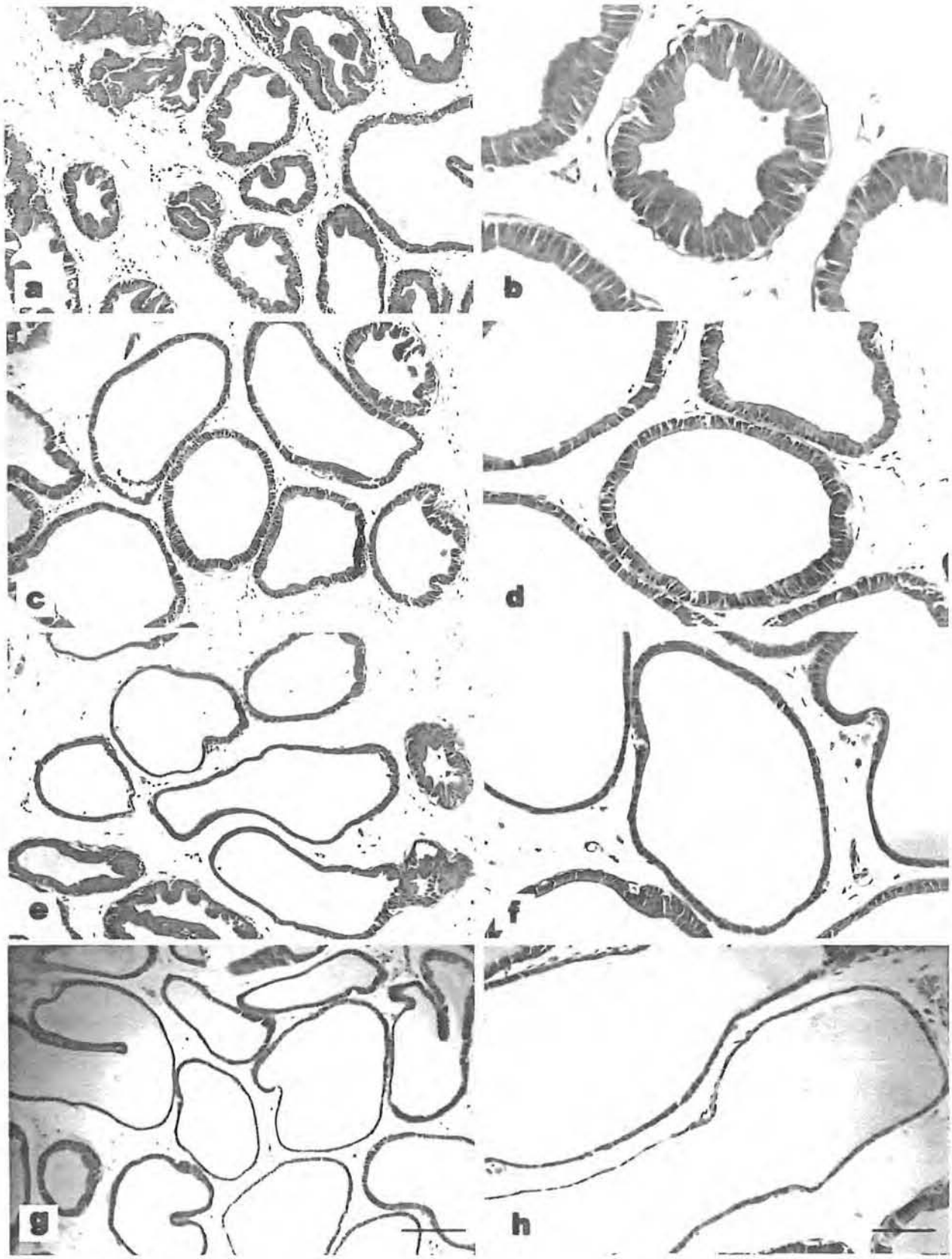
a
b
c
d
e
f
g
h

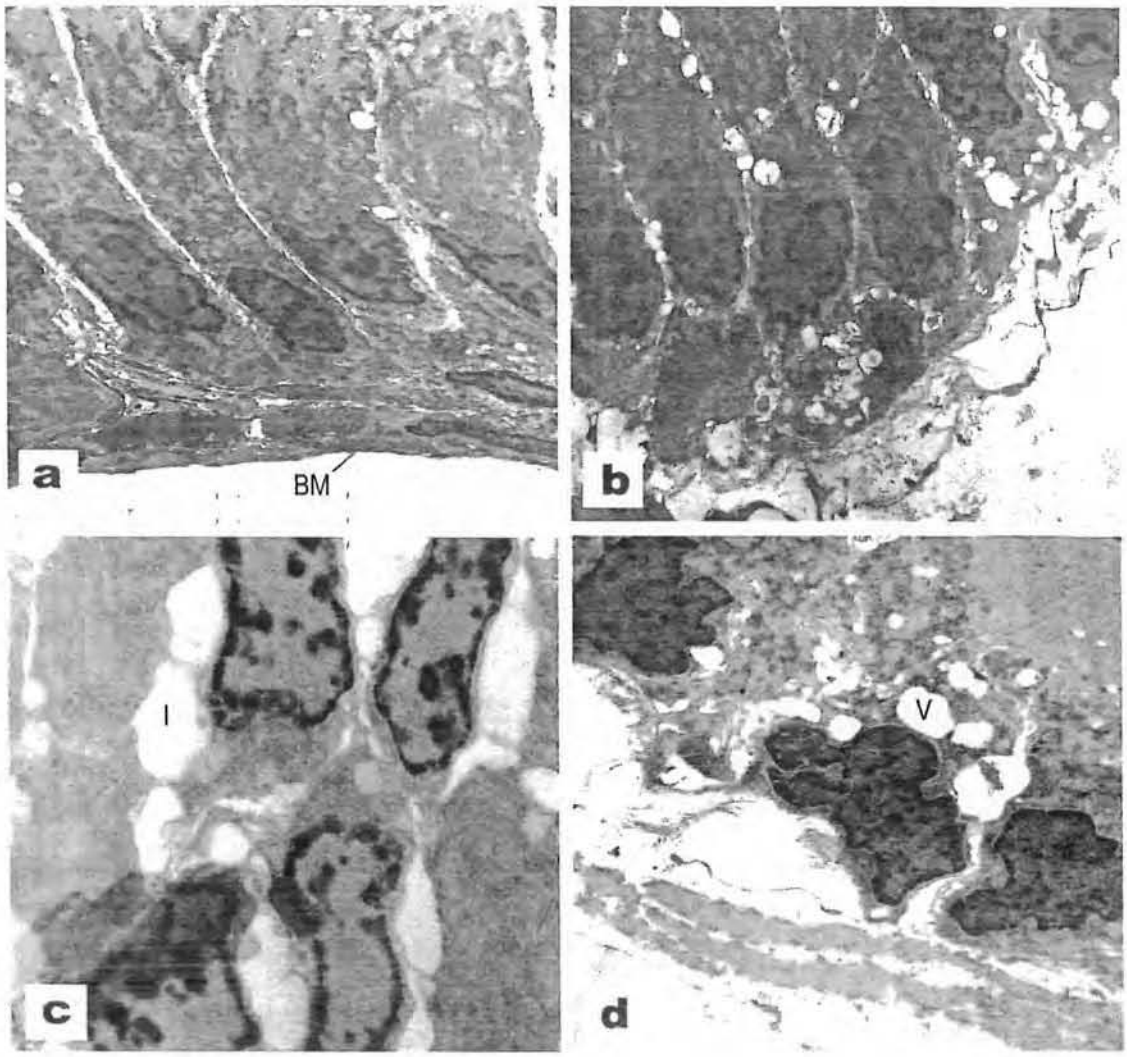

Figure 3.41 Electronmicrographs of prostate from control and kisspeptin treated rats.

a: Prostate of control rat showing well developed Golgi complex in supranuclear region. In the perinuclear cytoplasm, endoplasmic reticulum was observed with parallel and flattened cisternae.
b: The prostate of rats treated with 10 pg kisspeptin dose contained numerous vacuoles. Nuclear shape became irregular with invagination of the nuclear envelope. The basement membrane became thin and ruptured.
c: The prostate of rats treated with 1 ng kisspeptin. The damage was more pronounced. Pyknotic nuclei, large vacuoles and intercellular spaces (I) were evident.
d: The prostate at 1 μg dose is typified by marked atrophy. Intercellular spaces were widened. Nuclei were irregular shaped, chromatin was condensed, fragmented and scattered throughout the nucleoplasm. The cisternae of the Golgi complex were dilated.
Magnification a-b ×5,000, c-d ×12,000.

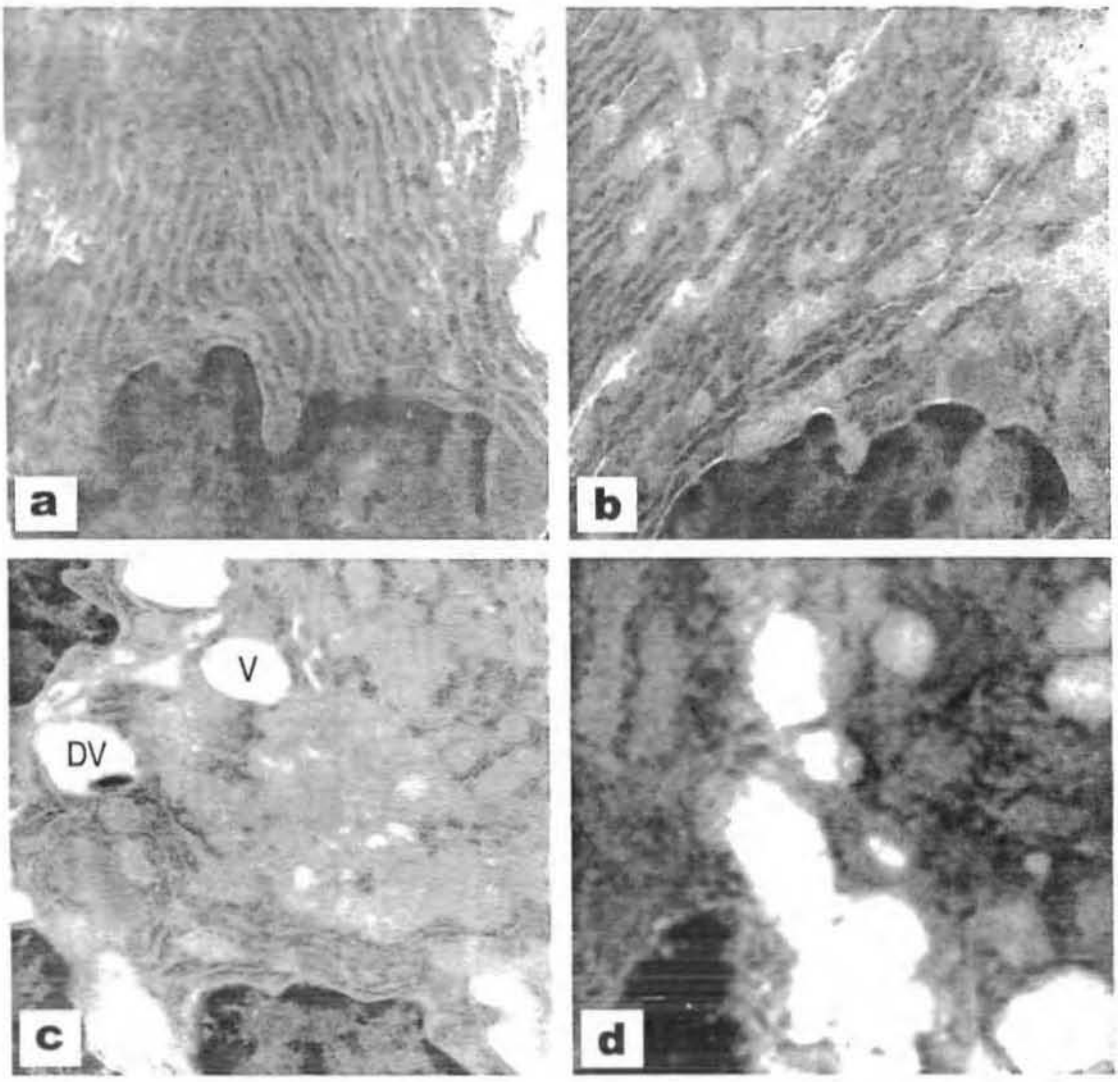

Figure 3.42 Details of the supranuclear region of prostate of control and kisspeptin treated rats.

a: The prostate of the control group was complex. The glandular cells had well developed Golgi apparatus in the apical portion of cytoplasm. The perinuclear cytoplasm contained endoplasmic reticulum.

b: The prostate of rats treated with 10 pg kisspeptin contained endoplasmic reticulum and the Golgi complex with dilatation of the cisternae.

c: The prostate of rats treated with 1 ng kisspeptin. The glandular epithelium was not developed. The cisternae of endoplasmic reticulum and the Golgi complex were dilated very much. Digestive vacuoles (DV) containing cell remnants were observed in the perinuclear cytoplasm. Large vacuoles (V) were observed.

d: The prostate of rats treated with 1 μg kisspeptin. Prostate was characterised by marked atrophy. Nuclei became irregularly shaped. The cisternae of the Golgi complex and endoplasmic reticulum were dilated.

Magnification a-d = ×30,000.

3.3.6 DNA fragmentation

In the control prostate DNA was intact. A smear of fragmented DNA was observed only at 1 μg kisspeptin dose. Faint smears were also visible in the 1 ng and 10 pg doses (Fig. 3.43A).

The degree of % DNA fragmention gradually increased where higher doses were administered. It increased significantly ($p < 0.05$) in 10 pg treatment group and ($p < 0.001$) in 1 ng and 1 μg groups as compared to control. The increase in % DNA fragmentation was found to be dose dependent (Fig. 3.43B).

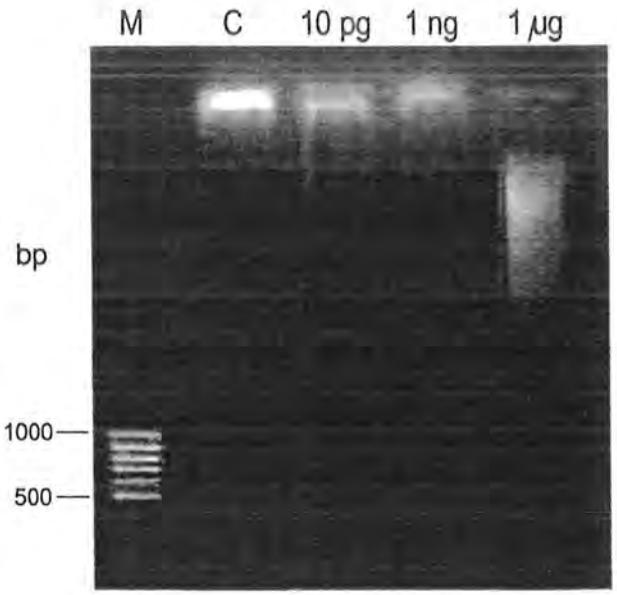

A

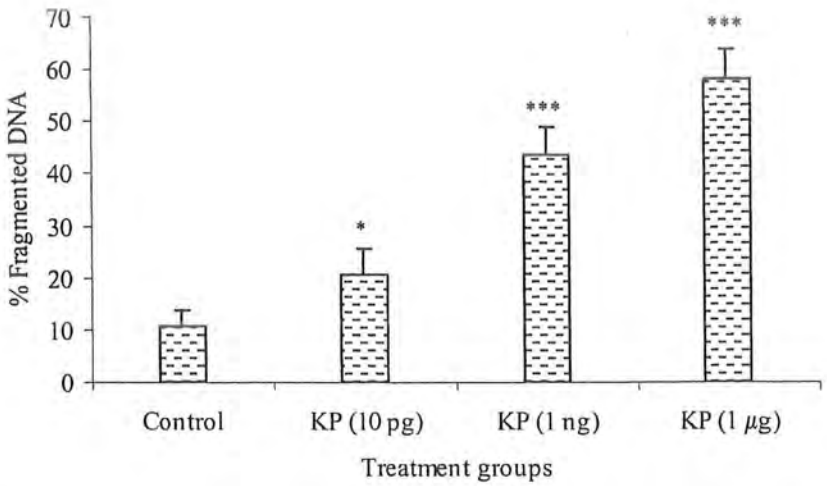

B

Figure 3.43 A) DNA ladder assay from rat prostate. A smear of DNA was noticeable in 1 μg dose group. Control (lane C) shows intact DNA. M= 100-bp DNA ladder.

B) DNA fragmentation assay. Percentage of fragmented DNA relative to total DNA increased dose dependently with kisspeptin treatment. Values are expressed as mean ± SE. $^{*}p < 0.05$, $^{***}p < 0.01$ compared with control.

Experiment 2: Indirect blockade of endogenous kisspeptin action after pretreatment with acyline, a GnRH antagonist

3.3.7 Prostate weight

No significant decrease was observed in prostate weight with kisspeptin alone treatment. It increased in saline (acyline pretreated) treated group as compared to kisspeptin alone treated group. Prostate weight decreased in kisspeptin (acyline pretreated) treated group compared to saline (acyline pretreated) group but the decrease did not approach significant levels.

3.3.8 Epithelial height

Epithelial height of secretory acini of prostate gland decreased significantly with kisspeptin alone ($p < 0.001$), saline (acyline pretreated) ($p < 0.001$) and kisspeptin (acyline pretreated) treated groups ($p < 0.05$) as compared to control. Intergroup comparison showed significant decrease of epithelial height in saline (acyline pretreated) treated group ($p < 0.01$) compared to kisspeptin (acyline pretreated) treated group. Kisspeptin alone treatment significantly decreased epithelial height as compared to saline (acyline pretreated) treated group (Fig. 3.45).

3.3.9 Histomorphology of prostate gland

Control prostate

Prostate gland of the control group contained many tubuloalveolar glands or secretory acini. The acini population was a mixture of smooth, round acini and those with infolding of the epithelium to form papillary projections of mucosa into the lumen of the gland. The acinar epithelium was lined with cuboidal or low columnar cells possessing basally-located nuclei and a supranuclear clear zone (Fig. 3.46 a-b). For further details see section 3.3.4.

Prostate gland from rats treated with kisspeptin alone

A pronounced dilatation of the prostatic lumen was observed with kisspeptin alone treatment. Epithelial folds were absent, cells of epithelium became cuboidal in

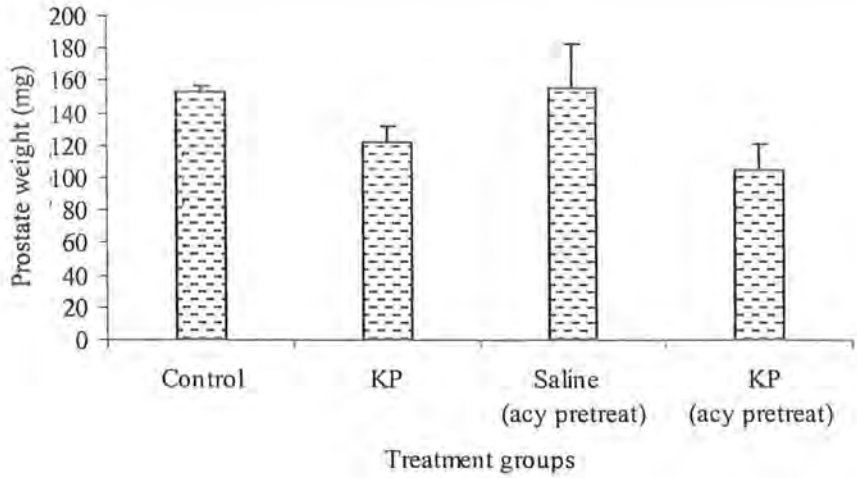

Figure 3.44 Prostate weight of prepubertal male rats following acyline and kisspeptin administration. Prostate weight decreased nonsignificantly with kisspeptin alone, saline (acyline pretreated) and saline (acyline pretreated) treatment compred to control. Values are expressed as mean ± SE.

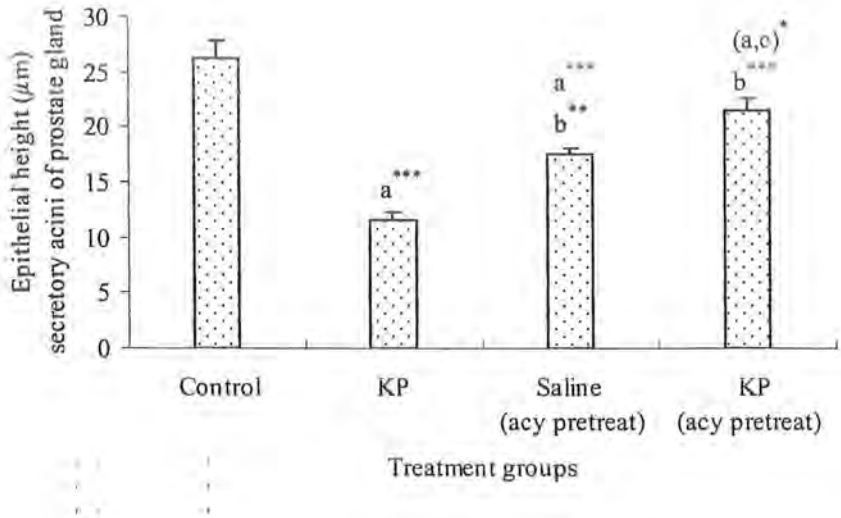

Figure 3.45 Mean epithelial height of secretory acini of prostate gland of prepubertal male rats following acyline and kisspeptin administration. Epithelial height decreased significantly with kisspeptin alone, saline (acyline pre-treat) and kisspeptin (acyline pretreated) treatment. Epithelial height decreased significantly in saline (acyline pretreated) compared to kisspeptin (acyline pre-treat). Values are expressed as mean ± SE. $^{*}p < 0.05$, $^{**}p < 0.001$, $^{***}p < 0.001$. a = difference from control, b = difference from kisspeptin alone (KP), c = significance between saline (acyline pretreated) and kisspeptin (acyline pretreated).

shape, basal cells were not conspicuous and the size of lumen was increased (Fig. 3.46 c-d).

Prostate gland from rats treated with saline (acyline pretreated)

In the prostate from rats treated with saline (acyline pretreated) epithelial folds were reduced. The height of epithelium also decreased (Fig. 3.46 e-f).

Prostate gland from rats treated with kisspeptin (acyline pretreated)

In the prostate of rats treated with kisspeptin treatment (acyline pretreated) the folds of epithelium were increased in number as compared to saline treatment (acyline pretreated). The height of epithelium also increased. Compared to control the epithelial height and number of epithelial folds showed a decreased (Fig. 3.46 g-h).

3.3.10 Electron microscopic examination

Control prostate

Ultrastructure of control non-treated prostate showed simple secretory epithelium with high columnar cells. The nuclei were situated in the basal region of the cell. In the perinuclear cytoplasm, endoplasmic reticulum consisted of parallel and flattened cisternae. The Golgi complex was well formed and was situated in the supranuclear region (Fig. 3.47 a). For further details see section 3.3.5.

Prostate gland treated with kisspeptin alone

The prostate in this group was characterized by marked atrophy, wide intercellular spaces, irregular shape nuclei, and condensed and fragmented chromatin that was scattered throughout the nucleoplasm. Digestive vacuoles containing cell remnants were also observed in the perinuclear cytoplasm. The cisternae of the Golgi complex were dilated (Fig. 3.47 b).

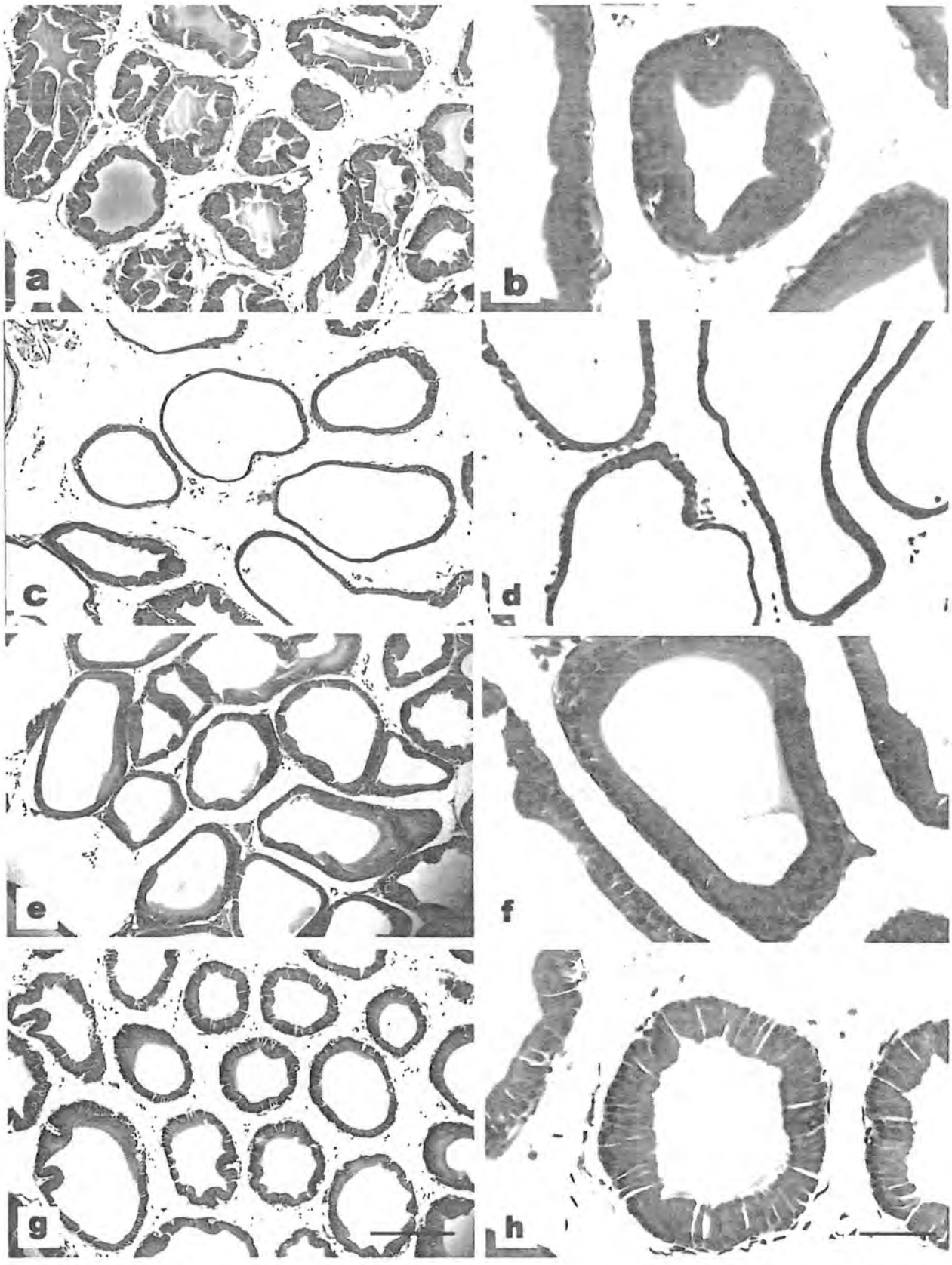
a
b
c
d
e
f
g
h

Prostate gland treated with saline (acyline pretreated)

The primary alterations were irregularity of nuclear shapes with invagination of the envelope and smaller nucleoli. Endoplasmic reticulum and Golgi apparatus were less organized with dilated cisternae. Vacuoles and cellular debris were present. Intracellular spaces were enlarged (Fig. 3.47 c).

Prostate gland treated with kisspeptin (acyline pretreated)

With this treatment there was some recovery in the prostate tissue than saline (acyline pretreated). The nuclei contained prominent nucleoli. The tissue still contained dilated Golgi apparatus and endoplasmic reticulum. Number of vacuoles decreased (Fig. 3.47 d).

3.3.11 DNA fragmentation

Normal prostate gland did not show any fragmentation of DNA. DNA fragmentation was evident in the saline treated (acyline pretreated) group. DNA extracted from kisspeptin (acyline pretreated) group showed no damage (Fig. 3.48 A).

The degree of % DNA fragmention increased highly significantly ($p < 0.001$) in the kisspeptin alone and saline (acyline pretreated) treated groups, but remained similar to kisspeptin (acyline pretreated) group as compared to control. Intergroup comparison showed that the % DNA fragmention increased significantly ($p < 0.001$) in the saline (acyline pretreated) group when compared to kisspeptin (acyline pretreated) group (Fig. 3.48 B).

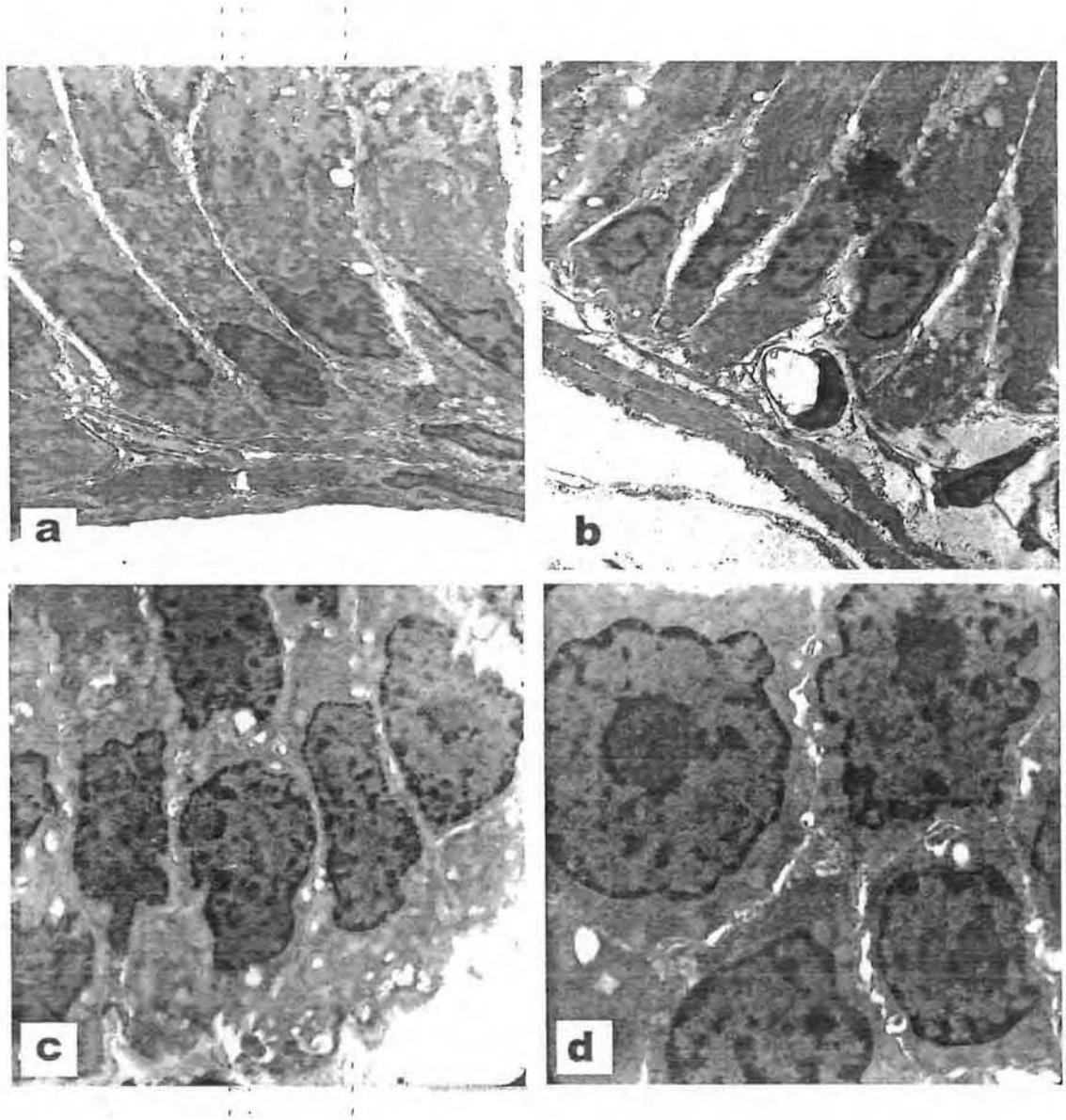

Figure 3.47 Electron micrographs of prostate tissue from control, kisspeptin alone, saline (acyline pretreated) and kisspeptin (acyline pretreated) rats.

a The prostate of control rats showing principal and basal cells containing well developed Golgi complex in supranuclear region. ×5, 000.

b: The prostate in this group was characterized by marked atrophy, wide intercellular spaces, irregular shaped nuclei, and condensed and fragmented chromatin scattered throughout the nucleoplasm. The cisternae of the Golgi complex were dilated. ×12,000.

c: The prostate of saline (acyline pretreated) contained endoplasmic reticulum and Golgi apparatus with dilated cisternae. Vacuoles were present. Nuclear shape became irregular with invagination of the envelope. The basement membrane was infolded. ×8,000.

d: The prostate of rats treated with kisspeptin (acyline pretreated). The tissue showed some recovery as compared to saline (acyline pretreated). ×12, 000.

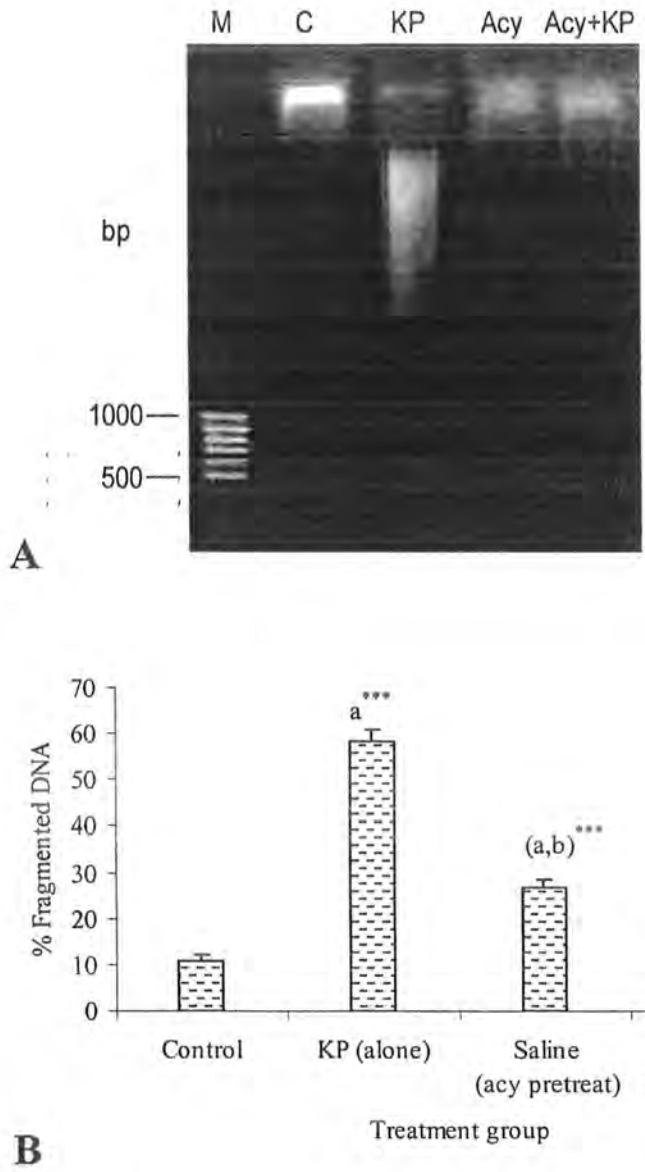

Figure 3.48 A) DNA ladder assay showing fragmented DNA, at alone kisspeptin dose, from rat prostate. With acyline treatment faint smear was observed while it remained intact with kisspeptin (acyline pretreated) treatment. M= 100-bp ladder (DNA size markers), C=control (saline treated), KP= kissprptin alone, Acy= Saline (acyline pre-treated), Acy+KP= Kisspeptin (acyline pre-treated).

B) DNA fragmentation assay. Percentage of fragmented DNA relative to total DNA increased significantly in all treated groups. It increased in kisspeptin (acyline pre-treated) treatment as compared to alone kisspeptin as well as saline (acyline pre-treated) treatment. Values are expressed as ± SE. $^{***}p < 0.001$.

DISCUSSION

DISCUSSION

The kisspeptin/GPR54 interaction has finally been identified in recent years as key regulator of the HPG axis (de Roux *et al.*, 2003; Seminara *et al.*, 2003). Although the acute effects of central and peripheral administration of kisspeptin have been explored in rats and mice (Gottsch *et al.*, 2004; Navarro *et al.*, 2004a; Navarro *et al.*, 2005a), effects of long term kisspeptin administration on structure and functional aspects of testicular tissue in general and in particular prepubertal testes remain elusive. Moreover, to date there is no report on the effect of kisspeptin administration on accessory sex glands, the seminal vesicle and prostate. The present study investigated the gonadal maturation and reproductive hormones status following kisspeptin challenge in reproductively immature male rats. Presently, subchronic 12 days i.p. kisspeptin administration at 1μg dose led to a significant decrease in type A spermatogonia, preleptotene spermatocytes, pachytene spermatocytes and step 7 spermatids, DSP, epithelium height, epididymes weight, prostrate and seminal vesicle weight. A significant decrease in prostate gland and seminal vesicle weight was accounted for by histological changes including the decrease in the height of secretory acini and dilatation of the lumen. Electron microscopy indicated dilatation of endoplasmic reticulum and Golgi apparatus cisternae, decrease in the number of secretory granules and appearance of the autophagic vacuoles. No effect was however found on body weight, testis weight, testis volume, GSI %, and seminiferous tubular diameter. At 1 ng dose, germ cell number, daily sperm production (DSP) and epithelial height decreased while the body weight, reproductive organ weights, GSI % and tubular diameter did not change significantly. At further low dose of 10 pg decrease in the above parameters did not lead to significant levels. A concomitant suppression of plasma LH and testosterone concentrations and, degeneration of testicular cells at 1 ng and 1 μg doses were the major outcomes.

Kisspeptin effects were further evaluated by blocking GnRH action using acyline as an antagonist. Body weight, testes weight, testes volume, GSI %, seminal vesicle and prostate weights were not altered. Plasma FSH, LH and testosterone concentrations decreased in the saline (acyline pretreated) treated group as well as

kisspeptin (acyline pretreated) treated group. Seminiferous tubular epithelium height decreased significantly in treated groups while seminiferous tubular diameter decreased non-significantly. In the kisspeptin (acyline pretreated) treated group, only type A spermatogonia decreased significantly while other parameters remained unaffected in contrast to saline (acyline pretreated) treated group where type A spermatogonia, preleptotene spermatocytes, pachytene spermatocytes, stage VII spermatids, elongated spermatid head count and DSP showed a decrease when compared with the control. Epithelial height of secretory acini of seminal vesicle and prostate decreased in both saline (acyline pretreated) and kisspeptin (acyline pretreated) groups compared to control. Histology and ultrastructure showed disorganization of the testicular tissue and cellular organelles involved in the secretory process as regards principal cells of the prostate and seminal vesicle tissues.

One of the salient findings of present study is that, despite significantly decreased LH and testosterone concentrations at 1 ng and 1 μg doses, subchronic administration of kisspeptin-10 did not affect FSH levels, which instead remained comparable to saline treated controls, at the end of the 12 day period. It appears that significant decrease in the testosterone concentration following the kisspeptin treatment was quite possibly due to significantly lowered LH concentration. This indicates that sharp decline in testosterone concentration was quite likely due to the active suppression of gonadal testosterone secretion. Alternatively, this might have been due to the degenerating testes as indicated by the histomorphological damage.

These present data are the first to disclose that in prepubertal male rat, persistent administration of kisspeptin may lead to obvious dissociation of gonadotropin levels, with selective decrease of LH secretion only. Loss of LH stimulation after continuous kisspeptin administration accompanied by persistent FSH levels casts doubts on a simple desensitization of the HPG axis as a contributing factor for the phenomenon. It appears that chronic kisspeptin input may have resulted in altered pattern of pulsatile GnRH release in terms of frequency and pulse amplitude, which might preferentially derive FSH secretion (Dalkin *et al.*, 1989). Notably, Dalkin *et al.* (1989) demonstrated that the frequency of GnRH stimulation can differentially regulate gonadotropin subunit mRNA expression and might be a

mechanism that allows a single GnRH peptide to selectively regulate the expression of gonadotropin subunit gene and hormone secretion. Navarro *et al.* (2005b) documented that i.c.v administration of KiSS-1 peptide significantly stimulated FSH secretion in prepubertal and adult rats. Yet, dose-response analyses *in vivo* demonstrated an ED_{50} value for the FSH-releasing effects of KiSS-1 of 400 pmol, *i.e.* approximately 100-fold higher than that of LH. In the present study the reason for unaltered FSH values might be the low dose. FSH concentration may alter at higher kisspeptin doses.

The present results differ slightly from those of Thompson *et al.* (2006) who showed that gonadotropin levels do not change significantly and there occurs a nonsignificant decrease in plasma concentration of total ($P = 0.07$) and free ($P = 0.11$) testosterone following chronic and continuous s.c. administration of kisspeptin-54 at the rate of 50 nmol/day for 13 days to adult male rats. One possibility is that in the present study kisspeptin-10 was used while they used kisspeptin-54 which is relatively more potent in releasing plasma LH and total testosterone (Thompson *et al.*, 2006; and Pheng *et al.*, 2009). However, it should be noted that kisspeptin-10 is the shortest active form of kisspeptin, consisting of 10 amino acid-amidated carboxy terminal sequence crucial for receptor interaction (Ohtaki *et al.*, 2001). In addition, the current study focused maturing rats while theirs (Thompson *et al.*, 2006) was conducted on adult rats.

Thompson *et al.* (2006) also conducted short term study of continuous s.c. administration of 50 nmol kisspeptin-54 demonstrating that kisspeptin treatment for one day increased plasma LH levels to nearly threefold concentration compared with saline treated controls. This increase in plasma LH was lost after 2 days of continuous kisspeptin treatment that became indistinguishable from saline treated control animals after 3 days of treatment. No effect was observed on plasma FSH after 1, 2 or 3 days of continuous s.c. kisspeptin administration. Similarly, an acute significant four fold increase in plasma testosterone compared with saline treated controls was observed after 1 day of kisspeptin-54 administration. This stimulatory effect too was lost after two days of continuous treatment with kisspeptin (Thompson *et al.*, 2006).

In the present study measurement of the hormone levels at alternate days was also conducted, however this was done for 1 μg dose only. FSH levels increased progressively from postnatal day 35 to 47 but remained similar to saline treated controls throughout the study period. In kisspeptin treated rats LH levels peaked after 4 days of treatment, and declined thereafter to become significantly lower than the controls after 12 days of treatment. To follow the general growth related pattern in both the control and treated rats, plasma testosterone levels increased with increasing age of rats, however kisspeptin treatment lowered testosterone levels compared to control animals after 6 days of treatment that remained lower thereafter. The control values observed in the present study appear similar to Zapatero-Caballero *et al.* (2003) who demonstrated that serum FSH levels decrease from day 5 to day 15, with a progressive rise until day 45. Circulating LH levels were quite variable and did not show significant changes with increasing age and serum total testosterone was hardly detectable during the neonatal and infantile periods and was undetectable between day 25-35, when it began to rise until day 50. Serum-free testosterone levels paralleled those of total testosterone until day 45 and remained unchanged afterwards (Zapatero-Caballero *et al.*, 2003).

Presently, it seems logical to presume that kisspeptin perhaps acted to suppress an early maturation of gonads as the male gonads have to develop fully at a later stage and sperms are first produced in the testes around day 45 with optimal production occurring at 75 days (Russell, 1992). However, testicular degeneration observed by Thompson *et al.* (2006) does not conform to this notion since they collected data from adult male rats. Thus it is suggested that suppressed levels of LH and testosterone could simply be the pharmacological effect of kisspeptin treatment.

Significant decreases in germ cells, daily sperm production, total support capacity of Sertoli cells and Sertoli efficiency and meiotic index and an increase in coefficient of mitosis indicated germ cell loss, which may have occurred through apoptotic mechanisms. Histomorphological examination of the seminiferous tubules appears to support this phenomenon.

Presently, cellular data fully supports kisspeptin mediated suppression of LH and testosterone concentrations at stage VII of the spermatogenic cycle resulting into

excessive degeneration of the seminiferous epithelium. Presently, scanty round and elongated spermatids were consistently observed, all indicating germ cell maturation arrest. A previous report by Kerr (1995) demonstrated that FSH and testosterone appear to act on the seminiferous epithelium at different stages of the spermatogenic cycle in the rat testis, the former possibly during stages I-VI and the latter at stages VII-VIII, with stages IX-XIV showing normal germ cell development if the previous stages had been properly maintained. Also, McLachlan *et al.* (1994) showed that LH withdrawal suppressed spermatogenesis and resulted in significant reductions in the numbers of spermatogonia, preleptotene spermatocytes, pachytene spermatocytes, and round spermatids while elongated spermatids were undetectable. Similarly acute removal of the testosterone produced a distinctive pattern of spermatogenic cell degeneration. When testosterone was removed by the use of the Leydig cell cytotoxin ethane dimethane sulphonate (EDS) for a period of few days, there occurred a sharp increase in the number of pyknotic nuclei and cytoplasmic vacuoles (markers of cellular degeneration) in several stages of the cycle, particularly affecting pachytene spermatocytes and spermatids (Kerr *et al.*, 1993).

Expression of both KiSS-1 and GPR54 has been reported in the ovaries and testes of rodents (Kotani *et al.*, 2001; Ohtaki *et al.*, 2001, Terao *et al.*, 2004; Castellano *et al.*, 2006), a direct testicular effect may be speculated to provide a functional kisspeptin-GPR54 system for local regulation of reproductive status at the level of gonads. Some reports of the effects of GnRH agonists also suggest an extrapituitary direct inhibitory action on the gonads (Hsuch and Schaeffer 1985; Van Kroonenburgh *et al.*, 1986). Thompson *et al.* (2009) have recently shown that a single i.c.v. injection of kisspeptin-54 caused testicular degeneration, suggesting that the action was GnRH-mediated.

Earlier, Thompson *et al.* (2006) also showed testicular degeneration in adult rats after s.c. administration of kisspeptin for 13 days. No work has however been conducted on sexually immature male rats as yet. The present is therefore the first quantitative study on spermatogenesis in kisspeptin treated prepubertal male rats. Appropriate comparison of the present data cannot therefore be made from the existing studies. On sex basis, the current results are in striking contrast to an earlier

study carried out on maturing female rats (Navarro *et al.*, 2004b), and also to that of Roa *et al.* (2008) in terms of hormone concentrations in which both FSH and LH levels were significantly elevated at day 7 after constant i.c.v infusion of kisspeptin 10 to prepubertal female rats. Strikingly, these two studies are also contradictory to each other because Navarro *et al.* (2004b) showed that chronic central administration of kisspeptin to immature female rats induced the precocious activation of the gonadotrophic axis, as estimated by advanced vaginal opening, elevated uterus weight, and increased serum levels of luteinizing hormone (LH) and oestrogen, while Roa *et al.* (2008) documented that despite significantly elevated gonadotropin levels uterus weights and age of occurrence of vaginal opening did not change.

The possibility that kisspeptin may affect the microvasculature of testis cannot be ignored. As Mayerhofer and Dube (1989) showed that three months of daily s.c. injections of gonadotropin-releasing hormone agonist (GnRH-A) [D-Trp6, des-Gly-NH2(10)]GnRH ethylamide to adult male dogs significantly decreased the diameter of seminiferous tubules and clearly altered the ultrastructure of testicular microvasculature as compared to capillaries and venules in untreated controls.

Presently, ultrastucture of the testicular epithelium demonstrated three major changes in the testicular tissue in kisspeptin treated rats. Firstly, the presence of pyknotic Leydig and Sertoli cell nuclei and associated cytoplasmic vacuolizations. Secondly, the appearance of large intercellular spaces between the Sertoli cells and lastly, consistent ultrastructural change noticeable was the loss of lamination with decreased thickness of the basal lamina. These changes increased dose dependently.

Close relationship between the Leydig cells and blood vessels suggests that these cells are at high risk of exogenous toxicants and appearance of multivacuolated Leydig cells is possibly a form of cell involution. Leydig cells are known to have receptors for LH that stimulates these cells to produce testosterone (Johnson *et al.*, 1972). Both LH and testosterone are responsible for normal spermatogenesis in male rats (Steinberger 1971; Zirkin, 1998). Depletion of LH receptors and decrease in peripheral LH by exogenous testosterone administration results in the reduction of testosterone secretion (Johnson *et al.*, 1972; Bijlsma *et al.*, 1982; Ichihara *et al.*, 2001). Lowered testosterone levels might also be due to the negative feedback

suggesting that kisspeptin works by causing the pituitary gland to release the hormones that cause the testicles and adrenal glands to make testosterone. The pituitary gland then runs out of its hormones, and testosterone production drops. Thus decreased testosterone levels following the kisspeptin administration could be involved in the involution of seminiferous epithelium (Paniagua *et al.*, 1986).

Sertoli cells foster the development and maintain the viability of germ cells. They secrete hormonal and nutritive factors into a specialized compartment, formed by tight junctions between the adjacent Sertoli cells (blood-testis barrier), that surrounds the germ cells. Sertoli cells are also the sites of attachment to germ cells. They serve both to maintain a close association between these two cell types and to provide physical support to the germ cells (Richburg, 2000). Damage to Sertoli cells that was observed presently may account for germ cell degeneration.

The basement membrane plays an important role in maintaining the structural and functional integrity of tissues (Richardson *et al.*, 1998). It provides structural stability of organs and sends signals to cells through cell surface receptors (Timple, 1996). Altered basement membrane structure as seen presently, was most likely associated with severe functional impairment of testes. Lamination of the basement membrane is a normal character, and was found in control animals as a regular feature. This laminated membrane is believed to contain alkaline phosphatase and acts as a semi permeable biochemical barrier (Gravis *et al.*, 1977). Thus, a loss of this barrier would enable toxic materials to cross the basal lamina into the seminiferous tubules. If the biochemical blood-testis barrier is lost as a result of ultrastructural damage caused to the basal lamina, spermatogenesis would be easily impaired. Increase in testicular temperature, reflux of adrenal metabolites, and stasis of testicular venous drainage can all destroy the alkaline phosphatase biochemical barrier. Once this barrier is lost, toxic materials would lead to a dysfunction of the Sertoli cells and/or damage to spermatogenesis in the basal cells and in the adluminal testicular area (Gravis *et al.*, 1977; Cameron *et al.*, 1980). Detached germ cells found in the present study are possibly due to a disruption of the Sertoli-germ cells interaction. This may ultimately lead to sloughing of the germ cells from seminiferous epithelium (Richburg, 2000).

Ultrastructure of Leydig cells showed invagination of the nuclear membrane and vacuoles in the cytoplasm as well as dilated cell organelles. Since Leydig cells are the only source of testosterone production in testis, it is possible that kisspeptin treatment modulated Leydig cell function to reduce steroid production or promoted Leydig cell degeneration in treated animals. Presently, it might have contributed towards decreased plasma testosterone concentration in kisspeptin treated male rats as seen in the present study. This possibility is further strengthened by the observations that kisspeptin though significantly lowering the plasma testosterone levels subsequently caused a reduction of spermatogenesis in these prepubertal rats. Leydig cells are known to have receptors for LH that stimulate these cells to produce testosterone (Johnson *et al.*, 1972). As both LH and testosterone are responsible for normal spermatogenesis in male rats (Steinberger 1971; Zirkin 1998), therefore, depletion of LH receptors and decrease in peripheral LH by exogenous testosterone administration result in the reduction of testosterone secretion (Johnson *et al.*, 1972; Bijlsma *et al.*, 1982; Ichihara *et al.*, 2001). It has been suggested earlier that decrease in testosterone level could be involved in the involution of seminiferous epithelium Paniagua et al., 1986).

Presently, kisspeptin treatment significantly elevated internucleosomal DNA fragmentation at all doses. The effect appeared to be dose dependent. DNA fragmentation was detected concomitant with the decrease in organ weights and a compromise of histological status. A quite many DNA ladder assays showed smears while clear bands of nearly 200 bp in some or multiples of 200 bp were evident in others. Studies suggest that activation of endogenous endonucleases which fragment the DNA into oligonucleosomal fragments of 200 base pairs is the earliest and most characteristic biochemical event common to all processes of apoptosis (Wyllie, 1980; Compton, 1992). Apoptosis is characterized by chromatin condensation, activation of some caspases and fragmentation of DNA at internucleosomal linker sites giving rise to discrete bands of multiples of 180–200 bp (Carson and Ribeiro, 1993). Although exceptions do exist, this form of DNA degradation has been very widely observed in apoptosis. Different types of DNA fragmentation have been reported during apoptosis, in the presence or absence of the characteristic internucleosomal DNA cleavage (ladder-like) pattern (Bortner *et al.*, 1995). Histomorphological data appears

to support apoptosis hypothesis, because germ cell nuclei were found regressed and pyknotic with kisspeptin treatment. At higher doses multinucleated germ cell formation was also frequent.

Testosterone is essential for the maintenance of height of the mucosal epithelium required for productions of continuous seminal vesicle and prostate secretions. It also influences the function of smooth muscle in the seminal vesicles (Fawcett, 1986). The growth and active secretion of seminal vesicle epithelium and other accessory reproductive tissues are dependent on the presence of circulating androgens (Brandes, 1974; Higgins *et al.*, 1976). Deprivation of androgens to sensitive tissue such as the seminal vesicles decreases cell size, structural integrity and morphological characteristics (Brandes, 1974; Veneziale *et al.*, 1977a). The prostatic epithelial height is known to be androgen-dependent (Gonzales *et al.*, 2005). Secretory activity by the prostate and seminal vesicles therefore is a sensitive, androgen dependent function. Decreased levels of plasma testosterone or interface with androgen receptors in these tissues may result in a reduced secretion leading to atrophic changes. In the present study Golgi complex and endoplasmic reticulum were found dilated, number of secretory granules lowered and characteristic structure of seminal vesicle was lost following kisspeptin administration. The dilatation of endoplasmic reticulum and Golgi complex reflects a decrease in protein synthesis as previously evidenced by Veneziale *et al.* (1977b). Aumuller *et al.* (1981) demonstrated that the autophagic vacuole formation and dilation of cisterns of the Golgi complex and of the granular endoplasmic reticulum can be interpreted as signs of degradation of biological membranes.

Experiments analyzing changes in the accessory sex glands in response to androgen deprivation have shown that castration (Vilamaior *et al.*, 2000), diabetes (Carvalho *et al.*, 2003) and chronic alcoholism (Sa'ttolo *et al.*, 2004) caused alterations in the accessory glands, especially in the prostate, in response to testicular alterations. These changes include epithelial degeneration and atrophy of organelles involved in the secretory process accompanied by biomembrane destructuring which lead to an altered aspect of luminal secretion (Carvalho *et al.*, 2003; Sa'ttolo *et al.*, 2004). Aumuller and Seitz (1990) confirmed that membrane degradation in the

accessory sex glands, such as dilatation of the Golgi cisternae and disintegration of the granular endoplasmic reticulum is a typical characteristic of androgen depletion caused by alterations in the hypothalamus-pituitary-gonadal axis. In conclusion, chronic administration of kisspeptin is found to be a determinant of changes in the cell morphology in the prostate which might have influenced the glandular function. The present is the first study of the effects of kisspeptin on the ultrastucture of testis and accessory sex glands; therefore comparison with other studies is not possible at present. However, histomorphological alterations at light and ultrastructural level necessitate the biochemical analyses of the seminal vesicle and prostate gland to investigate the seminal fluid fructose concentration, the concentrations of calcium, citrate, phosphate and pH of the prostatic fluid, parameters crucial to these organs.

The present study showed that in acyline treated rats there occured significant decrease in the population of type A spermatogonia, preleptotene spermatocytes, pachytene spermatocytes and step 7 spermatids with a concomitant decrease in plasma LH and testosterone concentrations. These results are parallel to those of Zhengwei *et al.* (1998) who reported that proportion of the type A spermatogonia, preleptotene, leptotene, zygotene and pachytene spermatocytes were all reduced in cetrorelix (GnRH antagonist) treated monkey testes and suppressed serum testosterone concentrations to castrate levels. In the present experiments pretreatment of rats with a single injection of acyline protected against kisspeptin induced decline in spermatogenesis. This was indicated by quantitative assessment of testicular histology at stage VII of spermatogenesis and testicular spermatid head counts. In instances of testicular damage produced by various chemical or physical agents, revival of spermatogenesis can be induced by suppression of testosterone and FSH by treatment with GnRH analogs (Kangasniemi *et al.*, 1995; Meistrich and Kangasniemi, 1997; Blanchard *et al.*, 1998; Meistrich and Shetty, 2003). The mechanisms causing failure of spermatogonial differentiation following cytotoxic therapies and how the suppression of testosterone restores this ability to differentiate are not yet known (Boekelheide *et al.*, 2005). Meistrich *et al.* (2001) showed that GnRH antagonist is more effective at stimulating the recovery of tubule differentiation and sperm counts in irradiated rats than a GnRH agonist. The present study also suggests that pretreatment with acyline can recover testicular degeneration. Thompson *et al.* (2009)

demonstrated that continuous s.c. administration of kisspeptin-54 caused testicular degeneration after only 12 h, while gonadotropins were still raised, suggesting that the testicular degeneration is independent of the desensitization of the HPG axis to kisspeptin-54 and pretreatment with cetrorelix blocked kisspeptin-induced testicular degeneration, and a single i.c.v. injection of kisspeptin-54 caused testicular degeneration, suggesting it to be GnRH-mediated. Therefore together with recent studies the present study also suggests that kisspeptin may act via both routes, central as well as peripheral.

Medical treatments required for life-threatening diseases or exposure to environmental toxicants may jeopardize the fertility of men and women of reproductive age. In men, such exposures can lead to effects ranging from temporary oligospermia to permanent azoospermia, and occasionally to androgen insufficiency. In women, such exposures can result in a range of effects from temporary amenorrhea to premature menopause and permanent amenorrhea, with the associated estrogen insufficiency. Methods to prevent these effects on fertility and to restore gonadal function after the toxic treatment are of particular importance to men and women of child bearing age. A variety of biochemical and biological approaches such as thiol radioprotectors, prostaglandin analogs, growth factors, blockers of apoptotic pathways, and reduction in blood flow, have been tested to protect the testes in experimental animal model systems against radiation and chemotherapy (reviewed in Meistrich *et al.*, 2007). However, the greatest research interest in nearly all clinical trials involved hormonal modulation in attempts to prevent or reverse damage to the germ line from radio- and chemotherapy. Given results of the present study it can be suggested that kisspeptin/GPR54 system may act as one of the targets for the pharmacological intervention of the reproductive system.

Conclusion and Future prospects

It is finally concluded that chronic kisspeptin administration to prepubertal rats causes severe testicular degeneration and a differential desensitization of the HPG axis followed by a decrease in the populations of germ cells, elongated spermatid head count and daily sperm production. Interestingly, the effect appears to be dose dependent, as mild effect on hormone lowering and testicular morphology was noticeable at 1ng dose, while no effect was found at 10 pg dose. In contrast, excessive degeneration of histological parameters and suppression of gonadotropins and testosterone was observed at 1 μg dose.

Antagonist for kisspeptin is available now. It Inhibits kisspeptin-10 stimulation of inositol phosphate in CHO cells expressing human gpr-54 and release of GnRH, pulsatile GnRH release in pubertal female rhesus monkeys, kisspeptin-10 stimulated LH in intact and castrated rats and mice and in ovariectomized ewes (Roseweir *et al.,* 2009). The development of kisspeptin antagonists provides a valuable tool for investigating the physiological and pathophysiological roles of kisspeptin in the regulation of reproduction and offers a unique therapeutic agent for treating hormone-dependent disorders of reproduction, including infertility, delayed and precocious puberty and metastatic prostate cancer. Further pharmacological and pathological studies using kisspeptin antagonist are required to be carried out. There was no antagonist available at the time the present study was conducted therefore attempt was made to indirectly block kisspeptin actions via acyline, a potent GnRH antagonist.

Kisspeptin is a peptide of diverse and multifunctional nature, involving various physiological systems and acting at all levels of the reproductive axis—brain, pituitary, gonad, and accessory organs. Kisspeptin exercises a crucial role in stimulating GnRH release, relaying steroid hormone negative and positive feedback signals to GnRH neurons, serving as a gatekeeper to the onset of puberty, and relaying photoperiodic information. Other less well defined actions of kisspeptin may include a role in the control of insulin and/or glucagon secretion, perhaps local control of ovulation, and blocking ectopic implantation (Oakely *et al.*, 2009). The field of "reproductive kisspeptinology" has blossomed and matured in the past 6 yr; however,

much is yet to be learned and important questions remain unanswered. For example, what specific neurotransmitters and signaling molecules control kisspeptin secretion? What is the role of kisspeptin's cotransmitters in the ARC (dynorphin, NKB, and others?) in the regulation of GnRH secretion? How do circadian signals from the SCN interact with the kisspeptin neurons in the AVPV? What activates kisspeptin neurons at puberty? What is the molecular basis for sexual differentiation of kisspeptin neurons? What molecular form(s) of the various kisspeptin fragments represent the endogenously active molecule? What is the physiological significance of kisspeptin signaling outside of the hypothalamus? What are the molecular mechanisms by which testosterone inhibits the expression of Kiss1 in the ARC but induces its expression in the AVPV and PeN? How do progesterone and the progesterone receptor (PR) influence Kiss1 gene expression? What are the electrophysiological properties of Kiss1 neurons in the AVPV and ARC? What is the functional significance of enhanced Kiss1 production during pregnancy? (Oakely *et al.*, 2009).

Several investigational tools may aid in answering these questions. For example, generation of a mouse expressing green fluorescent protein under the *Kiss1* promoter (*Kiss1*-GFP), a *Kiss1*-cre mouse, a floxed *Kiss1* mouse, or a *Kiss1* ribo-tagged mouse could prove invaluable to answer these questions. Another frontier in kisspeptin biology is the development of novel ligands (antagonists and agonists) to the kisspeptin receptor. Such analogs may prove useful in the treatment of people with hypogonadotropic hypogonadism and other reproductive disorders (*e.g.*, precocious puberty, endometriosis, metastatic prostate cancer, and ovulation induction) and may even provide a novel strategy for hormonal birth control (for both males and females). Beyond this, kisspeptin has been implicated for a role in a variety of other physiological control systems (*e.g.*, metabolism, vascular biology, pregnancy, cancer)—thus, improved understanding of kisspeptin and its receptor may benefit scientific research across a wide swath of the physiological community, not just reproductive endocrinology (Oakely *et al.*, 2009).

Further work is required to elucidate the mechanisms involved in the kisspeptin-induced testicular degeneration and reversal of these effects. Parallel quantitative studies on adult testes are also required to be conducted for comparing testes status in

maturing and mature animals. Enzymes involved in the testicular pathway like 17α HSD and 5α reductase should also be investigated. Plasma free and bound testosterone, cholesterol, albumin, androgen binding proteins and involvement of elements should also be measured in response to kisspeptin administration. Semen characters like fructose, citric acid and zinc may provide new insights into kisspeptin involvement. should also be measured. Similarly, kisspeptin may be involved in the activation of excitatory neurotransmission and deactivation of inhibitory neurotransmission to GnRH neurons.

PUBLICATIONS

1. Ramzan F, Qureshi IZ. Intraperitoneal kisspeptin-10 administration induces dose-dependent degenerative changes in maturing rat testes. Life Sciences 2011; 88: 246–256. doi:10.1016/j.lfs.2010.11.019 (impact factor = 2.52).

2. Ramzan F, Qureshi IZ. Kisspeptin administration dose dependently induces degenerative changes in histology and ultra structure of seminal vesicles and prostate gland of maturing rats. (Submitted to regulatory peptides).

Conference presentation

Intraperitoneal administration of kisspeptin-10 induces dose-dependent degenerative changes in prepubertal rat testes (presented in National Symposium on Current trends in Cellular, Medical and Environmental physiology. 17^{th} -19^{th} May, 2010).

Life Sciences 88 (2011) 246–256

Contents lists available at ScienceDirect

Life Sciences

journal homepage: www.elsevier.com/locate/lifescie

Intraperitoneal kisspeptin-10 administration induces dose-dependent degenerative changes in maturing rat testes

Faiqah Ramzan, Irfan Zia Qureshi *

Laboratory of Animal and Human Physiology, Department of Animal Sciences, Faculty of Biological Sciences, Quaid-i-Azam University 45320, Islamabad, Pakistan

ARTICLE INFO

Article history:
Received 3 May 2010
Accepted 15 November 2010
Available online 26 November 2010

Keywords:
Kisspeptin
Metastin
Hypothalamic-pituitary-gonadal axis
Prepubertal testes
Seminiferous tubules
Spermatogenesis

ABSTRACT

Aims: Kisspeptin, a peptide secreted by hypothalamic neurons, is a critical regulator of reproduction and puberty but its role in the regulation of gonadal maturation in sexually immature males is elusive. The present study investigated the effects of 12 days of pulsatile kisspeptin administration on gonadotropins and testosterone release and maturation of immature male gonads.

Main methods: Kisspeptin-10 was administered intraperitoneally at different dosage concentrations (1 μg, 1 ng, and 10 pg) to 5 weeks old prepubertal male rats, twice daily for 12 days. Plasma LH, FSH and testosterone concentrations were measured through competitive-binding radioimmunoassay. Spermatogenesis was studied mainly at stage VII of the spermatogenic cycle through light and electron microscopy.

Key findings: At the end of the treatments plasma LH and testosterone concentrations were reduced significantly at 1 ng and 1 μg kisspeptin doses ($P<0.05$; $P<0.01$). Type A spermatogonia, preleptotene spermatocytes, pachytene spermatocytes, step 7 spermatids, elongated spermatids and daily sperm production decreased significantly ($P<0.05$). Sertoli cell efficiency and total support capacity of Sertoli cells were reduced at all doses ($P<0.05$). Meiotic index decreased ($P<0.05$) at 1 μg dose only, whereas coefficient of mitosis increased at 1 ng and 1 μg ($P<0.01$) kisspeptin doses. Histologically, degeneration of seminiferous tubules was evident showing tubular necrosis, multinucleated giant cell formation, intratubular vacuolization, widened lumen and deshaped germ cells. Marked ultrastructural changes characterized by thin basal laminae, enlarged intratubular spaces, abnormal acrosome and disrupted germ cells were noticeable.

Significance: In conclusion long-term kisspeptin-10 administration negatively regulates gonadal maturation in prepubertal testes.

Introduction

Initiation of reproduction in a maturing animal is a complex process and requires the interaction of forebrain, pituitary and gonads. The onset of puberty is triggered by the activation of neurons in the hypothalamus that produce gonadotropin releasing hormone (GnRH). The amplified secretion of GnRH evokes the release of luteinizing hormone (LH) and follicle stimulating hormone (FSH), which then awaken the gonads (Ebling and Cronin, 2000; Plant and Barker-Gibb, 2004). Although this cascade has been well characterized for many mammalian species; the molecular and cellular events at the central level that actually initiate this process, remain unknown. Recently, it was shown that dysfunctional or deletional mutations in the gene encoding the G protein-coupled receptor, GPR54, cause hypogonadotropic hypogonadism, (de Roux et al., 2003; Seminara et al., 2003). Very soon, kisspeptin, a product of the *Kiss1* gene was found to be the endogenous ligand of GPR54 (Seminara et al., 2003; Plant et al., 2006). The gene for kisspeptin encodes a 145-amino-acid precursor peptide that is proteolytically cleaved into a family of peptides collectively referred to as kisspeptins, the most abundant of which is an amidated 54-amino-acid protein, kisspeptin-54. Further cleaving gives rise to shorter products namely kisspeptin-14, kisspeptin-13 and kisspeptin-10 (Kotani et al., 2001; Muir et al., 2001; Mead et al., 2007).

Both kisspeptin and GPR54 (now called Kiss1r, Oakley et al., 2009) transcripts are expressed in a variety of tissues including the placenta, several brain regions, spinal cord, testes, ovaries, liver, small intestine, pancreas, heart, kidney and uterus (Roa et al., 2008). Expression of both the *Kiss1* and *Kiss1r* mRNA is regulated developmentally as well as hormonally in the hypothalamus, with a sharp increase at prepubertal age in both male and female rats, changes throughout the estrous cycle in adult females, and increases after gonadectomy; an effect that is prevented by sex steroid replacement (Navarro et al., 2004a; Irwig et al., 2004). Kisspeptins potently stimulate LH secretion in mice (Gottsch et al., 2004) and rats, in both males and females, in prepubertal and adult rats (Navarro et al., 2004a,b), and as well as in juvenile agonadal male monkeys (Shahab et al., 2005).

These studies collectively point out that kisspeptins are likely to be the most potent elicitors of GnRH/gonadotropin secretion (Roa et al.,

* Corresponding author. Tel.: +92 51 90643013; fax: +92 51 2601176.
E-mail addresses: irfanzia@qau.edu.pk, irfanziaqureshi@gmail.com (I.Z. Qureshi).

0024-3205/$ – see front matter © 2010 Elsevier Inc. All rights reserved.
doi:10.1016/j.lfs.2010.11.019

REFERENCES

REFRENCES

Abercrombie, M. (1946). Estimation of nuclear population from microtome sections. *Anat. Rec.* **94**: 239-247.

Allen, E. (1918). Studies on cell division in the albino rat. *J. Morphol.* **31**: 133-185.

Almenara, A., Escalante, G., Gazzo, E., Gonzales, G. F. (2000). Transillumination to evaluate spermatogenesis: Effect of testosterone enanthate in adult male rats. *Arch. Androl.* **46**: 21-8.

Anderson, R. U., Wise, D., Sawyer, T. and Chan, C. A. (2006) Sexual dysfunction in men with chronic prostatitis/chronic pelvic pain syndrome: improvement after trigger point release and paradoxical relaxation training. *J. Urol.* **176**: 1534–1538.

Arriazu, R., Pozuelo, J. M., Martin, R., Rodriguez, R. and Santamaria, L. (2005). Quantitative and immunohistochemical evaluation of PCNA, androgen receptors, apoptosis, and glutathione-*S*-transferase P1 on preneoplastic changes induced by cadmium and zinc chloride in the rat ventral prostate. *Prostate* **63**: 347-357.

Aumuller, G. and Seitz, J. (1990). Protein secretion and secretory processes in male accessory sex glands. *Int. Rev. Cytol.* **121**: 127–230.

Aumuller, G., Giers, K., Giers, U., Volk, A. and Seitz, J. (1981). p-Chlorophennylalanine induced proliferation of the seminal vesicle epithelium. *Cell Tissue Res.* **219**: 159–172.

Bartsch, G. and Rohr, H. P. (1980). Comparative light and electron microscopic study of the human, dog and rat prostate. An approach to an experimentalmodel for human benign prostatic hyperplasia (light and electron microscopic analysis)—a review. *Urol. Int.* **35**: 91-104.

Becker, J. A., Mirjolet, J. F., Bernard, J., Burgeon, E., Simons, M. J., Vassart, G., Parmentier, M. and Libert, F. (2005). Activation of GPR54 promotes cell cycle arrest and apoptosis of human tumor cells through a specific transcriptional program not shared by other Gq-coupled receptors. *Biochem. Biophys. Res. Commun.* **326**: 677–86.

Bijlsma J. W., Duursma, S. A., Thijssen, J. H. and Huber, O. (1982). Influence of nandrolondecanoate on the pituitary-gonadal axis in males. *Acta Endocrinol. (Copenh)* **101**: 108-12.

Billig, H., Furuta, I., Rivier, C., Tapanainen, J., Parvinen, M. and Hsueh, A. J. (1995). Apoptosis in testis germ cells: developmental changes in gonadotropin dependence and localization to selective tubule stages. *Endocrinology* **136**: 5-12.

Biswas, S., Ferguson, K., Stedronska, J., Boffoe, G., Mansfield, M. and Koskab, N. (1978). Fructose and hormone levels in semen: their correlation with sperm counts and motility. *Fertil. Steril.* **30**: 200-204.

Blanchard, K. T., Lee, J., Boekelheide, K. (1998). Leuprolide, a gonadotropin-releasing hormone agonist, reestablishes spermatogenesis after 2,5-hexanedione- induced irreversible testicular injury in the rat, resulting in normalized stem cell factor expression. *Endocrinology* **139**: 236–244.

Bloom, W. and Fawcett, D. W. (1976). Male reproductive system. In: A textbook of histology. 10th ed. W. B. Saunders Company. Philadelphia, London, Toronto, pp. 805-855.

Boekelheide, K., Schoenfeld, H., Hall, S. J., Weng, C. C. Y., Shetty, G., Leith, J., Harper, J., Sigman, M., Hess, D. L. and Meistrich, M. L. (2005). Gonadotropin-releasing hormone antagonist (cetrorelix) therapy fails to protect non-human primates (*macaca arctoides*) from radiation-induced spermatogenic failure. *J. Androl.* **26**: 222–234.

Boraschi, D. and G. Maurizi. (1998). Quantitation of DNA fragmentation with diphenylamine. In: Apoptosis - A Laboratory Manual of Experimental Methods. D. Boraschi, P. Bossù and A. Cossarizza (Eds.), GCI Publications, L'Aquila, pp. 153-161.

Bortner, C. D., Oldenburg, N. E. and Cidlowski, J. A. (1995). The role of DNA fragmentation in apoptosis. *Trends Cell Biol.* **5**: 21–6.

Bourguignon, J. P., Alvarez Gonzalez, M. L., Gerard, A. and Franchimont, P. (1994). Gonadotropin releasing hormone inhibitory autofeedback by subproducts antagonist at *N*-methyl-D-aspartate receptors: a model of autocrine regulation of peptide secretion. *Endocrinology* **134:** 1589–92.

Bourguignon, J. P., Gerard, A., Mathieu, J., Mathieu, A. and Franchimont, P. (1990). Maturation of the hypothalamic control of pulsatile gonadotropin-releasing hormone secretion at onset of puberty. I. increased activation of N-methyl-D-aspartate receptors. *Endocrionology* **127**: 873-881.

Brandes, D. (1974) Hormonal regulation of fine structure. In: Male Accessory Sex Organs. Structure and Function in Mammals. D. Brandes (Ed). Academic Press, New York. pp. 183-222

Cameron, D. F., Snydle, F. E., Ross, M. H. and Drylie, D. M. (1980). Ultrastructural alterations in the adluminal testicular compartment in men with varicocele. *Fertil. Steril.* **33**: 526-533.

Carson, D. A. and Ribeiro, J. M. (1993). Apoptosis and disease. *Lancet* **341**:1251–4.

Carvalho, C. A. F., Camargo, A. M., Cagnon, V. H. A. and Padovani, C. R. (2003). Effects of experimental diabetes on the structure and ultrastructure of the coagulating gland of C57BL/6j and NOD mice. *Anat. Rec.* **270**: 129–136.

Castaño, J. P., Martı´nez-Fuentes, A. J., Gutie´rrez-Pascual, E., Vaudry, H., Tena-Sempere, M. and Malagon, M. M. (2009). Intracellular signaling pathways activated by kisspeptins through GPR54: Do multiple signals underlie function diversity. *Peptides* **30**: 10-15.

Castellano, J. M., Gaytan, M., Roa, J., Vigo, E., Navarro, V. M., Bellido, C., Dieguez, C., Anguilar, E., Sanchez-Criado, J. E., Pellicer, A., Pinilla, L., Gaytan, F. and Tena-Sempere, M. (2006). Expression of KiSS-1 in rat ovary: putative local regulator of ovulation? *Endocrinology* **147**: 4852-4862.

Catt, K. and Dufau, M. L. (1991). Gonadotropic hormones: Biosynthesis, secretion, receptors and actions. W.B. Saunders, Philadelphia, PA.

Christensen, A. K. (1975). Leydig cells. In: Handbook of Physiology. D. W. Hamilton and R. O. Greep (Eds.), Section 7. American physiological Society, Washington, DC. Vol. 5, pp.57-94.

Christenson, A. K. and Mason, N. R. (1965). Comparative ability of seminiferous tubules and interstitial tissues of rat testes to synthesize androgens from progesterone-4-1^{4}C *in vitro*. *Endocrinology* 76: 646-656.

Cicero, T. J., Schmoeker, P. F., Meyer, E. R., Miller, B. T., Bell, R. D., Cytron, S. M. and Brown, C. C. (1986). Ontogeny of the opioid-mediated control of reproductive endocrinology in the male and female rat. *Pharmacol. Exp. Ther.* **236(3):** 627-33.

Clegg, E. (1960). The age at which male rats become fertile. *J Reprod. Fertil.* **1**: 119-120.

Clermont, Y. (1960). Cycle of the seminiferous epithelium of the guinea pig. A method for identification of stages. *Fertil. Steril.* **11**: 563-573.

Clermont, Y. (1962). Quantitative analysis of spermatogenesis of the rat, a revised model for the renewal of spermatogonia. *Am. J. Anat.* **111**: 111-129.

Clermont, Y. (1972). Kinetics of spermatogenesis in mammals: seminiferous epithelium cycle and spermatogonial renewal. *Physiol. Rev.* **52**: 198-236.

Clermont, Y. (1993). Introduction to the Sertoli cell. In: The Sertoli cell. L. D. Russell and M. D. Griswold (Eds.), Cache River Press xxii-xxv.

Clermont, Y. and Leblond, C. P. (1953). Renewal of sermatogonia in the rat. *Am. J. Anat.* **93**: 475-502.

Colledge, W. H. (2004). GPR54 and puberty. *Trends Endocrinol. Metab.* 15: 448-453.

Compton, M. M. (1992). A biochemical hallmark of apoptosis: Internucleosomal degradation of the genome. *Cancer Met. Rev.* **11**:105-119.

Constantin, S., Caligioni, C. S., Stojilkovic, S. and Wray, S. (2009). Kisspeptin-10 facilitates a plasma membrane-driven calcium oscillator in gonadotropin-releasing hormone-1 neurons. *Endocrinology* **150**:1400–1412.

Corder, R., Walker, C. D., Gaillard, R. C. and Aubert, M. L. (1992). Inhibition of sexual maturation in male rats by melatonin: evidence linking the mechanism of action to changes in regulation of hypothalamic neuropeptide Y. *J. Neuroendocrinol.* **4**: 1-7.

Courot, M., Hochereau-de Reviers, M. T. and Ortarant, R. (1970). Spermatogenesis. In: The Testis. A. D. Johnson, W. R. Gomes and N. L. VanDemark (Eds.), Vol. 1. Academic Press, New York.

Crowley, W., Parker, S. L., Sahu, A. and Kalra, S. P. (1995). Interacting transmembrane signals regulating GnRH and LH secretion. In: The

Neurobiology of Puberty. T. M. Plant and P. A. Lee (Eds.), Bristol, UK. pp. 41–54.

Crown. A., Clifton, D. K. and Steiner, R. A. (2007). Neuropeptide signaling in the integration of metabolism and reproduction. *Neuroendocrinology* **86** 175-182.w

Cunha, G. R., Donjacour, A. A., Cooke, P. S., Mee, S., Bigsby, R. M., Higgins, S. J. and Sugimura, Y. (1987). The endocrinology and developmental biology of the prostate. *Endocr. Rev.* **8**: 338–362.

Cunha, G. R., Hayward, S.W. and Wang, Y. Z. (2002). Role of stroma in carcinogenesis of the prostate. *Differentiation* **60**: 473–485.

Curtis, G. M. (1918). The morphology of the mammalian seminiferous tubule. *Am. J. Anat.* **24**: 339.

Cutler, L., Egli., C. A., Styne, D. M., Kaplan, S. L. and Grumbach, M. M. (1985). Hormone ontogeny in the ovine fetus. XVIII. The effect of an opioid antagonist on luteinizing hormone secretion. *Endocrinology* **116**: 1997-2002.

Dalkin, A. C., Haisenleder, D. J., Ortolano, G. A., Ellis, T. R. and Marshall, J. C. (1989). The frequency of gonadotropin-releasing-hormone stimulation differentially regulates gonadotropin subunit messenger ribonucleic acid expression. *Endocrinology* **125**: 917–924.

d'Anglemont de Tassigny X., Fagg, L. A, Dixon, J. P., Day, K., Leitch, H. G., Hendrick, A. G., Zahn, D., Franceschini, I., Caraty, A., Carlton, M. B., Aparicio, S. A. and Colledge, W. H. (2007) Hypogonadotropic hypogonadism in mice lacking a functional Kiss1 gene. *Proc. Natl. Acad. Sci. U. S. A.* **104:** 10714-10719.

Daoust, R., and Clermont, Y. (1955). Distribution of nucleic acids in germ cells during the cycle of the seminiferous epithelium in the rat. *Am. J. Anat.* **96**: 255-283.

Davis, A. M., Grattan, D. R., Selmanoff, M. and McCarthy, M. M. (1996). Sex differences in glutamic acid decarboxylase mRNA in neonatal rat brain: implications for sexual differenciation. *Horm. Behav.* **30**: 538-552.

Davis, A. M., Ward, S. C., Selmanoff, M., Herbison, A. E. and McCarthy, M. M. (1999). Developmental sex differences in amino acid neurotransmitter levels in hypothalamic and limbic areas of rat brain. *Neuroscience* **90**: 1471-1482.

de Kretser, D. M. and Kerr, J. B. (1988). The cytology of the testis. In: The Physiology of Reproduction. E. Knobil and J. D. Neill (Eds.), Vol. 1. New York, Raven Press Ltd, pp. 837–932.

De Marzo, A. M., Meeker, A. K., Epstein, J. I. and Coffey, D. S. (1998). Prostate stem cell compartments: Expression of the cell cycle inhibitor $p27^{Kip1}$ in normal, hyperplastic, and neo plastic cells. *Am. J. Pathol.* **153**: 911-919.

de Rooij, D. G. and Russell, L. D. (2000). All you want to know about spermatogonia but were afraid to ask. *J. Androl.* **21**: 776-798.

de Roux, N., Genin, E., Carel, J. C., Matsuda, F., Chaussain, J. L. and Milgrom, E. (2003). Hypogonadotropic hypogonadism due to loss of function of the KiSS1-derived peptide receptor GPR54. *Proc. Natl. Acad. Sci. U. S. A.* **100**: 10972–10976.

Decavel, C. and van den Pol, A. N. (1990). GABA: A dominant neurotransmitter in the hypothalamus. *J. Comp. Neurol.* **302**: 1019-1037.

DeKlerk, D. P. and Coffey, D. S. (1978). Quantitative determination of prostatic epithelial and stromal hyperplasia by a new technique. *Biomorphometrics Invest. Urol.* **16**: 240–245.

di Saint´ Agnese, P. A. and Cockett, A. T. (1996). Neuroendocrine differentiation in prostatic malignancy. *Cancer* **78**:357-361.

Donnel, L. O., Meachem, S. J., Stanton, P. G., Machlachlan, R.I. (2006). Endocrine regulation of spermatogenesis, In: The Physiology of Reproduction. E. Knobil and J. D. Neill (Eds.), 3rd ed. Vol. 1. Elsevier Academic Press, New York, pp. 1017-1148.

Dufau, M. L. (1988). Endocrine regulation and communicating functions of the Leydig cell. *Ann. Rev. Physiol.* **50**: 483-508.

Dullaart, J. (1977). Immature rat pituitary glands in vitro: age and sex-related changes in luteinizing hormone releasing hormone-stimulated gonadotrophin release. *J. Endocrinol.* **73:** 309–19.

Dym, M. and Fawcett, D. W. (1971). Further observations on the numbers of spermatogonia, spermatocytes and spermatids connected by intercellular bridges in the mammalian testis. *Biol. Reprod.* **4**: 195-215.

Ebling, F. J., Schwartz, M. L. and Foster, D. L. (1989). Endogenous opioidregulation of pulsatile luteinizing hormone secretion during sexual maturation in the female sheep. *Endocrinology* **125**: 369-383.

Ekwall, H., Jansson, A., Sjoberg, P. and Ploen, L. (1984). The differentiation of the rat testis between 20 and 120 days of age. *Arch. Androl.* **13**: 27-36.

El-Alfy, M., Luu-The, V., Huang, X. F., Berger, L., Ladrie, F. and Pelletier, G. (1999). Localization of Type 5 17β-hydroxy steroid dehydrogenase, 3 β-hydroxy steroid dehydrogenase and androgen receptor in the human prostate by in situ hybridization and immunocytochemistry. *Endocrinology* **140**: 1481-1491.

El-Alfy, M., Pelletier, M. G., Mermo, L. S. and Labrie, F. (2000) Unique features of the basal cell of human prostate epithelium. *Microsc. Res. Tech.* **51**:436-446.

Evans, N. P. and Karsch, F. J. (1995). Operation of the gonadotropin-releasing hormone pulse generator. In: The Neurobiology of Puberty. Great Britain, Bourne Press.

Ewing, L. L., Zirkin, B. R., Cochran, R. C., Kromann, N., Peters, C. and Ruiz-Bravo, N. (1979). Testosterone secretion by rat, rabbit, guinea pig, dog, and hamster testes perfused in vitro, correlation with Leydig cell mass. *Endocrinology* **105:** 1135-1142.

Fawcett, D. W. (1986). Male reproductive system. In: a textbook of histology. W. Bloom and D. W. Fawcett (Eds.), 11th ed. Philadelphia: W.B. Saunders Company: 796–850.

Fawcett, D. W., Ito, S., and Slautterbackm D.B. (1959). The occurrence of intercellular bridges in groups of cells exhibiting synchronous differentiation. *J. Biochem. Cytol.* **5**: 453-458.

Fawcett, D. W., Leak, L. V. and Heider, P. M. (1970). Electron microscopic observations on the structural components of the blood-testis barrier. *J. Reprod. Fertil.* Suppl 10, 105-122.

Fawcett, J. W. and Keynes, R. J. (1986). Muscle basal lamina: A new graft material for peripheral nerve repair. *J. Neurosurg.* **65**: 354–363.

Fawell, S. E., Higgins, S. J. (1984). Androgen regulation of specific mRNAs, endoplasmic reticulum and Golgi-system. *Mol. Cell Endocrinol.* **37**: 15-27.

Ferin, M., Wehrenberg, W. B., Lam, N. Y., Alston, E. J. and Vande Wiele, R. L. (1982). Effects and site action of morphine on gonadotropin secretion in the female rhesus monkey. *Endocrinology* **111**: 1652-1656.

Flügge, G., Wuttke, W. and Fuches, E. (1986). Postnatal development of transmitter systems: sexual differentiation of the GABAergic system and effects of muscimol. *Int. J. Dev. Neurosci.* **4**: 319-326.

Funes, S., Hedrick, J. A., Vassileva, G., Markowitz, L., Abbondanzo, S., Golovko, A., Yang, S., Monsma, F. J. and Gustafson, E. L. (2003). The KiSS-1 receptor GPR54 is essential for the development of the murine reproductive system. *Biochem. Biophys. Res. Commun.* **312**: 1357-1363.

Gartner, L. P. and Hiatt, J. L. (1997). Male reproductive system. In: Color textbook of histology. Philadelphia: W.B. Saunders, pp. 403–420.

George, F. W. and Wilson, J. D. (1994). Sex determination and differentiation, In: The Physiology of Reproduction, E. Knobil and J. D. Neill (Eds.), 2nd ed. New York: Raven Press, Ltd.

Gonzales, G. F. (1989) Functional structure and ultrastructure of seminal vesicles. *Arch Androl* **22**: 1-13.

Gonzales, G. F. (1994). Test for androgen activity at the male reproductive tract in infertile men. *Arch Androl.* **32**: 235-42.

Gonzales, G. F. and Villena, A. (2001). True corrected seminal fructose level: a better marker of the function of seminal vesicles in infertile men. *Int. J. Androl.* **24**: 255-260.

Gonzales, G. F., Miranda, S., Nieto, J., Fernandez, G., Yucra, S., Rubio, J., Yi, P. and Gasco, M. (2005). Red Maca (*Lepidium meyenii*) reduced prostate size in rats, *Reprod. Biol. Endocrinol.* **3**: 5.

Gonzales, G. F., Garca-Hjarles, M. and Napuri, R. (1988). Corrected seminal fructose levels: an index of the secretory activity of the seminal vesicles. *Arch. Androl.* **21**: 135-142.

Goroll, D., Arias, P. and Wuttke, W. (1994). Ontogenic changes in hypothalamic levels of amino aci neurotransmitters in the female rat. *Brain Res. Dev. Brain Res.* 77: 183-188.

Gottsch, M. L., Cunningham, M. J., Smith, J. T., Popa, S. M., Acohido, B. V., Crowley, W. F., Seminara, S., Clifton, D. K. and Steiner, R. A. (2004). A role for kisspeptins in the regulation of gonadotropin secretion in the mouse. *Endocrinology* **145**: 4073–4077.

Gravis, C. J., Chen, I. L. and Yates, R. D. (1977). Ultrastructure and cytochemistry of epinephrine-induced testicular degeneration. In: Male reproductive system. R. D. Yates and M. Cordon (Eds.), Masson Publishing. New York, USA, pp. 35-55.

Grosser, P. M., O'Byrne, K. T., Williams, C. L., Thalabard, J. C., Hotchkiss, J. and Knobil, E. (1993). Effects of naloxone on estrogen induced changes in hypothalamic gonadotropin-releasing hormone pulse generator activity in the rhesus monkey. *Neuroendocrinology* **53**: 115-119.

Gudermann, T., Nürnberg, B. and Schultz, G. (1995). Receptors and G proteins as primary components of transmembrane signal transduction. I. G-protein-coupled receptors: structure and function. *J. Mol. Med.* **73**: 51–63.

Hagenas, L., Ploen, L., Ekwall, H., Osman, D. I. and Ritzen, E. M. (1981). Differentiation of the rat seminiferous tubules between 13 and 19 days of age. *Int. J. Androl.* **4**: 257-264.

Hall, P. F., Irby, D. C. and de Kretser, D. M. (1969). Conversion of cholesterol to androgens by rat testes, comparison of interstitial cells and seminiferous tubules. *Endocrinology* **84**: 488-496.

Hansson, V., Jégou, B., Attramadal, H., Jahnsen, T., Le Gac, F., Tvermyr, M., Frøysa, A. and Horn, R. (1983). Regulation of Sertoli cell function and response. In: Recent Advances in Male Reproduction: Molecular Basis and Clinical Implications. R. D'Agata, M. B. Lipsett, P. Polosa, and H. J. van der Molen, (Eds.), Raven Press, New York, pp. 53-68.

Hayashi, N., Sugimura, Y., Kawamura, J., Donjacour, A. A. and Cunha, G. R. (1991). Morphological and functional heterogeneity in the rat prostatic gland. *Biol. Reprod.* **45**: 308-321.

Hayward, S. W., Baskin, L. S., Haughney, P. C. and Cunha, G. R. (1996) Epithelial development in the rat ventral prostate, anterior prostate and seminl vesicle. *Acta Anat.* **155**: 81-93

Hedlund, T. E., K. A. Moffatt, M. R. Uskokovic and G. J. Miller. (1997). Three synthetic vitamin D analogues induce prostate-specific acid phosphatase and prostate-specific antigen while inhibiting the growth of human prostate cancer cells in a vitamin D receptor-dependent fashion. *Clin. Cancer Res.* **3**: 1331–1338.

Heller, C. G., and Clermont, Y. (1964). Kinetics of the germinal epithelium in man. *Rec. Prog. Horm. Res.* **20**: 545-575.

Herbst, K. L., Coviello, A. D., Page, S., Amory, J. K., Anawalt, B. D. and Bremner, W. J. (2004). A Single Dose of the Potent Gonadotropin-Releasing Hormone Antagonist Acyline Suppresses Gonadotropins and Testosterone for 2 Weeks in Healthy Young Men. *J. Clin. Endocrinol. Metab.* **89(12)**: 5959–5965.

Hess, R. A. (1990). Quantitative and qualitative characteristics of the stages and transitions in the cycle of the rat seminiferous epithelium: light microscopic observations of perfusion-fixed and plastic-embedded testis. *Biol. Reprod.* **43**: 525-542.

Higgins, S. J. and Burchell, J. M. (1978). Effects of testosterone on messenger ribonucleic acid and protein synthesis in rat seminal vesicle. *Biochem. J.* **174**: 543-51.

Higgins, S. J., Burchell, J. M. and Mainwaring, W. I. P. (1976) Testosterone control of nucleic acid content and proliferation of epithelium and stroma in rat seminal vesicles. *Biochem. J.* **160**: 43-74.

Hochereau, M. T. (1968). Etude des divisions spermatogiales et du renou- vellement de la spermatogonie souche chez le taureau. *Int. Cong. Anim. Reprod.* **1**: 149-152.

Holstein, A. F. and Roosen-Runge, E. C. (1981). Atlas of Human Spermatogenesis, Grosse Verlag, Berlin, pp. 1-224.

Hsueh, A. J. and Schaeffer, J. M. (1985). Gonadotropin-releasing hormone as a paracrine hormone and neurotransmitter in extra-pituitary sites. *J. Steroid. Biochem.* **23**: 757-764.

Huckins, C. (1971). The spermatogonial stem cell population in adult rats. I. their morphology, proliferation and maturation. *Anat. Rec.* **169**: 533- 558.

Ichihara, I., Kawamura, H., Nakano, T. and Pelliniemi, L. J. (2001). Ultrastructural, morphometric, and hormonal analysis of the effects of testosterone treatment on Leydig cells and other interstitial cells in young adult rats. *Ann. Anat.* **183**: 413-26.

Ingelmo, I. and Santamaría, L. (2007). The Prostate of the Rat. In: Advances in Anatomy, Embryology and Cell Biology. F. F. Beck, F. Clascá, M. Frotscher, D. E. Haines, H.-W. Korf, E. Marani, R. Putz, Y. Sano, T. H. Schiebler (Eds.), Springer: Berlin, Heidelberg, New York, pp. 38- 42.

Irwig, M. S., Fraley, G. S., Smith, J. T., Acohido, B. V., Popa, S. M., Cunningham, M. J., Gottsch, M. L., Clifton, D. K. and Steiner, R. A. (2004). Kisspeptin activation of gonadotropin releasing hormone neurons and regulation of KiSS-1 mRNA in the male rat. *Neuroendocrinology* **80**: 264–272.

Jennes, L., Stumpf, W. E. and Sheedy, M. E. (1985). Ultrastructural characterization of gonadotropin-releasing hormone (GnRH)-producing neurons. *J. Comp. Neurol.* **232:** 534–47.

Jesik, C. J., Holland, J. M. and Lee, C. (1982). An anatomic and histologic study of rat prostate. *Prostate* **3**: 81-97.

Johnson, L. C., Fisher, G., Silvester, L. J. and Hofheins, C. C. (1972). Anabolic steroid: effects on strength, body weight, oxygen uptake and spermatogenesis upon mature males. *Med. Sci. Sports* **4**: 43-5.

Kangasniemi, M., Wilson, G., Parchuri, N., Huhtaniemi, I. and Meistrich, M. L. (1995) Rapid protection of rat spermatogenic stem cells against procarbazine by treatment with a gonadotropin-releasing hormone antagonist (Nal-Glu) and an antiandrogen (flutamide). *Endocrinology.* **136**: 2881–2888.

Kaya, M. and Harrison, R. G. (1976). The ultrastructural relationships between Sertoli cells and spermatogenic cells in the rat. *J. Anat.* **121**: 279-290.

Kerr, J. B. (1995). Macro, Micro, and Molecular research on spermatogenesis: The quest to understand its control. *Microsc. Res. Tec.* **32**: 364-384.

Kerr, J. B., Loveland, K. L., O'Bryan, M. K. and de Kretser, D .M. (2006). Cytology of the testis and intrinsic control mechanism. In: Knobil, E., Neill, J.D. (Eds.), The Physiology of Reproduction. Elsevier Academic Press., New York, pp 1017-1148.

Kerr, J. B., Millar, M., Maddocks, S. and Sharpe, R. M. (1993). Stage-Dependent changes in spermatogenesis and Sertoli cells in relation to the onset of spermatogenic failure following withdrawal of testosterone. *Anat. Rec.* **235**: 547-559.

Kesner, J. S., Kaufman, J. M., Wilson, R. C., Kuroda, G. and Knobil, E. (1986). The effect of morphine on the electrophysiological activity of the hypothalamic luteinizing hormone-releasing hormone pulse generator in the rhesus monkey. *Neuroendocrinology* **43**: 686-688.

Ketelslegers, J. M., Hetzel, W. D., Sherins, R. J. and Catt, K. J. (1978). Developmental changes in testicular gonadotropin receptors: plasma gonadotropins and plasma testosterone in the rat. *Endocrinology* **103:** 212–22.

Kinbara, H. and Cunha, G. R. (1996). Ductal heterogeneity in rat dorsal-lateral prostate. *Prostate* **28**: 58-64.

Knorr, D. W., Vanha-Perttula, T. and Lipsett, M. B. (1970). Structure and function of rat testis through pubescence. *Endocrinology* **86**: 1298-1304.

Kotani, M., Detheux, M., Vandenbogaerde, A., Communi, D., Vanderwinden, J. M., Le Poul, E., Brezillon, S., Tyldesley, R., Suarez-Huerta, N., Vandeput, F., Blanpain, C., Schiffmann, S., Vassart, G. and Parmentier, M. (2001). The metastasis suppressor gene KiSS-1 encodes kisspeptins, the natural ligands of the orphan G protein-coupled receptor GPR54. *J. Biol. Chem.* **276**: 34631–34636.

Lapatto, R., Pallais, J. C., Zhang, D., Chan, Y. M., Mahan, A., Cerrato, F., Le, W. W., Hoffman, G. E. and Seminara, S. B. (2007) Kiss1K/Kmice exhibit more variable hypogonadism than Gpr54K/K mice. *Endocrinology* **148**: 4927-4936.

Leblond, C. P. and Clermont, Y. (1952). Definition of the stages of the seminiferous epithelium in the rat. *Ann. N. Y. Acad. Sci.* **55**: 548-573.

Lee, C., Kozlowski, J. M. and Grayhack, J. T. (1997). Intrinsic and extrinsic factors controlling benign prostatic growth. *Prostate* **31**:131–138.

Lee, D. K., Nguyen, T., O'Neill, G. P., Cheng, R., Liu, Y., Howard, A. D., Coulombe, N., Tan, C. P., Tang-Nguyen, A. T., George, S. R., O'Dowd, B. F., (1999). Discovery of a receptor related to the galanin receptors. FEBS Lett. **446**: 103-107.

Lejeune, H., Habert, R. and Saez, J. M. (1998). Origin, proliferation and differentiation of Leydig cells. *J. Mol. Endocrinol.* **20**: 1-25.

Levy, H., Dean, H. W. and Rubin, B. L. (1959). Visualization of steroid-3ß-ol activity in tissues of intact and hypophysectomized rats. *Endocrinology* **65**: 932-943.

Lewis-Jones, D. I., Aird, I. A., Biljan, M. M. and Kingsland, C. R. (1996). Effects of sperm activity on zinc and fructose concentrations in seminal plasma. *Hum. Reprod.* **11**: 2465-7.

Li, L. H. and Heindel, J. J. (1998). Sertoli cell toxicants. In: Reproductive and Developmental Toxicology. K.S. Korach, Editor, Marcel Dekker, New York pp. 655–691.

Lieber, M. M., Barham, S. S., Veneziale, C. M. (1980). In vitro propagation of seminal vesicle epithelial cells. *Invest. Urol.* **17**: 348.

Liu, X., Lee, K. and Herbison, A. E. (2008). Kisspeptin excites gonadotropin-releasing hormone neurons through a phospholipase C/calcium-dependent pathway regulating multiple ion channels. *Endocrinology* **149**: 4605–4614.

Luke, M. C. and Coffey, D. S. (1994). The male asseccory tissues. In: The Physiology of Reproduction, E. Knobil and J. D. Neill (Eds.), 2nd ed. New York: Raven Press, Ltd.

MacLaughlin D.T. and Donahoe, P. K. (1998). Müllerian-inhibiting substance activity and normal male sex determination. In: Reproductive and developmental toxicology. K.S. Korach (Ed.), Marcel Dekker, Inc. 1-10.

Maini, A., Archer, C., Wang, C. Y. and Haas, G. P. (1997). Comparative pathology of benign prostatic hyperplasia and prostate cancer. *In Vivo* **11**: 293-299.

Mallory, D. S., Bona-Gaio, A and Gallo, R. V. (1989). Neurotransmitter involvement in naloxone- induced stimulation of pulsatile LH release on day 8 of pregnancy in the rat. *Brain Res. Bull.* **22**: 1015-1021.

Matsumoto, A. M., Karpas, A. E., Southworth, M. B., Dorsa, D. M. and Bremner, W. J. (1986). Evidence for activation of the central nervous system-pituitary mechanism for gonadotropin secretion at the time of puberty in the male rat. *Endocrinology* **119:** 362–9.

Mayerhofer, A. and Dube, D. (1989). Chronic administration of a gonadotropin-releasing hormone (GnRH) agonist affects testicular microvasculature. *Acta Endocrinologica* **120**: 75-80.

McLachlan, R. I, Wreford, N. G., Meachem, S. J., de Kretser, D. M. and Robertson, D. M. (1994). Effects of testosterone on spermatogenic cell populations in the adult rat. *Biol. Reprod.* **51**: 945-955.

McNeal, J. E. (1968). Regional morphology and pathology of prostate. *Am. J. Clin. Pathol.* **49**: 347-357

McNeal, J. E. (1981). The zonal anatomy of the prostate. *Prostate* **2**: 35-49.

McNeal, J. E. (1988). Normal histology of prostate. *Am. J. Surg. Pathol.* **12**: 619-633.

Meachem, S., von Schonfeldt, V., and Schlatt, S. (2001). Spermatogonia, stem cells with great potential. *Reproduction* **121**: 825- 834.

Meistrich, M. L. and Kangasniemi, M. (1997) Hormone treatment after irradiation stimulates recovery of rat spermatogenesis from surviving spermatogonia. *J. Androl.* **18**: 80 -87.

Meistrich, M. L. and Shetty, G. (2003). Inhibition of spermatogonial differentiation by testosterone. *J. Androl.* **24**: 135 -148.

Meistrich, M. L., Shuttlesworth, G., Huhtaniemi, I. and Reissmann, T. (2001). GnRH agonists and antagonists stimulate recovery of fertility in irradiated LBNF1 rats. *J. Androl.* **22**: 809-817.

Meistrich., M. L., Zhang, Z., Porter, K. L., Bolden-Tiller, O. U. and Shetty, G. (2007). Prevention of adverse effects of cancer treatment on the germline, In: Male-Mediated Developmental Toxicity D. Anderson and M. H. Brinkworth. Cambridge, Royal Society of Chemistry:114–123.

Moens, P. B. and Go, V. L. W. (1972). Intercellular bridges and division patterns of rat spermatogonia. *Z. Zellforsch.* **127**: 201-208.

Montgomery, T. H. (1912). Human spermatogenesis, spermatocytes and spermiogenesis. A study in inheritance. *J. Acad. Natl. Sci. Phil.* **15**: 1-22.

Montgomery, T. H. (1901). A study of the chromosomes of the germ cells of the metazona. *Trans. Am. Phil. Soc.* **20**: 154-236.

Moyle, W. R. and Campbell, R. K. (1995). Gonadotropins, In: Endocrinology. L. J. De Groot (ed) WB Saunders Company, Philadelphia, pp 230–241.

Muir, A. I., Chamberlain, L., Elshourbagy, N. A., Michalovich, D., Moore, D. J., Calamari, A., Szekeres, P. G., Sarau, H. M., Chambers, J. K. and Murdock, P. (2001). AXOR12, a novel human G protein-coupled receptor, activated by the peptide KiSS-1. *J. Biol. Chem.* **276**: 28969–28975.

Murono, E. P. and Payne, A. H. (1979). Testicular maturation in the rat. In vivo effect of gonadotropins on steroidogenic enzymes in the hypophysectomized immature rat. *Biol Reprod* **20**: 911–7.

Nagano, M., Avarbockm M. R. and Brinster, R. L. (1999). Patterns and kinetics of mouse donor spermatogonial stem cell colonization in recipient testes. *Biol. Reprod.* **60**: 1429- 1436.

Nash, K. T., Phadke, P. A., Navenot, J. M., Hurst, D. R., Accavitti-Loper, M. A., Sztul, E., Vaidya, K. S., Frost A. R., Kappes, J. C., Peiper, S. C. and Welch, D. R. (2007). Requirement of KISS1 secretion for multiple organ metastasis suppression and maintenance of tumor dormancy. *J. Natl. Cancer Inst.* **99**: 309–21.

Navarro, V. M., Castellano, J. M., Fernandez-Fernandez, R., Barreiro, M. L., Roa, J., Sanchez-Criado, J. E., Aguilar, E., Dieguez, C., Pinilla, L. and Tena-Sempere, M. (2004a). Developmental and hormonally regulated messenger ribonucleic acid expression of KiSS-1 and its putative receptor, GPR54, in rat hypothalamus and potent luteinizing hormone-releasing activity of KiSS-1 peptide. *Endocrinology* **145**: 4565–4574.

Navarro, V. M., Castellano, J. M., Fernandez-Fernandez, R., Tovar, S., Roa, J., Mayen, A., Barreiro, M. L., Casanueva, F. F., Aguilar, E., Dieguez, C., Pinilla, L. and Tena-Sempere, M. (2005b). Effects of KiSS-1 peptide, the

natural ligand of GPR54, on follicle stimulating hormone secretion in the rat. *Endocrinology* **146**: 1689–1697.

Navarro, V. M., Castellano, J. M., Fernandez-Fernandez, R., Tovar, S., Rao, J., Mayen, A., Nogueiras, R., Vasquez, M. J., Barreiro, M. L., Magni, P., Aguilar, E., Dieguez, C., Pinilla, L. and Tena-Sempere, M. (2005a). Characterization of the potent luteinizing hormone-releasing activity of KiSS-1 peptide, the natural ligand of GPR54. *Endocrinology* **146**: 156-163.

Navarro, V. M., Fernandez-Fernandez, R., Castellano, J. M., Roa, J., Mayen, A., Barreiro, M. L., Gaytan, F., Aguilar, E., Pinilla, L., Dieguez, C. and Tena-Sempere, M. (2004b). Advanced vaginal opening and precocious activation of the reproductive axis by KiSS-1 peptide, the endogenous ligand of GPR54. *J. Physiol.* **561**: 379–386.

Nemeth, J. A. and Lee, C. (1996). Prostatic ductal system in rats: regional variation in stromal organization. *Prostate* **28**:124-128.

Nicander, L. (1967). An electron microscopical study of cell contacts in the seminiferous tubules of some mammals. *Z. Zellforsch.* **83**: 375-397.

Nicander, L., Abdel- Raouf, M. and Crabo, B. (1961). On the ultrastructure of the seminiferous tubles in bull calves. *Acta. Morphol. Neerl. Scand.* **4**: 127-135.

Oakberg, E. F. (1956). A description of spermiogenesis in the mouse and its use in analysis of the cycle of the cycle of the seminiferous epithelium and germ cell renewal. *Am. J. Anat.* **99**: 391- 413.

Oakley, A. E., Clifton, D. K. and Steiner, R. A. (2009). Kisspeptin Signaling in the Brain. *Endocr. Rev.* **30 (6)**: 713-743.

Ohtaki, T., Shintani, Y., Honda, S., Matsumoto, H., Hori, A., Kanehashi, K., Terao, Y., Kumano, S., Takatsu, Y., Masuda, Y., Ishibashi, Y., Watanabe, T., Asada, M., Yamada, T., Suenaga, M., Kitada, C., Usuki, S., Kurokawa, T., Haruo O., H., Nishimura, O. and Fujino, M. (2001). Metastasis suppressor gene KiSS-1 encodes peptide ligand of a G-protein-coupled receptor. *Nature.* **411**: 613–617.

Ojeda, S. R. and Skinner, M. K. (2006). Puberty in the rat, In: The Physiology of Reproduction. In: Knobil, E., Neill, J. D. (Eds.), 3rd ed. Elsevier Academic Press. New York, pp.2061-2126.

Ojeda, S. R. and Urbanski, H. F. (1994). Puberty in the rat, In: *The Physiology of Reproduction*, E Knobil and JD Neill (Eds.), 3rd ed. New York: Raven Press.

Ojeda, S. R., Andrews, W. W., Advis, J. P. and White, S. S. (1980). Recent advances in the endocrinology of puberty. *Endocr. Rev.* **1**: 228–57.

Ortavant, R. (1959). Spermatogenesis and morphology of the spermatozoon, In: Reproduction in domestic animals. H. H. Cole and P. T. Cupps (Eds.), Vol.2. Academic Press, New York.

Pahdke, A. M., Samant, N. R. and Deval, S. D. (1973). Significance of seminal fructose in male fertility. *Fertil. Steril.* **24**: 894-903.

Painter, T. S. (1923). Studies in mammalian spermatogenesis. II. The spermatogenesis of man. *J. Exp. Zool.* **37**: 291- 338.

Paniagua, R., Amat, P., Nistal, M. and Martin, A. (1986). Ultastructure of Leydig cells in human ageing testes. *J. Anat.* **146**: 173-83.

Parreira, G. G., Ogawa, T., Avarbock, M. R., Franca, L. R., Brinster, R. L., and Russell, L. D. (1998). Development of germ cell transplants. *Biol. Reprod.* **59**: 1360-1370.

Perey, B., Clermont, Y. and Leblond, C. P. (1961). The wave of the seminiferous epithelium in the rat. *Am. J. Anat.* **108**: 47.

Pheng, V., Uenoyama, Y., Homma, T., Inamoto, Y., Takase, K., Yoshizawa-Kumagaye, K., Isaka, S., Watanabe, T. X., Ohkura, S., Tomikawa, J., Maeda, K. I. and Tsukamura, H. (2009). Potencies of centrally or peripherally injected full length kisspeptin or its C-terminal decapeptide on LH release in intact male rats. *J. Reprod. Dev.* **55**: 378-382.

Pierce, J. G. and Parsons, T. F. (1981). Glycoprotein hormones: structure and function. *Ann. Rev. Biochem.* **50**: 465-495.

Pochron, S. T. and Wright, P. C. (2002). Dynamics of testis size compensates for variation in male body size. *Evol. Ecol. Res.* **4**: 577-585.

Prince, F. P. (1999). Mitochondrial christae diversity in human Leydig cells, a revised look at cristae morphology in these steroid producing cells. *Anat. Rec.* **254**: 534-541.

Quaynor, S., Hu, L., Leung, P. K., Feng, H., Mores, N., Krsmanovic, L. Z., Catt, K. J. (2007). Expression of a functional G protein-coupled receptor 54-

kisspeptin autoregulatory system in hypothalamic gonadotropin releasing hormone neurons. *Mol. Endocrinol.* **21**: 3062–70.

Regaud, C. (1901). Etudes sur la structure des tubes seminiferes et sur la spermatogenese chez les mammiferes. *Arch. Anat. Microsc.* **4**: 101- 156.

Reiter, E., Hennuy, B., Bruyninx, M., Cornet, A., Klug, M., McNamara, M., Closset, J., Hennen, G. (1999). Effects of pituitary hormones on the prostate. *Prostate* **38(2)**: 159-165.

Reynolds, R. M., Logie, J. J., Roseweir, A. K., McKnight, A. J. and Millar, R. P. (2009) A role for kisspeptins in pregnancy: facts and speculations. *Reproduction* **138**: 1-7.

Richardson, L. L., Kleinman, H. K. and Dym, M. (1998). Altered basement membrane synthesis in the testis after tissue injury. *J. Androl.* **19**: 145-55.

Richburg, J. H. (2000). The relevance of spontaneous-and Chemically-induced alteration in testicular germ cell apoptosis to toxicology. *Toxicol. Lett.* **112-113**: 79-86.

Roa, J., Aguilar, E., Dieguez, C., Pinilla, L. and Tena-Sempere, M. (2008). New frontiers in kisspeptin/GPR54 physiology as fundamental gatekeepers of reproductive function. *Front. Neuroendocrinol.* **29**: 48–69.

Roa, J., Vigo, E., García-Galiano, D., Castellano, J. M., Navarro, V. M., Pineda, R., Diéguez, C., Aguilar, E., Pinilla, L. and Tena-Sempere, M. (2008). Desensitization of gonadotropin responses to kisspeptin in the female rat: analyses of LH and FSH secretion at different developmental and metabolic states. *Am. J. Physiol. Endocrinol. Metab.* **294**: 1088–1096.

Roosen-Runge, E. C. and Leik, J. (1968). Gonocyte degeneration in the postnatal male rat. *Am. J. Anat.* **122**: 275-300.

Roseweir, A. K., Kauffman, A. S., Smith, J. T., Guerriero, K. A., Morgan, K., Pielecka-Fortuna, J., Pineda, R., Gottsch, M. L., Tena-Sempere, M., Moenter, S. M., Terasawa, E., Clarke, I. J. Steiner, R. A. and Millar, R. P. (2009) Discovery of potent kisspeptin antagonists delineate physiological mechanisms of gonadotropin regulation. *J. Neurosci.* **29(12)**: 3920 -3929.

Roth, C., Leonhardt, S., Theiling, K., Lakomek, M., Jerry, H. and Wuttke, W. (1998). Ontogeny of the GnRH, glutaminase and glutamate decarboxylase-

gene expression in the hypothalamus of female rats. *Brain Res. Dev. Brain Res.* **110**: 105-114.

Rowely, M. J., Berlin, J. D., and Heller, C. G. (1971). The ultrastructure of four types of human spermatogonia. *Z. Zellforsch.* **112**: 139- 157.

Russell, E. and Sinha Hikim, C. (1995). Histological and histopathological evaluation of the testis. Vanguard Productions, Inc.

Russell, L. D. (1977). Desmosome-like junctions between Sertoli and germ cells in the rat testis. *Am. J. Anat.* **148**: 301-312.

Russell, L. D. (1992). Normal development of the testis, In: Pathobiology in the aging rat. U. Mohr, D. L. Dungworth and C. C. Capen (Eds.), ILSI press, Washington D.C. pp. 395-405.

Russell, L. D., Ettlin, R. A., Sinha Hikim, A. P. and Clegg, E. D. (1990). Histological and Histopathological Evaluation of the Testis. Clearwater, FL: Cache River Press.

Ryu, B. Y., Orwing, K. E., Avarbock, M. R. and Brinster, R. L. (2003). Stem cell and niche development in the postnatal rat testis. *Dev. Biol.* **263**: 253-263.

Saez, J. M. (1994). Leydig cells: endocrine, paracrine, and autocrine regulation. *Endocr. Rev.* **15**: 574-626.

Saito, S. (1995). Inhibin functions in male rats. *Arch. Androl.* **34:** 101–4.

Sanborn, B. M., Wagle, J. R., Steinberger, A, and Lamb, D. J. (1983). Sertoli cell as an androgen target, In: Recent Advances in Male Reproduction: Molecular Basis and Clinical Implications. R. O'Agata, M.B. Lipsett, P. Polosa and H.J. van der Molen (Eds.), Raven Press, New York, pp. 69-78.

Santen, R. J. (1995). The testis, In: Endocrinology and metabolism. P. Felig, J. D. Baxter and L. A. Frohman (Eds.), McGraw-Hill, pp. 885-972.

Sa´ttolo, S., Carvalho, C. A. F. and Cagnon, V. H. A. (2004). Influence of hormonal replacement on the ventral lobe of the prostate of rats (*Rattus norvegiccus albinus*) submitted to chronic ethanol treatment. *Tissue Cell* **36**: 417–430.

Schulze, C. (1984). Sertoli cells and Leydig cells in man. *Adv. Anat. Embryol. Cell Biol.* **88**: 1-104.

Schulze, W. and Rehder, U. (1984). Organization and morphogenesis of the human seminiferous epithelium. *Cell. Tiss. Res.* **237**:395–407.

Segaloff, D. L. and Ascoli, M. (1993). The lutropin/choriogonadotropin receptor. 4....years later. *Endocr. Rev.* **14**: 324-347.

Segatelli, T. M., Franca, L. R., Pinheiro, P. F. F., Almeida, C. C. D., Martinez, M. and Martinez, F. E. (2004). Spermatogenic Cycle Length and Spermatogenic Efficiency in the Gerbil (*Meriones unguiculatus*). *J. Androl.* 25: 872-880.

Seminara, S. B., Messager, S., Chatzidaki, E. E., Thresher, R. R., Acierno, J. S., Shagoury, J. K., Bo-Abbas, Y., Kuohung, W., Schwinof, K. M., Hendrick, A. G., Zahn, D., Dixon, J., Kaiser, U. B., Slaugenhaupt, S. A., Gusella, J. F., O'Rahilly, S., Carlton, M. B., Crowley, W. F., Aparicio, S.A. and Colledge, W. H. (2003). The GPR54 gene as a regulator of puberty. *N. Engl. J. Med.* **349**: 1614–1627.

Sertoli, E. (1865). Sulla struttura dei canalicoli seminiferi dei testiculo. *Arch. Sci. Med.* **2**: 267-295.

Setchell, B. P. and Waites, G. M. H. (1975). The blood-testis barrier. In: Handbook of Physiology. D. W. Hamilton and R. O. Greep, (Eds.), Section 7, Williams and Wilkins, Baltimore. pp. 143-172.

Seung, H., Wolfe, G. and Rocca, M. (2003). Male Reproductive Toxicology, In: Current Protocols in Toxicology. M. D. Maines, L.G. Costa, E. Hodgson, D. J. Reed, and Sipes, I. G. (Eds.), John Wiley & Sons, Inc., Chap. 16, pp. 15.7.1-16.7.6.

Shahab, M., Mastronardi, C., Seminara, S. B., Crowley, W. F., Ojeda, S. R. and Plant, T. M. (2005). Increased hypothalamic GPR54 signaling: a potential mechanism for initiation of puberty in primates. *Proc. Natl. Acad. Sci. U. S. A.* **102**: 2129–2134.

Sharpe, R. M., Turner, K. J., McKinnell, C., Groome, N. P., Atanassova, N., Millar, M. R., Buchanan, D. L. and Cooke, P. S. (1999). Inhibin B levels in plasma of the male rat from birth to adulthood: effect of experimental manipulation of Sertoli cell number *J. Androl.* **20**: 94–101.

Shinohara, T., Orwing, K. E., Avarbock, M. R. and Brinster, R. L. (2001). Remodeling of the postnatal testis is accompanied by dramatic changes in

stem cell number and niche accessibility. *Proc. Natl. Acad. Sci. USA* **98**: 6186-6191.

Shinohara, T., Orwing, K. E., Avarbock, M. R. and Brinster, R. L. (2002). Germ line stem cell competition in postnatal mouse testes. *Biol. Reprod.* **66**: 1491-1497.

Sirinathsinghji, D. J. S., Motta, M. and Martini, L. (1985). Induction of precocious puberty on female rat after chronic naloxone administration during neonatal period: the opiate "brake" on prepubertal gonadotropin secretion. *J. Endocrinol.* **104**: 299-307.

Smith, J. T., Dungan, H. M., Stoll, A., Gottsch, M. L., Braun, R. E., Eacker, S. M., Clifton, D. K. and Steiner, R. A. (2005). Differential Regulation of KiSS-1 mRNA. Expression by sex steroids in the brain of the male mouse. *Endocrinology* **146(7)**: 2976-2984.

Stafford, L. J., Xia, C., Ma, W., Cai, Y. and Liu, M. (2002) Identification and characterization of mouse metastasis-suppressor KiSS1 and its G-protein-coupled receptor. *Cancer Res.* **62**: 5399–5404.

Steinberger, E. (1971). Hormonal control of mammalian spermatogenesis. *Physiol. Rev.* **51**: 1-22.

Steinberger, E. (1976). Biological action of gonadotropins in the male. *Pharmacol. Ther. [B]* **2**: 771–86.

Sugimura, Y., Cunha, G. R. and Donjacour, A. A. (1986). Morphogenesis of ductal networks in the mouse prostate. *Biol. Reprod.* **34**: 961-971.

Sutton, S, W., Mitsugi, N., Plotsky, P. M. and Sarkar, D. K. (1988). Neuropeptide Y (NPY): a possible role in initiation of puberty. *Endocrinology* **123**: 2152-2154.

Sutton, W. S. (1903). The chromosomes in heredity. *Biol. Bull.* **4**: 231-251.

Swift, H. H. (1950). The deoxyribose nucleic acid content of animal nuclei. *Physiol. Zool.* **23**: 169-200.

Tanner, J. M. (1962). Growth at Adolescence. 2nd ed. Blackwell Scientific Publications, Oxford.

Tao, Y. X., Lei, Z. M. and Rao, C. V. (1998). Seminal vesicles are novel sites of luteinizing hormone/human chorionic gonadotropin receptor gene expression. *J. Androl.* **19**: 343-7.

Teles, M. G., Bianco, S. D., Brito, V. N., Trarbach, E. B., Kuohung, W., Xu, S., Seminara, S. B., Mendonca, B. B., Kaiser, U. B. and Latronico, A. C. (2008) A GPR54-activating mutation in a patient with central precocious puberty. *N. Engl. J. Med.* **358**: 709-715.

Tena-Sempere, M. (2006). The roles of kisspeptins and G protein-coupled receptor-54 in pubertal development. *Curr. Opin. Pediatr.* **18**:442–447

Terao, Y., Kumano, S., Takatsu, Y., Hattori, M., Nishimura, A., Ohtaki, T. and Shintani, Y. (2004). Expression of KiSS-1, a metastasis suppressor gene, in trophoblast giant cells of the rat placenta. *Biochimica Biophysica Acta (BBA) - Gene Structure and Expression.* **1678**: 102-110.

Thompson, E. L., Amber, V., Stamp, G. W., Patterson, M., Curtis, A. E., Cooke, J. H., Appleby, G. F., Dhillo, W. S., Ghatei, M. A., Bloom, S. R. and Murphy, K. G. (2009). Kisspeptin-54 at high doses acutely induces testicular degeneration in adult male rats via central mechanisms. *Br. J. Pharmacol.* **156**: 609-625.

Thompson, E. L., Murphy, K. G., Patterson, M., Bewick, G. A., Stamp, G. W. H., Curtis, A. E., Cooke, J. H., Jethwa, P. H., Todd, J. F., Ghatei, M. A. and Bloom, S. R. (2006). Chronic subcutaneous administration of kisspeptin-54 causes testicular degeneration in adult male rats. *Am. J. of Physiol. Endocrinol. Metab.* **291**: 1074–1082.

Timms, B. G., Mohs, T. J. and Didio, L. J. (1994). Ductal budding and branching patterns in the developing prostate. *J. Urol.* **151**: 1427–1432.

Timpl, R. (1996). Macromolecular organization of basement membranes. *Curr. Opin. Cell Biol.* **8**: 618-24.

Tovar, S., Vázquez, M. J., Navarro, V. M., Fernández- Fernández, R., Castellano, J. M., Vigo, E., Rao, J., Casanueva, F. F., Anguilar, E., Pinilla, L., Dieguez, C. and Tena-Sempere, M. (2006). Effects of single or repeated intravenous administration of kisspeptin upon dynamic LH secretion in conscious male rats. *Endocrinology* **147**: 2696-2704.

Van Kroonenburgh, M. J., Beck, J. L., Vemer, H. M., Rolland, R., Thomas, C. M. and Herman, C. J. (1986). Effects of a single injection of a new depot formulation of an LH-releasing hormone agonist on spermatogenesis in adult rats. *J. Endocrinol.* **111**: 449–454.

Veneziale, C. M., Bums, J. M., Lewis, J. C. and Buchi, K. A. (1977b). Specific protein synthesis in isolated epithelium of guinea pig seminal vesicle: effects of castration and androgen replacement. *Biochem. J.* **166**: 167-173.

Veneziale, C. M., Steer, R. C. and Buchi, K. A. (1977a). Guinea pig seminal vesicle epithelium: a model for androgen action in regulatory mechanisms affecting gonadal hormone action. Baltimore: University Park Press: 103-168.

Vilamaior, P. S. L., Felisbino, S. L. and Taboga, S. R. (2000). Collagen fiber reorganization in the rat ventral prostate following androgen deprivation. A possible role for smooth muscle cell. *Prostate* **45(3)**: 253-258.

Vilar, O., Perez del Cerro, and Mancini, R. E. (1962). The Sertoli cell as a "bridge cell" between the basal membrane and the germinal cells. *Exp. Cell. Res.* **27**: 158-161.

Vitale, R., Fawcett, D. W. and Dym, M. (1973). The normal development of the blood–testis barrier and the effects of clomiphene and estrogen treatment. *Anat. Rec.* 176,331–344.

von Ebner, V. (1888). Zur Spermatogenese bei den Saugthieren. *Arch. Mikr. Anat.* **31**: 236-292.

von Ebner, V. (1871). Untersuchungen iiber den Bau der Samenkanalchen und die Entwicklung der Spermotozoiden bei den Sanagentieren und beim Menschen. *Rollet Untersuch Inst. Phyiol. Histol.* **2**: 200-236.

von La Valette, and St. George, A. J. H. (1876). Ueber die Genese der Samenkorper. *Arch. Mikrosk. Anat.* **12**: 797- 825.

von La Valette, and St. George, A. J. H. (1885). Spermatologische Beitrage. *Arch. Mikr. Anat.* **25**: 581-593.

Watson, M. L. (1952). Spermatogonia in albino rat as revealed by electron microscopy. *Biochim. Biophys. Acta.* 8: 369-374.

Wattenberg, L. W. (1958). Microscopic histochemical demonstration of steroid-3ß-ol dehydrogenase activity in tissue sections. *J. Histochem. Cytochem.* **6**: 225-232.

Wettstein, R. and Sotelo, J. R. (1967). Electron microscope serial reconstruction of the spermatocyte 1 nuclei at pachytene. *J. Microsc.* **6**: 557- 576.

Winiwater, H. (1901). Recherche sur 1'ovogenese et forganogenese de 1' ovaire des mamiferes. *Arch. Biol.* **17**: 33-199.

World Health Organization (WHO) (1999). Laboratory Manual for the Examination of human semen and sperm-cervical mucus interaction. 4th ed. Cambridge, U.K. Cambridge University Press.

Wray, S and Gainer, H. (1987). Effect of neonatal gonadectomy on the postnatal development of LHRH cell subtypes in male and female rats. *Neuroendocrinology* **45**: 413-419.

Wray, S. and Hoffman, G. (1986). Postnatal morphological changes in rat LHRH neurons correlated with sexual maturation. *Neuroendocrinology* **43**: 93-7.

Wyllie, A.H. (1980). Glucocoticoid-induced thymocyte apoptosis is associated with endogenous endonuclease activation. *Nature* **284**: 555-556.

Yen, S. S. C. and Jaffe, R. B. (1978). Reproductive Endocrinology W.B. Saunders, Philadelphia, PA.

Ying, S. Y. (1988). Inhibins, activins, and follistatins: gonadal proteins modulating the secretion of follicle-stimulating hormone. *Endocr. Rev.* **9**: 267-293.

Zanato, V. F., Martins, M. P., Anselmo-Franci, J. A., Petenusci, S. O., Lamano[a2]Carvalho. T. L. (1994). Sexual development of male wistar rats. *Braz. J. Med. Biol. Res.* **27**: 1273-80.

Zhang, C., Roepke, T. A., Kelly, M. J. and Rønnekleiv, O. K. (2008). Kisspeptin depolarizes gonadotropin-releasing hormone neurons through activation of TRPC-like cationic channels. *J. Neurosci.* **28**: 4423–4434.

Zhengwei, Y., Wreford, N. G., Schlatt, S., Weinbauer, G. F., Nieschlag, E. and McLachlan, R. I. (1998). Acute and specific impairment of spermatogonial development by GnRH antagonist-induced gonadotrophin withdrawal in the adult macaque (*Macaca fascicularis*). *J. Reprod. Fertil.* **112**: 139-147.

Zini, A., O'Bryan, M. K. and Schlegel, P. N. (2001) Nitric oxide synthase activity in human seminal plasma. *Urology* **58**: 85-9.

Zirkin, B. R. (1998). Spermatogenesis: its regulation by testosterone and FSH. Semin. Cell Dev. Biol. **9**: 417-21.

Zapatero-Caballero, H., Sanchez-Franco, F., Guerra-Perez, N., Fernandez-Mendez, C.. and Fernandez-Vazquez, G. (2003). Gonadotropin releasing hormone receptor gene expression during pubertal development of male rats. *Biol. Reprod.* **68**: 1764–1770.

APPENDIX I

Light microscopy

Phosphate buffered saline (PBS)

Potassium chloride	0.2 g
Potassium dihydrogen phosphate	0.2 g
Disodium hydrogen phosphate	2.1 g
Sodium chloride	8.0 g

The reagents were dissolved in dH_2O, pH was adjusted to 7.4. Final volume was made 1000 ml.

Preparation of 4 % Paraformaldehyde (PFA)

Paraformaldehyde	2 g
dH_2O	50 ml
PBS	5 ml
Sodium hydroxide	1 M

For the preparation of PFA, 33 ml of dH_2O was heated to 60°C to which paraformaldehyde powder (Sigma, St Louis, Missouri, USA) was added and mixed well. NaOH (1 M) was then added dropwise until the solution became just clear, 5 ml of PBS (phosphate buffered saline) was the added and pH was adjusted to 7.2. Final volume was raised to 50 ml with dH_2O. The solution was filtered with a 0.45 µm filter paper and stored at 4 °C until used.

Schiff's reagent

Basic fuchsin	1 g
dH_2O	200 ml
Potassium metabisulphite	2 g
Conc. HCl	2 ml
Activated charcoal	0.2 g

Basic fuchsin was dissolved in 200 ml of boiling dH_2O, flask was removed from the heat before adding. Solution was allowed to cool to 50°C and potassium metabisulphite was added with constant mixing, allowed to cool to room temperature and concentrated HCl was added, mixed and allowed to stand overnight in the dark. Activated charcoal was then added and the solution was mixed for 1-2 min. Stain was filtered through a Whatman No. 1 filter paper (125 mm). Solution was stored in a brown bottle at 4°C.

1% Periodic acid

Periodic acid	1 g
90 % ethanol	100 ml

Periodic acid was added to 90% ethanol and mixed.

Harris's Hematoxylin

Hematoxylin	1 g
Absolute alcohol	10 ml
Alum	20 g
Mercuric oxide	0.5 g
Glacial acetic acid	8 ml
dH_2O	200 ml

Hematoxylin (1 gm) was dissolved in 10 ml of absolute alcohol, 20 g alum was dissolved separately in the 200 ml warm dH_2O. Hematoxylin solution was then added to the alum solution and rapidly brought to boiling to which 0.5 g mercuric oxide was then added. The stain was rapidly cooled by plunging the flask into cold water and 8 ml glacial acetic acid was added after the solution cooled.

Eosin

Eosin crystals	1 g
dH_2O	100 ml
Acetic acid	0.05 ml

Eosin crystals were dissolved in dH_2O. To this acetic acid was added. The solution was kept in a brown bottle and used immediately.

APPENDIX II

Elongated spermatid head count and daily sperm production

Dimethyle sulfoxide (DMSO)/saline solution

NaCl (18.00 g) was taken in a 2 L container to which was added 1.60 L dH_2O. The contents were mixed vigorously and 200 ml of DMSO was then added. Final volume was made to 2 L with dH_2O.

Trypan blue stain, 0.1% (w/v)

To 10 mg trypan blue were added 10 ml dH_2O. The contents were stirred until dissolved.

APPENDIX III

DNA Parameters

Cell lysis buffer

1 M Tris-HCl solution pH 8.0	1 ml
0.5 M EDTA	5 ml
1 M NaCl	10 ml
Protein kinase	0.1 mg/ml

Final volume was made to 100 ml with dH_2O

Preparation of stock solution of EDTA

EDTA (ethylenediamine tetraacetic acid) solution (pH 8.0) was prepared before hand. For a 500 ml stock solution of 0.5 M EDTA, 73.06 g EDTA (FW = 146.13) were weighed and dissolved in 400 ml dH_2O, the pH was adjusted with NaOH. Final volume was made to 500 ml.

Preparation of stock solution of TBE

Tris	108 g
Boric acid	55 g
0.5 M EDTA	40 ml

A concentrated (10 ×) stock solution of TBE was made by dissolving Tris base (FW = 121.14) and boric acid (FW = 61.83) in approximately 900 ml deionized water. EDTA (pH 8.0) was then added and final volume was made to 1 L. This solution was stored at room temperature in glass bottles and discarded if a precipitate had formed.

Working Solution of TBE

For agarose gel electrophoresis, TBE was used at a concentraion of 1 × (1:10 dilution of the concentrated stock). Stock solution was diluted the by 10 × in dH_2O.

Chloroform/Isoamyl alcohol

Chloroform	24 ml
Isoamyl alcohol	1 ml

DNA washing buffer (TE buffer)

Tris (pH 7.5) 10 mM
EDTA 5 mM

DNA dissolving buffer (TE buffer)

Tris (pH 7.5) 10 mM
EDTA 1 mM

Preparation of phenol

1. An aliquot of phenol was allowed to melt in a water bath at 65°C.
2. 8-hydroxyquinoline was added to a final concentration of 0.1 % w/v to the phenol and mixed to dissolve the 8-hydroxyquinoline.
3. An equal volume of 0.5 M Tris HCl (pH 8.0) was added to the phenol, mixed for 15 min. Bottle was returned to a water bath at 65°C. Phases were allowed to separate, the top layer was siphoned off and discarded.
4. An equal volume of 0.1 M Tris Cl (pH 8.0) was added to the phenol. The procedure was repeated as in Step 3.
5. Extractions were repeated with 0.1 M Tris Cl (pH 8.0) until the supernatant was ~pH 7.8.
6. An equal volume of TE buffer was added to the phenol. The procedure was repeated as in Step 3. A ~1 cm layer of TE was left over the phenol.
7. The buffer saturated phenol was stored at 4°C for periods up to 2 months for RNA work and for 6 months for DNA work.

Note: Phenol would lose during the preparation of the TE buffered phenol, the protocol started with at least 2.5 × the final volume of phenol that was needed.

TTE solution

TE buffer pH 7.4

0.2 % Triton X-100 (store at 4°C)

Diphenylamine (DPA) solution

Glacial acetic acid	10 ml
Diphenylamine	150 mg
Conc. Sulfuric acid	150 µl
Acetaldehyde solution	50 µl

Glacial acetic acid was added to diphenylamine in a polypropylene tube and mixed thoroughly by repeated inversion until complete dissolution. Concentrated sulfuric acid was added and mixed. Acetaldehyde solution was then added and mixed thoroughly.

Caution: DPA was prepared fresh and used within 60 min. It is an irritant.

Acetaldehyde solution

Acetaldehyde	16 mg
Deionized water	10 ml

Acetaldehyde (16 mg) was added to 10 ml deionized water.

APPENDIX IV

Transmission electron microscopy

Pipes Buffer [0.2M] (Piperzine-N, N-bis [2-ethanesulfonic acid]) FW: 302

Pipes	6 g
dH_2O	100 ml
NaOH	1 N

Pipes were added to dH_2O. 1 N NaOH was added drop wise until solid components dissolved. After adjusting the pH to 6.8, the volume was raised to 100 ml and stored at 4 °C.

5% Glutaraldehyde

Glutaraldeyhde	5 ml
dH_2O	25 ml
0.2 M Pipes buffer	10 ml

Glutaraldeyhde was added to of 0.2 M Pipes buffer, the pH was adjusted to 6.8 with 1 N NaOH and the total volume was raised to 25 ml with dH_2O.

Osmium tetroxide (0.2 %)

2 % Osmium tetroxide	1 ml
Pipes buffer	9 ml

I ml of 2 % aqueous stock solution was added to 9 ml of Pipes Buffer which was prepared fresh before use.

5% Uranyl Acetate

Uranyl acetate	5 g
dH_2O	100 ml

Uranyl acetate was dissolved in dH_2O, filtered and sterilized with 0.2 μm cellulose acetate filter and stored in cuvettes covered with aluminum foil to save from direct light, the solution was used as stain to enhance electron density.

Ethanol Series

Ascending grades of ethanol 30%, 50 %, 70 %, 100 % were used as dehydrating agents.

Spur Resin

The spur resin was prepared as following:

ERL / VCD 4206 (Vinylcyclohexene dioxide)	10 Parts
DER736 (Diglycidyl ether of propylene glycol)	6 Parts
NSA (Nonyl succnic anhydride)	26 Parts
S1 (Dimethylaminoethanol)	0.4 Parts